Modeling and analysis of Picture Archiving and Communication System (PACS)

by

Hassan Khanmoradi

CCSP-TR-89/7

A thesis submitted in partial fulfillment of the requirements for the degree of Doctor of Technology at the Royal Institute of Technology, Stockholm.

May 1989

STOCKHOLM

ACKNOWLEDGEMENTS

I like to express my gratitude to Professor Arne A. Nilsson, Director of the Center for Communications and Signal Processing (CCSP) at North Carolina State University, for making it possible for me to do the work which led to this thesis under his supervision. Arne's help, encouragement, and friendship over the last few years have been of great value to me and I thank him for it.

I also like to thank Drs Anders Hedin and Janos Werner for helping me through the course of this project.

I thank Professor Harry Perros of North Carolina State University for taking the trouble of being the "opponent" at the final defense.

This work was supported by CCSP and the Department of Telecommunications and Computer Systems at the Royal Institute of Technology.

KHANMORADI, HASSAN. Modeling and analysis of Picture Archiving and Communication System (PACS), 1989, Stockholm.

The Royal Institute of Technology, Department of Telecommunications-Computer systems.

ABSTRACT

This thesis presents analytical queueing models for performance evaluation of picture archiving and communications system (PACS). These systems are used for digitizing, storing, and retrieving medical images.

We have studied several generic queueing models of these systems. Our models are general enough to be applicable to PACS used in any environment. However we emphasized on PACS that are used in the radiology departments of hospitals for storing image information of patients.

We evaluated the response time of each model to get some insight into the performance of such systems. Our queueing models were for the image database structure, the communications medium, and the image processors of picture viewing stations.

We studied three different queueing models of the database, $E_r/M/1$, $E_r/M/1$ with spawning, and $E_r/Cox_2/1$ with spawning. The communication channels were modeled as a multi server G/M/m queueing system, and its arrival process was found by superimposing the departure processes from the database queues. The image processors were modeled as M/G/1 and M/G/1 queueing systems with bulk service.

Key words: Queueing system, communication channels, performance evaluation, image database, image processor, PACS.

TABLE OF CONTENTS

CHAPTER 1

INTRODUCTION

1.1-Introduction to Picture Archiving and Communication Systems (PACS)

At present the management of radiological information is done manually in most hospitals. Images from the digital modalities (e.g. Computer-tomography scanners, X-ray machines) are converted into films and stored in a room. These films are then distributed manually and interpretation is done by reading the films through light boxes.

With the advances in semiconductor technology and digital processing techniques it is now possible to automate these operations by using a digital system for archiving and communication of images.

A Picture Archiving and Communication System (PACS), is a digital system for acquiring, storing, moving and displaying picture or image information [1].

The fundamental concept in PACS is the digital representation of image information, and the digital image refers to the presentation of a picture in terms of 1's and 0's. In the world of computing, the digital image has been a concept since the mid- 1950's, especially in intelligence and space applications. In these fields pictures began as photographs and were converted to digital images in order to make them accessible to the computer.

In the medical environment, the ultimate goal of using digital images and PACS is to have a radiology department without film jackets.

The inherent nature of digital images and the power of computer allow instant free "copies" of images to be made and thrown away. These copies can be transmitted to remote sites without the original ever leaving the archives of the radiology department. The result is a radiology

department with much freer access to patient images and greater protection against lost or misplaced image information.

In this work we concentrate on modeling and analysis of PACS for medical environments [2]. A typical PACS consists of a database of medical images, display stations, acquisition systems and the communications medium. Two possible architectures of PACS are shown in Figure 1.1.

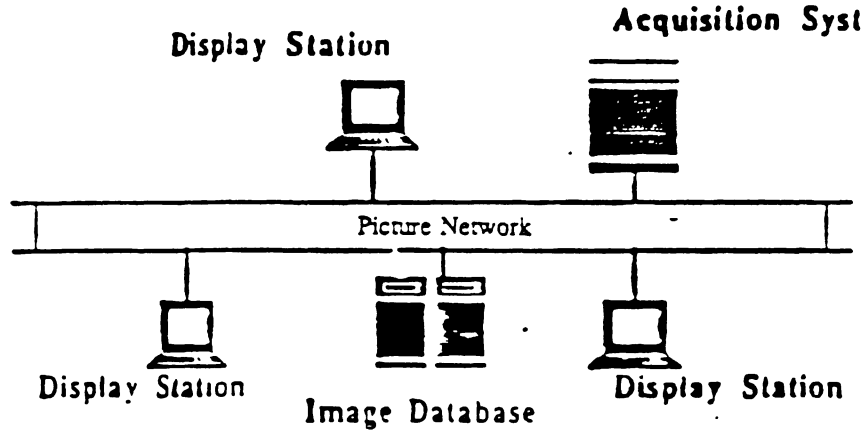

a) Distributed PACS

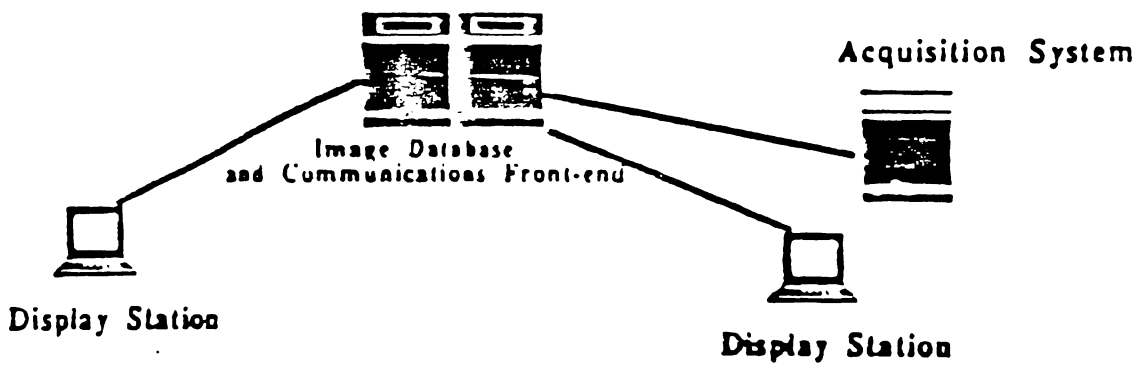

b) Centralized PACS

Figure 1.1 Two possible architectures for PACS.

The picture network must accommodate sources representing a variety of imaging modalities (e.g. X-ray machines, CT scanner etc), support various classes of viewing stations, and facilitate system growth. Image transmission differs from data transmission in that the basic unit of information transfer involves several orders of magnitude more data. An unencoded uncompressed image with 512x512 pixels and 8-bit intensity information for each pixel contains 262,144 bytes of information. In contrast, transactions of a few tens to a few thousands bytes are typical of computer terminals.

Fiber optics is an attractive transmission medium for communication between various nodes in a picture network. Its attractiveness results from its potentials for providing high data transfer rate, long transmission distance, ground isolation, absence of electromagnetic pickup and radiation (commonly found in a radiology department), and low error rate (10^{-9} or better). In [3] a fiber optic communication system linking a number of digital imaging modalities to a central radiology research computer is described. It is claimed that this system can transfer high resolutions images in less than a second over distances exceeding 2000 feet.

One of the most important components of a radiology information system is the Picture Viewing Station (P.V.S.) or the PACS console. For the radiologist, the P.V.S. serves as the main interactive device for consultation, replacing the film light box. PACS console is required to have long format high resolution displays, and reasonably fast response time. If the P.V.S. is to be used and accepted by the radiologists it must respond to the user's commands in a short time. The picture viewing station, will incorporate image processing appropriate to the viewers needs, such as zoom, pan, contrast enhancement and annotation of a region of an image or text. In addition the P.V.S has to be able to manipulate digitized images from a variety of imaging modalities, such as X-ray, Computer Tomography, Ultrasound imaging, Digital Subtraction Angiography etc [4]. The P.V.S. should display each image in an array of its acquisition system (see table 1) and in an optimal size for each type of

image. Many imaging studies are tomographic or involve multiple views. In the process of interpretation, the radiologist performs a rapid scanning search through all the pertinent, available image before, during, and after studying individual images. For computed tomography and ultrasound, 48 images must often be scanned quickly. More images are involved when comparisons with previous studies are required or when combinations of study modalities are necessary to assess the progress of disease and/or the effect of therapy [5].

ACQUISITION DEVICE	MATRIX	DEPTH
Digital Radiography (Chest X-ray)	$1024^2(4096^{2*})$	12 bits (16 bits)
Digital Subtraction Angiography	1024^{2*} (2048^2)	12 bits (16 bits)
Emission Computed Tomography	128^2	16 bits
Nuclear Medicine	256^2	16 bits
Nuclear Magnetic Resonance	512^2	16 bits
Ultrasound	512^2	8 bits (16 bits)
X-ray Computed Tomography	512^2	14 bits

() implies potential resolution or depth

* 17" x 17" image intensifier = 4 line pairs per millimeter

Table 1

One characteristic of PACS is that even in its most primitive mode of operation - acquisition , filing , and retrieval- it needs high speed image processors. The tens of megabits of each image has to be processed in a few seconds and the required throughput is far beyond the capability of the conventional computer hardware [6]. In [6] a modular multiprocessor system is described for high speed processing of images. It is based on 2048^2x8 extendable registers of full (or multiple) picture size, where each register is connected to a number of processing elements via a

standardized synchronous 32-bit picture data bus and 24-bit address bus. Processing element may be hardwired (fast but specialized), or programmable on different levels. Several modes of multiprocessing are possible, such as SIMD and pipelining, among others [6].

Some of the PACS consoles being used in radiology departments are, low cost multi_medium (voice, data and picture) workstations [7][8], specialized consoles such as "Physician's Review Console" [4], modular multiprocessor systems [6], highly advanced 3-D computer graphic workstations used in neurology, orthopaedics, and cardiology [9].

The picture archive, can be centralized, but part of it is likely to be decentralized at multiple nodes located throughout the network. In either case, it will depend heavily on new technology in the form of optical disks or new magnetic recording systems that provide substantial increase in information packing density. In [10] a number of optical data storage systems are reviewed, they range from electron beam recording on film [11] to laser beam holographic recording on micro-fiche [12], laser spot recording on optical disks [13] and [14], glass slide [15], and silver halide film diskette [16]. Among them, the bit by bit laser spot write (recording) and read techniques appear to be the most practical methods for optical storage. The storage density attainable by using the bit oriented laser spot method is about 10^8 bits per square inch [10]. One optical disk of 2 gigabyte storage can stores 1000 to 10000 pictures with a reasonable access time [17]. During a 10 year period a medium size hospital produces about five million pictures, most of them high resolution [18]. To provide enough storage mechanical disk exchanges ("jukeboxes"), for several hundred disks, or automatic magazines for several thousand, have to be used significantly increasing the access time [18]. For example up to 36000 X-ray images can be stored on one side of a 12-inch disk by melting holes 0.015 mm in size in material such as tellerium with a laser beam. Hospital personnel can call up a particular X-ray in less than 0.6 of a second in an on-line single disk system and up to less than 6 seconds in an on-line "jukebox" system. The "jukebox" is designed to hold up to 100 disks, thus storing 3,600,000 in hospitals with

a bed size of greater than 500 [19].

Due to the huge amount of data involved and the need for reasonable access time the picture archive must be organized in a hierarchical structure. This will enable the radiologists to have faster access to the images that are used frequently.

In [18], statistics on X-ray retrieval for several medium sized hospitals verses the year of filing are shown, Figure 1.2. It shows that for example in average 50% of one year old X-rays are retrieved in comparison to less than 0.5% of four year olds and more.

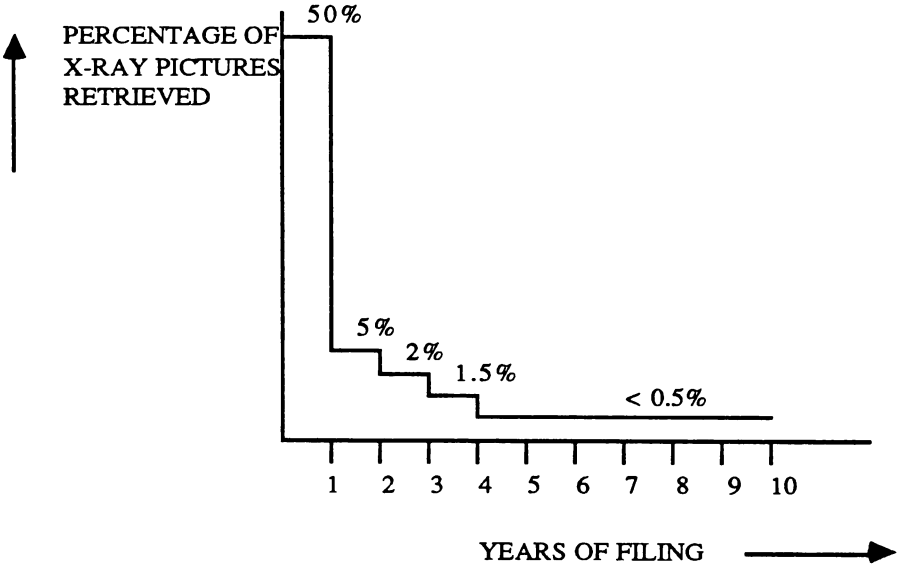

Figure 1.2. Average X-ray retrieval statistics.

It is reasonable from the performance point of view to increase the access time of older pictures in order to provide faster access to the more widely used pictures, i.e. the newer ones.

Retrieval statistics in Figure 1.2, indicates that a trade off between access time and age of images would be acceptable. This trade off requires

structuring the archive into a small "actual", a large "active", and a very large permanent section [18]. Images are stored according to their age, new images in the "actual", the old ones in the "active", and the very old images in the "permanent".

This hierarchical scheme is shown in Figure 1.3. Six levels of storage through which the image propagates- downward during the filing, and upward during the retrieval process are also shown.

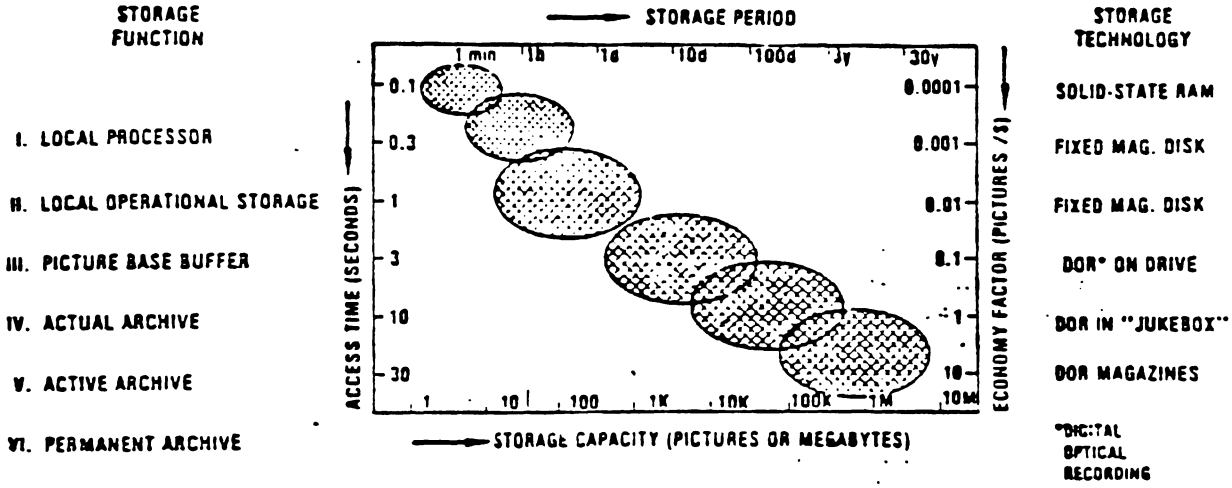

Figure 1.3. Hierarchy of Picture Store.

In accordance with the logical storage hierarchy, the parameters such as access time, storage period, storage capacity, and storage economy factor are found to be proportional functions of the level depth in Figure 1.3 [18].

The concept of a storage hierarchy helps in managing the storage problem physically, but it undermines efforts toward its logical management, that is how to map a storage address on its physical location. In [18] a very simple virtual addressing concept is introduced which alleviates this problem.

There are a number of prototype PACS or image transport networks in use at various universities, such as University of California [20], University of North Carolina [21], University of Arizona [4] and University

of Pennsylvania [3]. However the only commercially available full service PACS are the CommView™ from AT&T and Siemens PACS . There are a number of these PACS systems in use at various hospitals. In the following sections we briefly present the architecture of CommView™ with a focus on its functionality, we overview the design goals in implementing a PACS, we look at the motivation for performance evaluation, and in section 1.4 we present the outline of the dissertation.

1.2-Architecture of a commercial PACS (AT&T's CommView™)

AT&T's CommView™ system is designed to support the information movement and management needs of a radiology department [2]. The CommView™ product consists of four basic blocks shown in Figure 1.4.

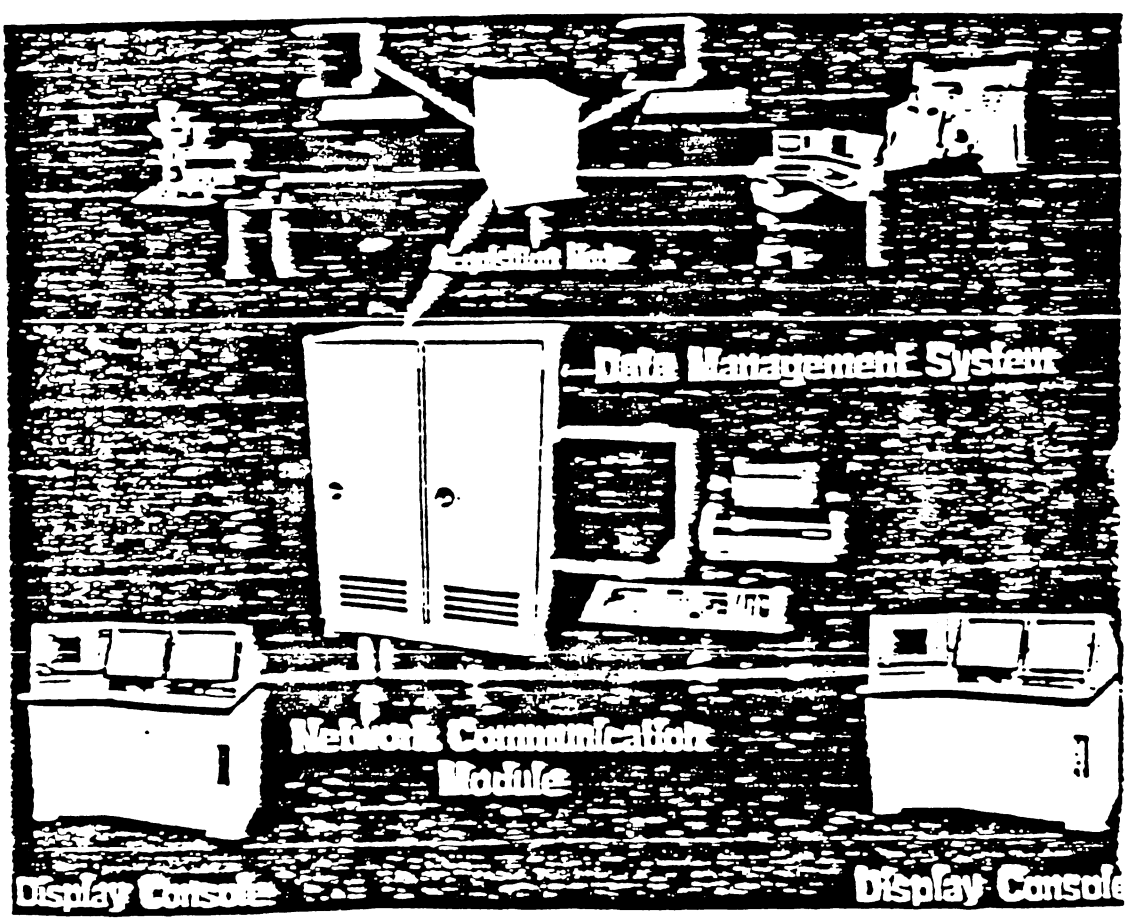

Figure 1.4. CommView™.

A building block approach is followed in designing the CommView™ architecture. A bulk of modules (CPU, Bus, Operating System, etc.) are common among the products in Figure 1.4. Each of the products is then built as a set by plugging in appropriate hardware and software modules.

Hardware Architecture- The foundation of the hardware architecture is the VME bus, a set of boards are added to the bus and these are briefly described below

*Single Board Computer- The single board computer features a CPU and 1 megabyte of on_board memory.

*Main Memory- Bulk random access memory is included in increments of megabytes.

*Terminal Interface Board- A six port interface board is used to support asynchronous I/O divides, e.g. data entry terminals, printers, etc.

*Disk Drive Interface- This includes the interfaces to the 86 megabytes winchester drives in the acquisition node and display consoles as well as those to the 300 megabytes magnetic and 1 gigabyte optical drives on the data management system.

*Network Interface- This peripheral provides a point to point data link over a wide variety of physical media. The medium could be dial up at 4.8 Kb/s or fiber optic at speeds up to 40 Mb/s.

*Image Acquisition- The frame grabber is programmable and allows interfacing to all the modalities commonly seen in radiology departments.

*Image Display- The graphics board drives a 1024x1024 display screen and provides a number of commonly requested manipulations in hardware, such as pan, scroll, zoom, etc.

*Image Compression- The compression board is programmable and can be programmed to execute bit preserving or non bit preserving algorithms.

Software Architecture- The software architecture is a layered design, consisting of three layers: the operating system, the core level software, and the application level software. Figure 5 illustrates this hierarchy.

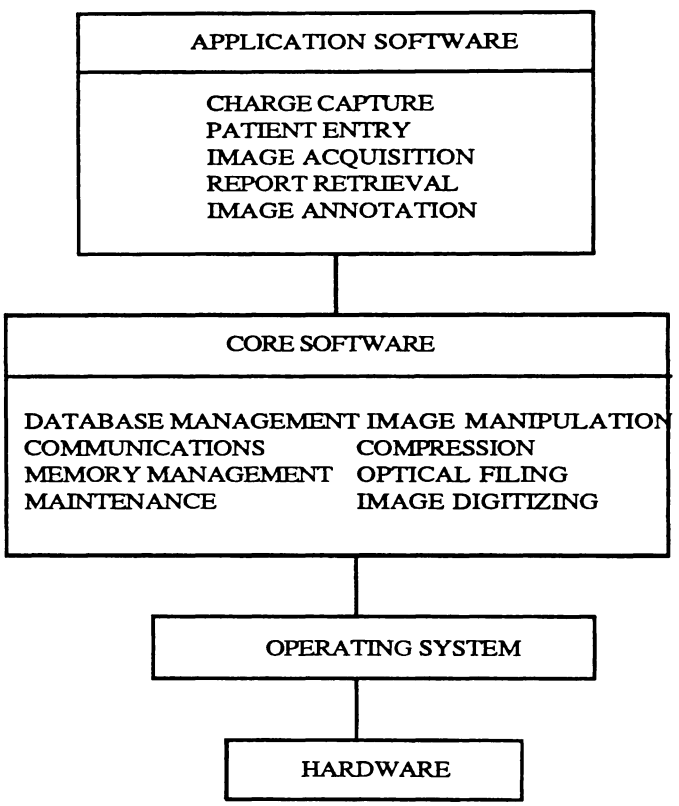

Figure 1.5. Software Layered Architecture.

For further information on each layer the interested reader is referred to reference [2].

In the next four sections we briefly overview the basic architectures of

the products outlined above.

1.2.1-Acquisition Node

The hardware/software base is augmented by a single fiber optic board or remote access interface board for the connection to the data management system. The acquisition node has interfaces of up to five (possibly different) modalities including a film scanner if desired. For each modality, a separate control terminal is required. Figure 1.6 shows this architecture.

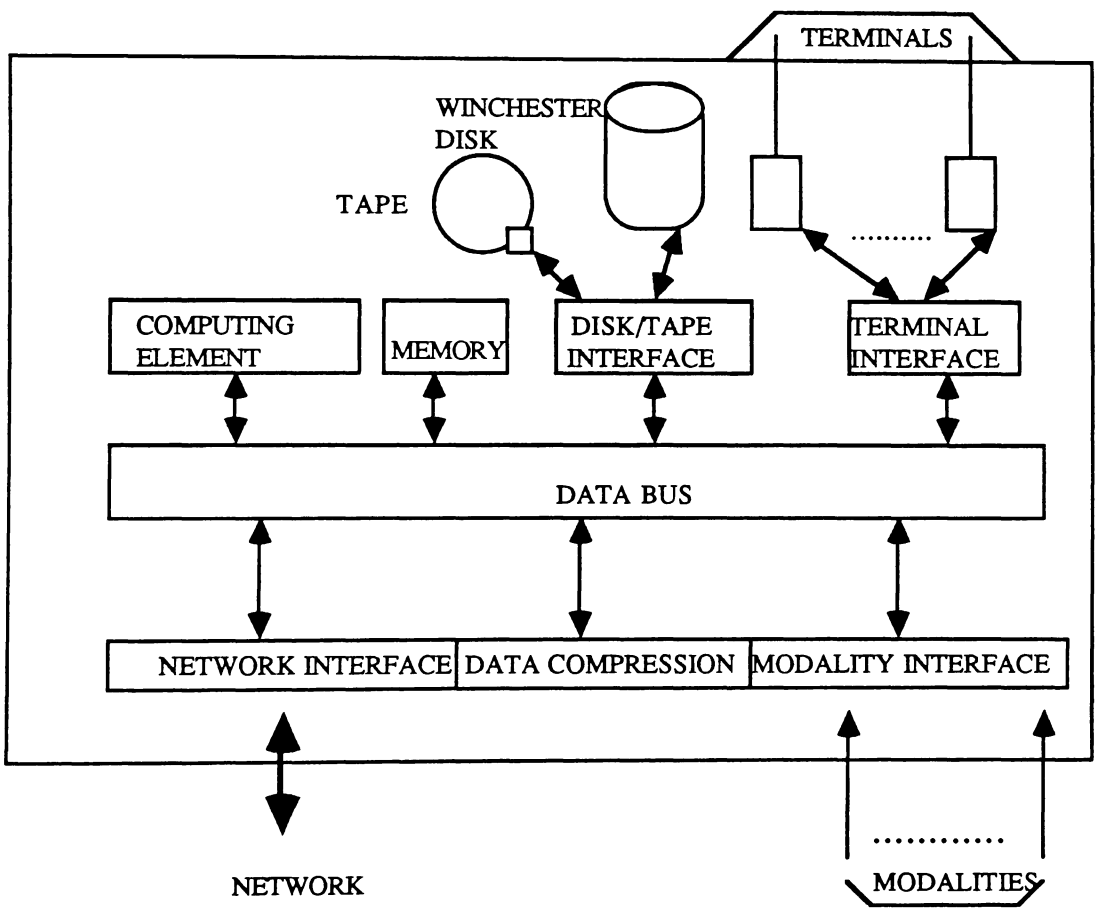

Figure 1.6. Acquisition Node Architecture.

1.2.2-Display Console Architecture

The hardware/software base is augmented by a single fiber optic or remote interface board for the physical level and link level connection to the database management system. The display console has multiple graphics terminals and a text display terminal. Figure 1.7 shows this architecture.

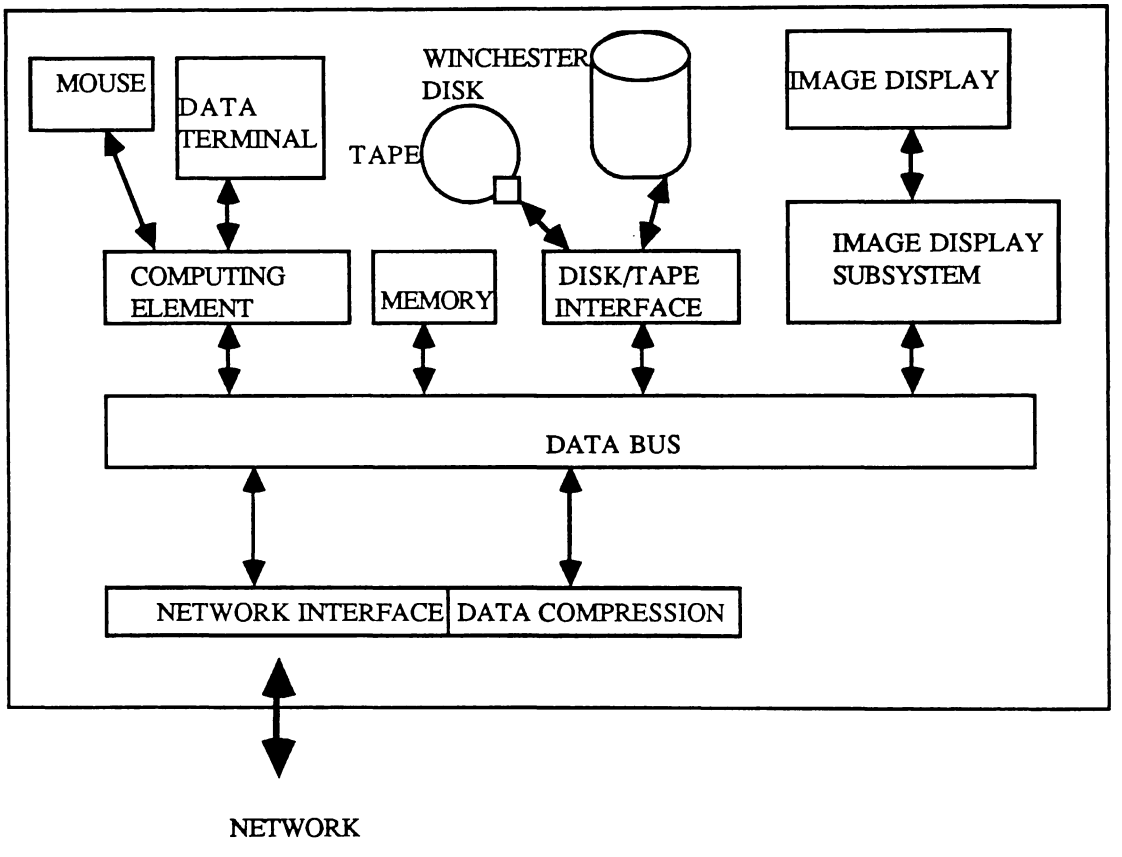

Figure 1.7. Display Console Architecture.

1.2.3-Database Management System

The hardware/software base is augmented by additional magnetic disk storage (2.4 gigabyte) for retention of records of current patients and

optical disks for long term storage of those records. currently, terminal interfaces are provided for up to eight Data Entry Terminals. Figure 1.8 shows this architecture.

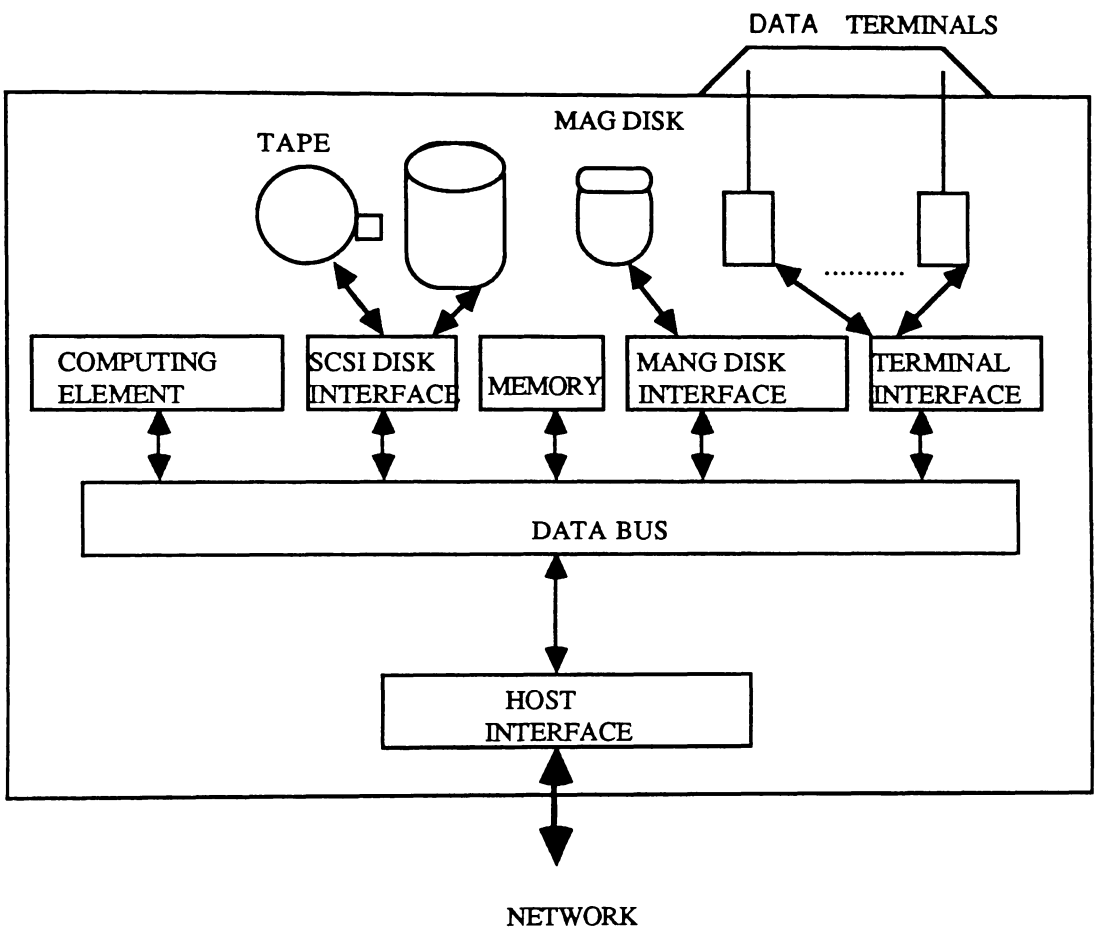

Figure 1.8. Data Management System Architecture.

1.2.4-Network Communications Module

The communications module provides a session layer connection oriented service and a file transfer service between the various nodes in the CommView™ system. It utilizes fiber optic links for local communications (distances of up to 3 kilometers) and an interface to either a private or a

public switched network for remote access. Compression and decompression are provided to reduce the transmission time for teleradiology and storage requirements.

1.3-Design goals in implementing a PACS

As noted in [22], the design goals in implementing a PACS are modularity, reliability, and reasonable response time.

Modularity. The continued growth of radiological image production and interpretation is certain. Improved system components will be developed as technology advances. Both of these factors lead to a modular approach in designing PACS . Such an approach requires the partitioning of the network into subnets. This partitioning must be done in a way that minimizes the traffic between subnets.

Subdivision of the picture archive into disjoint sets residing on separate subnets is another design objective, to facilitate modular growth and to prevent traffic bottleneck at the interface between the archive and the network.

Reliability. The goal of a reliable system is obvious. Modular systems are to some extent fault tolerant in the face of failure. Errors in transmission are likely to be low in high speed local area networks [23] , and stored images would be transmitted with a very small probability of error (see section 2.1). Operational reliability is especially important in PACS for two reasons. The first is the nature of "life and death" decisions that are based on the stored data. The consequences of data loss, alteration, or inaccessibility can be drastic. Secondly, the cost of such systems (in order of $1 million) will generate an implicit expectation of reliability in the buyer's mind. A basic study of the reliability aspects of PACS can be found in [24].

Response time. Retrieval of an entire medical exam, not part of it, in a reasonable amount of time is the most concrete and challenging of the

design goals [22]. Until the radiologists makes a preliminary review of a medical exam, he finds it hard to begin detailed interpretation of a single image. The images stored in the archive have to be available to the radiologist in a short time. This requires that the components of PACS perform in an optimal way to reduce the delay in retrieval, transmission and processing of images.

1.4-Motivation for performance evaluation

As mentioned in the previous section, fast response time is the major criteria in designing and implementing PACS. In order for PACS to be accepted by a radiologist, it must respond to his commands in a reasonable time, and this entails that the components of PACS have to be designed to perform in an optimal way.

For this reason, in the work reported here, we have embarked on performance evaluation of PACS. Our analysis here will provide the system designer with the necessary tools to measure the response time of each component of PACS as realistically as possible. These analysis can be used to evaluate the time it takes to retrieve, transmit, and process the huge amount of data that is needed for storage and presentation of medical images.

In our performance evaluation, we analyze various queueing models of components of PACS. These models are for the image archive, the communication channels and the image processor in the picture viewing stations. We have used abstract models, so that minor alterations in the design of a component do not invalidate the model.

1.5-Outline of the dissertation

In chapter 2 we present the performance models of PACS. These are generic queueing models of the image archive, the communication channels, and the picture viewing stations. Three analytical models of the image archive together with two models of the picture viewing stations

and one model of the communication channels are presented. Based on the three models of the image archive, we use three different queueing models of PACS for our performance studies. These models have the same type of queueing system representing their communication channels. Two of these models also have the same type of queueing system representing their picture viewing stations.

We also look at the structure of an image database currently in use at the University of California at Los Angeles (UCLA).

In chapter 3, we study our first performance model (model 1). The analysis of the image database is presented in details, we present the distribution of number of packets in the database, the average delay, the distribution of inter_departure intervals, and the analysis for the superposition of departure processes from the database queues. We then analyze the distribution of inter_arrival intervals to the communication channels, the average buffer occupancy in the input buffer of the communication channels and the average delay in transmitting images through the communication channels. Average buffer occupancy in the input buffer of the picture viewing stations and the delay in the image processor of the picture viewing stations is also presented.

In chapter 4, we study the second model (model 2). Detailed analysis of the image database queues and the queue representing the image processor in the picture viewing stations are presented, together with the distribution of the inter_arrival intervals to the communication channels. This model has the same type of queueing system representing its communication channels as the first model. The analysis for average buffer occupancy of the input buffer of the communication channels, and the transmission delay are the same as the one for model 1 and are not repeated in this chapter.

In chapter 5, we present the detailed analysis of the image database and the distribution of inter_arrival intervals to the communication channels. The queueing models of the communication channels and the image

processor of the picture viewing stations are the same as in the model 2, their analysis are also the same as the one presented for model 2 and are not repeated in the chapter.

In chapter 6, we use the analytical results obtained in chapters 3, 4 and 5 and the results from our simulation models of the queueing systems of models 1, 2 and 3 to present the performance curves.

In chapter 7, we present some topics that could be investigated in the future with regard to the queueing models of PACS.

CHAPTER 2

QUEUEING MODELS OF PACS

2.1-Modeling a PACS

In our modeling effort, we concentrate on studying analytical models for distributed PACS environment, see Figure 1.1. A block diagram of a distributed PACS is shown below.

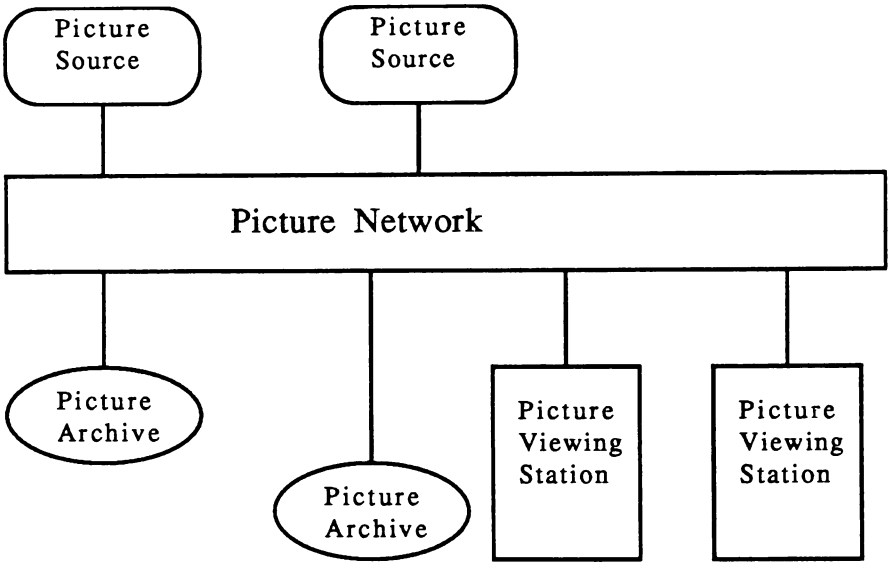

Figure 2.1. A distributed PACS block diagram.

Our analysis are focused on measuring the delay that the request packets from Picture Viewing Stations (P.V.S.) experience in the image database, the transmission delay for data packets retrieved from the database, and the time it takes to process images in the image processor of the picture viewing station. Here we first look at the delay in the communication channels, the Open System Interconnection (OSI) reference model proposed by the International Standard Organization has been used for modeling the picture network layer of PACS [22]. From the seven layers of the OSI, the top four layers provide a sufficiently high level of

abstraction such that the difference from the conventional networks, handling normal messages, are small. Here we look only at the the three lower levels of the protocol layers, the physical layer, the picture link layer (data link layer), and the picture network layer (network layer).

Physical layer. This layer provides a raw transmission facility with a capacity of say C bits per second, and a bit error rate of e . This channel can transmit D bits of data from source to destination in t seconds.

$$t = \frac{D}{C} \qquad (2.1)$$

The propagation time is very small compared to t and is neglected here. If we choose a Standard Image Frame (SIF) as an image with 512 x 512 pixels and 8 bits of intensity information for each pixel, then a 1024 x 1024 x 8 image corresponds to four SIFs, and a 2048 x 2048 x 8 image corresponds to 16 SIFs. The transmission time t given in (2.1) is plotted in Figure 2.2 [22] against the channel capacity C, with various values for D. It can be seen that transmission times less than one second require channel capacity greater than 2 Mbps for a D corresponding to one SIF and more.

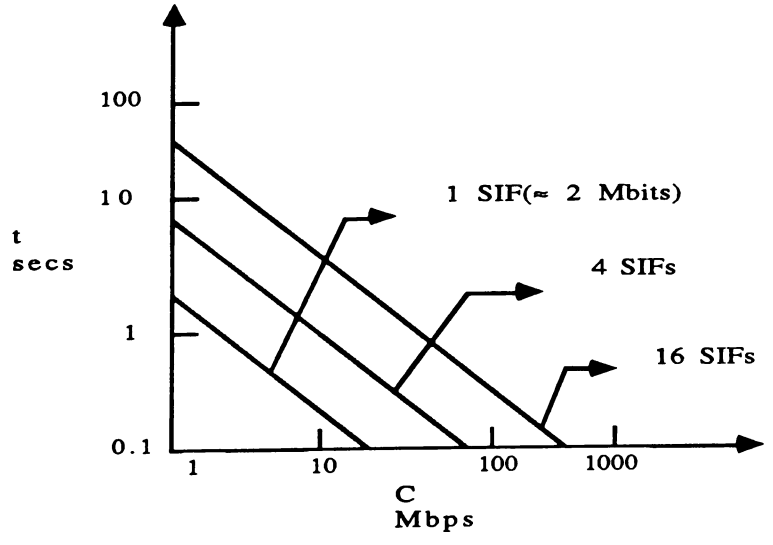

Figure 2.2. Transmission time verses channel capacity.

Picture link layer. This layer takes the raw transmission facility provided by the physical layer and transforms it into a channel that can transmit images with a small probability of error. Images are transmitted in packets of fixed length and we assume that each packet corresponds to an SIF. The picture link layer protocol must allow for the retransmission of erroneous packets and acknowledgements from the destinations.

The protocol that accomplishes the retransmission of damaged frames requires the attachment of a prefix and a suffix to the data frame. The prefix is to aid in frame synchronization, to number sequentially the frames and to pass along other control information. The suffix is to provide error checking. The acknowledgement from the destination may be a separate transmission or "piggy backed" on data bound in the opposite direction. We assume prefix and suffix together occupy H bits and the acknowledgement A bits. In [22], the delay factor, δ, is defined as $\frac{\text{actual transmission time}}{\text{ideal transmission time}}$ -1, and the mean number of retransmissions is given by

$$\bar{k} = \sum_{k=0}^{\infty} k(1- \alpha)^k \alpha = \frac{1}{\alpha} -1 \qquad (2.2)$$

where α is the probability of a successful transmission, given by

$$\alpha = (1- e)^H(1- e)^D(1-e)^A = (1- e)^{D_t} \qquad (2.3)$$

assuming the independence of errors, D_t is the total bits in a frame, where $D_t = H + D + A$.

On average there are a total of $\bar{k}$ + 1 transmissions, including the successful one. Thus, the total transmission time for the picture link layer is

$$\tau_L = \frac{D_t}{C}(\bar{k}+1) = t\,\frac{D_t}{\alpha D} \qquad (2.4)$$

The delay factor for this layer is

$$\delta = \frac{\tau_L}{t} - 1 = \frac{D_t}{\alpha D} - 1 \approx D_t\, e \qquad (2.5)$$

where the approximation holds for $H+A \ll D$ and $D_t\, e \ll 1$. Transmission of a complete SIF (2.1×10^6 bits) does not degrade the transmission time measurably for $e < 10^{-9}$, an achievable error rate for local area networks [25]. In summary, easily achievable constraints ($H+A \ll D$ and $D_t\, e \ll 1$) insures that $\delta \approx 0$ and that transmission time at picture link layer is given by relation (2.1).

Picture network layer. The third layer of PACS interfaces the host computers at the picture source, archive, and viewing station to the network. At the transmitting node a set of images from an exam is partitioned into packets that contain routing and control information. The flow of packets into the network is adjusted to match network traffic. At the destination, this layer assembles the packets which constitute an image, and an exam is presented as a set of images. In this study, we concentrate on the delay at the destination node as one of our performance parameters, that is the delay in the picture viewing station. In our analysis of the performance of the picture processor in the P.V.S. we accommodate the delay which occurs in assembling packets as part of the response time of the image processor.

In our performance evaluation of PACS, we assume that the delay in the picture link layer is negligible and we concentrate on the he delay in transmitting these images through picture network's physical layer, the delay in retrieving images from the image archive, and the delay in the image processor of the picture viewing station. We also assume that the communication between various nodes in the system is through a broadband communication medium, where the capacity of the link is shared by all the nodes for sending and receiving images.

In the next section we discuss the structure of an image database designed and operated at UCLA [20], in section 2.3 we present a generic queueing model for image archives. In section 2.4 we present a queueing model for the communication channels. Section 2.5 is devoted to the queueing model of the image processor in the picture viewing stations, and in section 2.6 we present various queueing models of PACS.

2.2-Structure of the image database of a Clinical Radiology Imaging System (CRIS)

The functions of Clinical Radiology Imaging System (CRIS) [20], are shown in Figure 2.3.

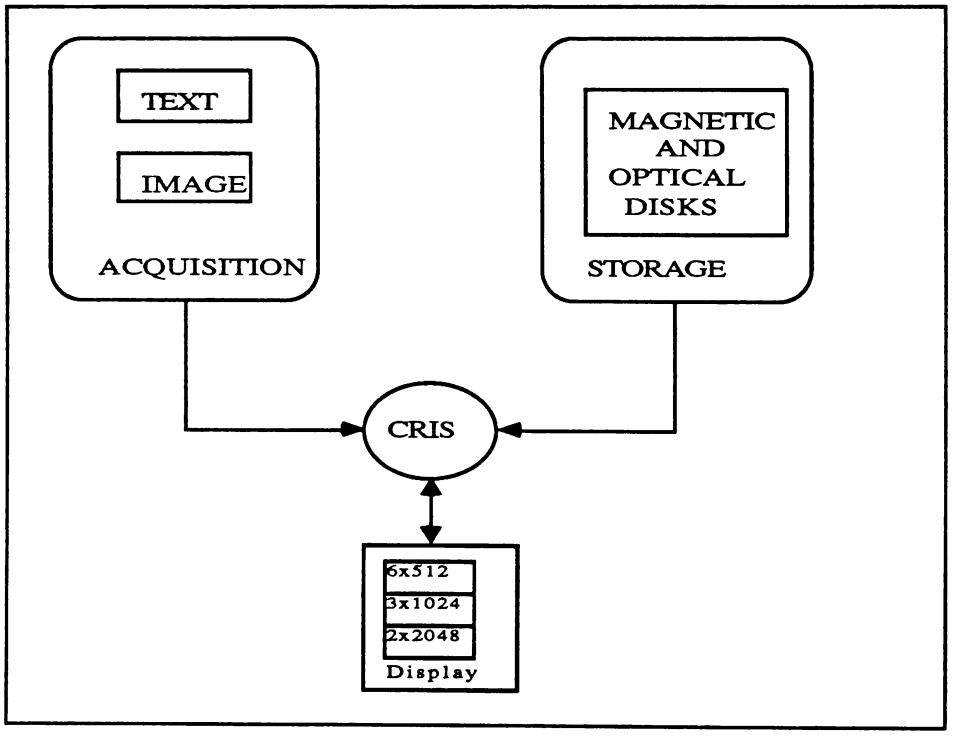

Figure 2.3. The functions of CRIS.

As can be seen in Figure 2.3, the CRIS is a centralized PACS. The CRIS database is made up of sub-systems, each composed of one or more

computer programs (processes), such as image reformat process, archive process, and storage manager process etc, which operate in parallel on a VAX-11/750 in a pediatric radiology department. Processes are coordinated through dynamic data structures that include system event flags and disk- resident queues, for more details see [20].

The flow of image and text data from image modalities to the storage medium in the CRIS system is shown in Figure 2.4.

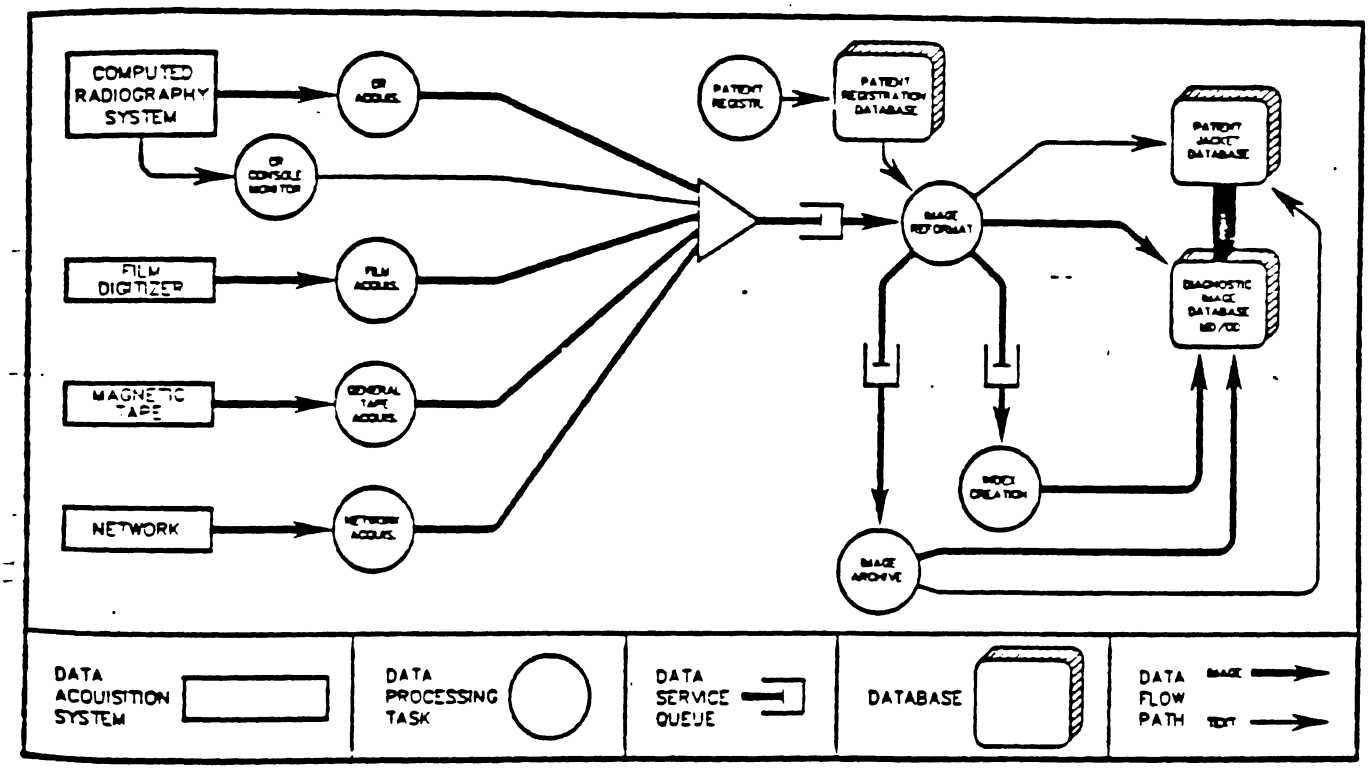

Figure 2.4. The flow of image and text data in the CRIS system from data acquisition (left) to database storage (right).

Image information enters the pediatric radiology PACS from: (1) Fuji Computed Radiology System, (2) a laser film digitizer, (3) a magnetic tape drive, and (4) a digital network.

Each of these four image modalities has its own software to handle the details of image interfacing. Image data is copied to a VAX magnetic disk

as quickly as possible in whatever form best meets the acquisition modality. Raw images are put into VAX magnetic disk, and once acquisition is complete a "request to process" is placed in the image reformat queue.

The image reformat process, using a priority weighting scheme [20], extracts the next request from the queue and creates a "standard format image file". The standard UCLA Radiological Image Format (UCLA-RIF) includes a multi-block image header into which is placed image-descriptive information.

After an image is in standard form, it remains on magnetic disk for one or two days. The actual duration of stay on this active storage device is determined by a storage manager process, which uses a patient/image decision algorithm to determine which files to retain in the magnetic storage , see [26] for the algorithm.

All images acquired by CRIS are archived on optical disk by the archive process, this process also retrieves file from optical disk, and stores them on the magnetic disk.

All image data is accompanied by related text information including patient demographic data, procedure description, date, and time as well as the individual image descriptions and previous radiological reports. This text data is handled as part of the data acquisition and storage stream. Basic patient information enters the system via the patient registration subsystem known as Pediatric Radiology Patient Registration System (PRPRS), see Figure 2.4.

Text data plays a critical role in the acquisition of Computed Radiography (CR) images, the Computed Radiography system uses custom built hardware that directly transfers image data to CRIS VAX [20]. Text for CR images is inserted from a console monitor attached to the operator's console.

This hardware/software subsystem reads all text information on the CR screen and sends pertinent patient to the CRIS image management software. By transferring this text the console monitor primes the CRIS system for the reception of CR images.

Film digitization and the loading of images from magnetic tape or digital network both carry on an interactive dialog with the technician. This results in image text data that accompanies the image through CRIS system.

A collection of patient text and image information is called a patient jacket. The patient jacket database is the heart of CRIS system. The most important field in each record is the patient code, which is generated automatically by CRIS at the acquisition of the patient's first image and is used in all references to images or text files within the system.

The patient jacket database is composed of a master patient index file and a master jacket file, which are used to access patient image and text data, see Figure 2.5.

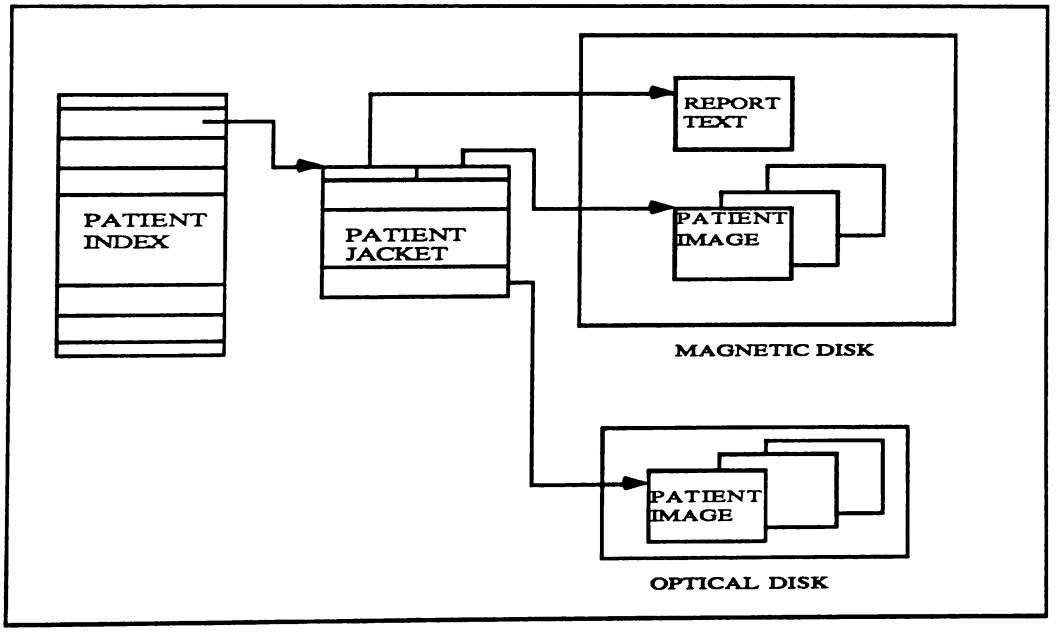

Figure 2.5. CRIS master patient jacket database structure

The final element in the CRIS image management chain is the permanent file storage system. All files in the CRIS system are sent to the optical disk archive for storage. Active patient files are kept on magnetic disk where management is done exclusively through the CRIS patient jacket database. Files that are no longer active are purged from magnetic disk, and access is through the optical disk archive database.

The optical disk subsystem is composed of an archive process attached to an image archive queue. It is a general file-oriented module which stores VAX files on two-sided optical disk cartridges. In the current system, each Hitachi 301 optical disk cartridge can store 1.3 gigabyte per side, and each side of the cartridge is given a unique optical disk volume name by CRIS.

The operation of the optical disk subsystem is transparent to the other CRIS modules. The only contact CRIS has with the archive is through the archive queue, where requests are entered and the success of image transfer is indicated by queue status field. This transparency is crucial for the growth of archive system. Optical storage is a new technology, and the use of a file oriented archive queue allows CRIS to accommodate other types of devices which may be interfaced to the queue in the future. This could include optical library units (jukeboxes) as well as different types of storage technology, such as optical tape.

2.3-Queueing model of the image archive

As mentioned in chapter 1, in a distributed system the image archive is likely to be decentralized at multiple nodes located throughout the network. Here we assume that each node consists of tens of disks put together in a "jukebox" configuration.

We present the queueing model of a single database node in the network, this model can be used for any node in the system where the storage structure and image retrieval mechanism is as described below.

The jukebox configuration has the capability for serving multiple simultaneous user request. Because of this feature, we model our database manager as a number of archive processes concurrently serving requests from picture viewing stations.

In our archive model a medical exam consists of a random number of images, which may be of varying sizes, an image consists of a random number of SIFs (depending on its type and size), and we assume that each SIF is stored as a block of data in the database. It should be noted that an image could occupy a fraction of an SIF, if the image size is not an integer number of SIFs. We also assume that database blocks can not be individually addressed except in the case when one block corresponds to a full image. The database blocks are the logical units in the communications between session layers of communicating devices.

We assume that the "request packets" from the picture viewing stations contain requests for one or more medical exams.

We also assume that these packets are routed by a scheduler to archive processes in the order of arrival, that is, the first goes to process 1, the second to process 2 and so on. When the last process is reached the scheduler repeats itself. The archive process provides service by first locating the exam header (e.g. through patient index and patient jacket in CRIS), then it proceeds to sequentially read off all the images that are in an exam.

As an exam features a set of images and images are stored as a number of SIFs on the disk, unless we have a request for a single image which consists of one or a fraction of an SIF, a request forces the archive process to retrieve blocks of data until all the blocks making an image, and all the images comprising an exam are collected. As soon as a block of data is retrieved, it is sent for transmission to the picture viewing station which requested it.

The "request packets" containing a number of exam requests generate

sibling requests for retrieval of more medical exams until all the exam requests are served and the images are retrieved from the database. Thus we have a spawning mechanism when a "request packet" is in service unless the "request packet" asks for the retrieval of only one medical exam.

For the above system the following queueing model can be envisaged:

Each archive process is modeled as a single server. Each server is fed through a single queue (archive queue) of its own, formed by the requests sent to it by the scheduler, see Figure 2.6. The queueing discipline in the archive queues are FCFS, and we assume that the requests are of the same priority.

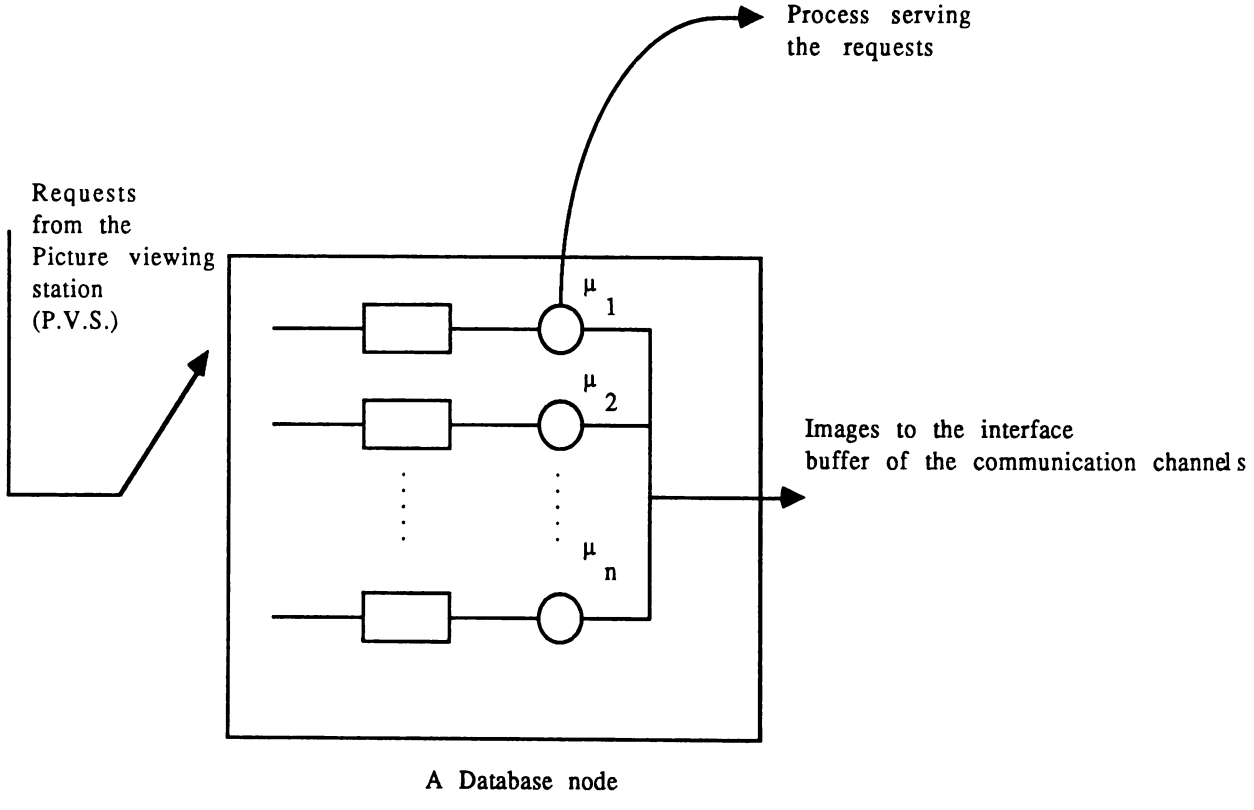

Figure 2.6. Queueing model of a database node.

Upon completing the retrieval of the images in the first medical exam

from the database, the archive process with some probability 'P' creates a sibling request for the retrieval of another exam (more images), which is spawned and put at the head of the archive queue. This is repeated at the completion of each service interval until the last medical exam in a "request packet" is retrieved from the database. The probability of spawning a sibling is related to the mean number of exam requests in a "request packet" and can be found from the following relationship

$$\bar{k} = \sum_{n=0}^{\infty} n(1-P)P^n = \frac{1}{1-P} \qquad (2.6)$$

where $\bar{k}$ is the mean number of exam requests in a "request packet".

With some statistics on the size of images and medical exams the probability, P, can be evaluated.

Since the archive processes are running under a time-sharing system with the same priority, it is unlikely that a process say j gets a quantum of CPU time immediately after it has completed retrieving an exam. For this reason, a random amount of time after a service interval (providing service to a request), expires through the scheduling mechanism before the process j is provided with more CPU time, see Figure 2.7 .

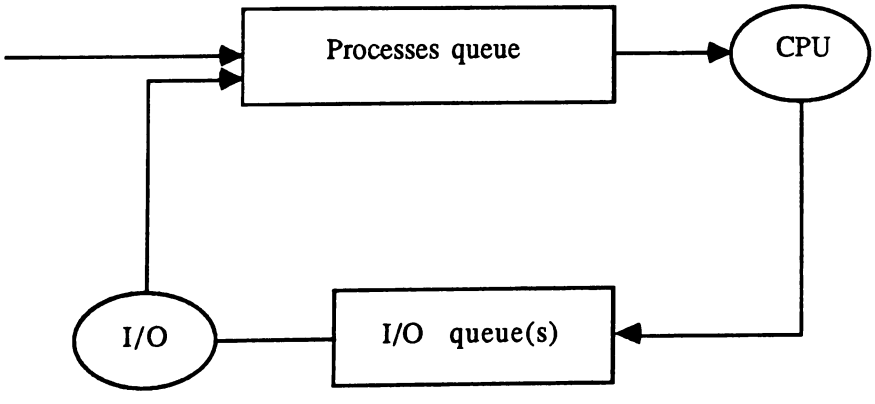

Figure 2.7. Simplified queueing in CPU.

Therefore, the "read" time, time it takes from the completion of the previous service interval, for an archive process to retrieve one more medical exam from the database, is a random variable. This time is the sum of access time to the disk (a constant), time to retrieve an exam from the disk (a random variable), and the scheduling time (a random variable). Since we have concurrent access to the disks, the I/O queueing time is negligible.

The service rate of the servers (archive processes) in the database is the number of medical exams that can be retrieved from the disk in a second. The service rate, μ_j ,of server j is

$$\mu_j = \frac{1}{\tau_j} \qquad (2.7)$$

where τ_j is the average "read" time (seconds) .

The exogenous and the spawned requests form the total arrival rate to each queue. Three models of the database with various assumptions on the service time distribution of archive processes are presented in section 2.6 .

2.4-Description of queueing model of the communication channels

The communications bandwidth is shared by all the database nodes in the system. We assume that each database node is provided with one or more dedicated transmission channels for communicating with picture viewing stations. Data packets retrieved from a database node are put in the interface buffer of the transmission channels associated with that node, see Figure 2.8. As soon as a channel is available, it is allocated for transmitting the next packet from the head of the queue.

The communication medium is modeled by a multi_server queue, in our analysis (chapters 3, 4, and 5) we assume that these servers are

homogeneous. The service rate of server i, in number of medical exams transmitted per sec, can be evaluated by the following

$$m_i = \frac{1}{\bar{m} \times \bar{n} \times \frac{D}{C}} \qquad (2.8)$$

where

$\bar{m}$ _ average exam size (in number of images)

$\bar{n}$ _ average size of an image (in number of SIFs)

D _ size of an SIF in bits.

C _ transmission rate of channel (bps) .

The model of Figure 2.8, represents the database nodes and the communication channels of a distributed PACS.

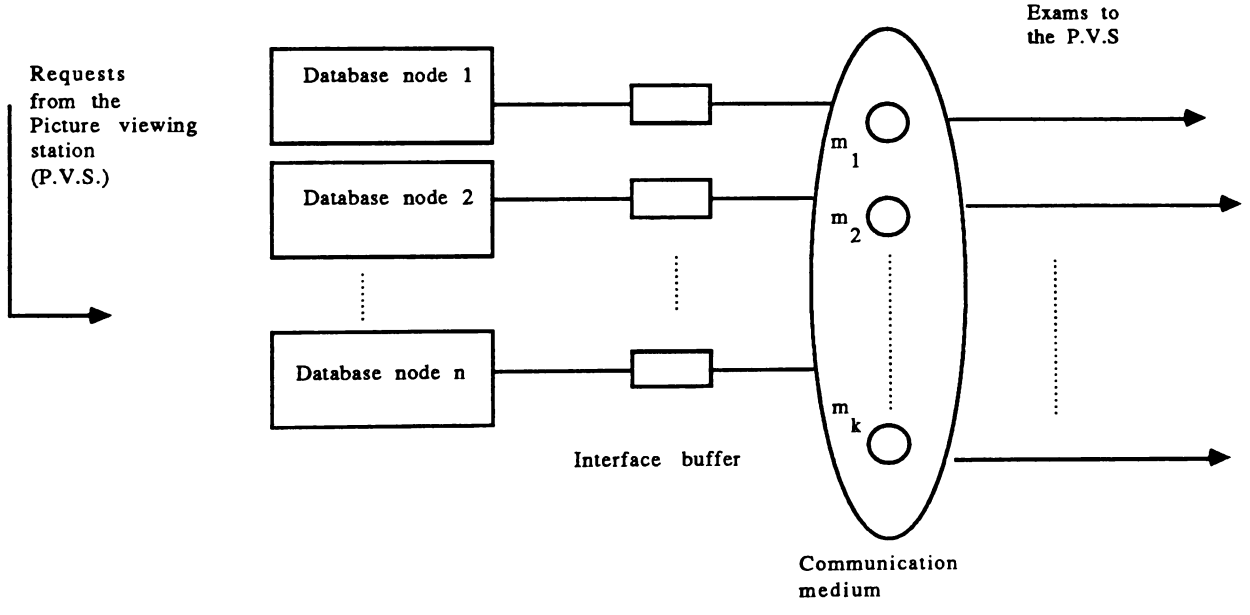

Figure 2.8. Queueing model of a distributed PACS.

2.5-Queueing model of the picture viewing station

Data packets transmitted through the communication channels are collected in the input buffer of the picture viewing stations. These

packets are then processed by the image processor to display the images on the monitors. We model the P.V.S as an image processor with one input buffer and a single server, which displays images by assembling data packets retrieved from the database. Two types of service mechanism are investigated. One is a server which needs a single packet to display an image. The other is a server which uses a "bulk" of packets to display an image. These two models are presented in the next section.

2.6-Various queueing models of PACS

In this work we analyze three different queueing models of distributed PACS. In all of these queueing systems we assume infinite buffer capacity and FIFO service mechanism. These models can also be used to evaluate the performance of heterogeneous subnets in a large distributed PACS.

The differences in the models, are in the queueing models of the database and the image processor. We use the same delay model of the communication channels in all three cases.

Each database node is modeled by two archive queues, however the analysis of the following chapters are general and can be applied to any number of queues in a database node. In all the models we assume that two communication channels are provided at each database node for transmission of images.

In the following subsections we present an overview of the PACS models and in chapters 3, 4 and 5 we analyze them in details.

2.6.1-Model 1: E_r/M/1 database queues and M/G/1 image processor queue

This model represents the case where "request packets" are for a single medical exam, i.e. no spawning. In this model we assume that the SIF or a block of storage in the database is large enough to contain the largest type of image that is going to be stored in the database. Therefore an image either occupies a whole SIF or a fraction of it depending on its size.

For this model, in equation (2.8) $\bar{n} \leq 1$.

We also make the following assumptions for this model:

1- No hierarchy of storage, i.e. the same access time to all the data.
2- Scheduling of request packets is as described in section 2.3.
3- Database servers have exponentially distributed service times.
4- Communication servers have exponentially distributed service times.
5- Request packets from picture viewing stations arrive according to a Poisson process.

With the scheduling of request packets as described in section 2.3, if we have r processes in the database (i.e. r queues), the inter-arrival intervals will have an Erlang-r distribution. Therefore each queue in the database will be an $E_r/M/1$ queueing system. Since the images consist of only one or a fraction of an SIF, and the communication servers have exponentially distributed service times, i.e. packets arrive at a P.V.S. at exponentially distributed service intervals, we model the image processor as an M/G/1 queue. Where the server needs to read only a single SIF from its input buffer to display an image on the monitor. In Figure 2.9, a two-queue database node with its communication channels is shown.

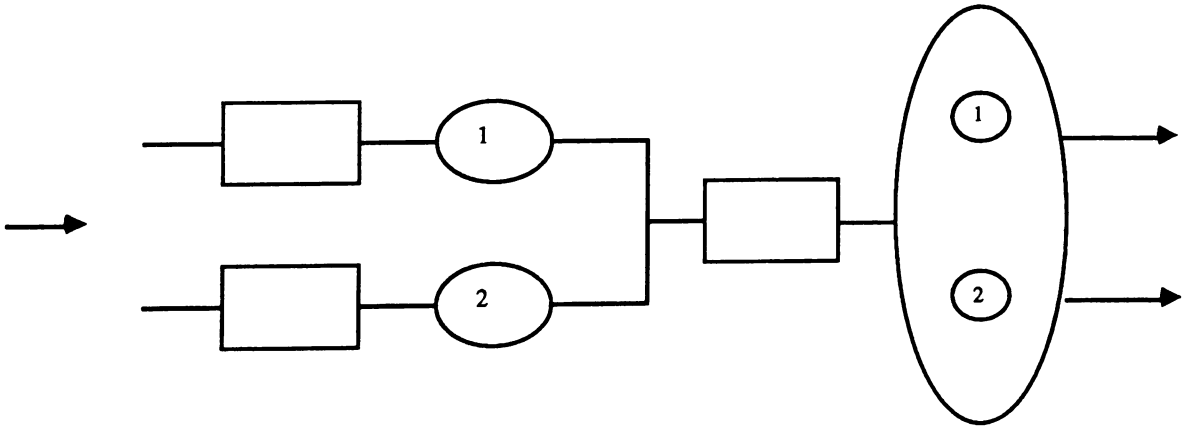

Figure 2.9. $E_2/M/1$ database queue and its communication channels.

2.6.2-Model 2: $E_r/M/1$ database queues with spawning and M/G/1 image processor queue with bulk service

In this model a "request packet" is for a number of medical exams, i.e. a spawning mechanism as described in section 2.3. We assume the images in this model consists of a number of blocks of data or SIFs.

We also make the following assumptions for this model:

1- No hierarchy of storage, i.e. the same access time to all the images.
2- Scheduling of request packets is as described in section 2.3.
3- Database servers have exponentially distributed service times.
4- Communication servers have exponentially distributed service times.
5- Spawning mechanism is as described in section 2.3 .
6- Request packets from picture viewing stations arrive according to a Poisson process.

With the scheduling of request packets as described in section 2.3, if we have r processes in the database (i.e. r queues), the inter-arrival intervals will have an Erlang-r distribution. Therefore each queue in the database will be an $E_r/M/1$ queueing system with spawning.

Since the images consist of many blocks of data, and the communication servers have exponentially distributed service times, i.e. Poisson arrival process for P.V.S., we model the image processor as M/G/1 queue with bulk service. Where the server needs to read a number of SIFs (a "bulk") from its input buffer to display a complete image on the monitor.

In Figure 2.10, a two-queue database node with its communication channels is shown

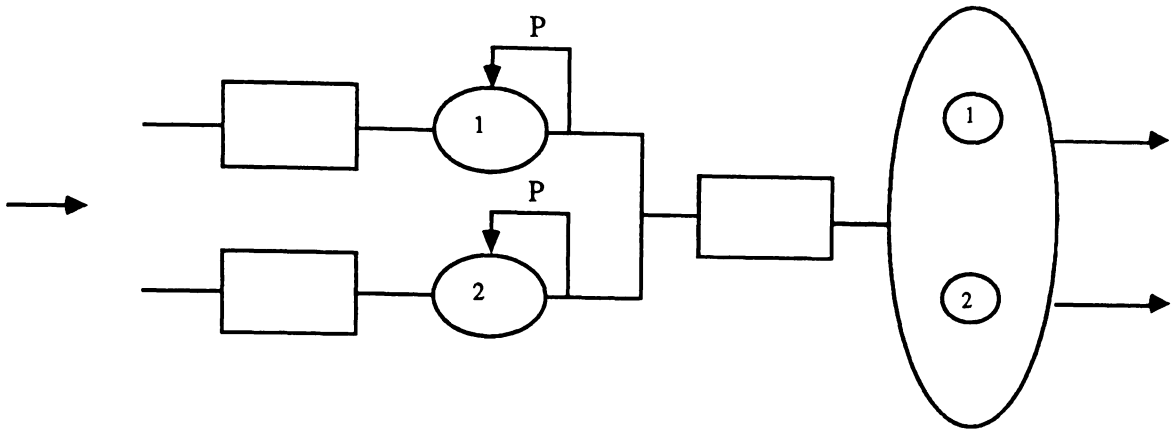

Figure 2.10. $E_2/M/1$ database queue with spawning and its communication channels.

2.6.3-Model 3: $E_r/Cox_2/1$ database queues with spawning and M/G/1 image processor queue with bulk service

As shown in Figure 1.2, the percentage of X-ray pictures usage, reduces sharply after they are one year old. This makes it reasonable for a designer of large image archive to provide faster access to more widely used images than the others through creating a hierarchical storage system, see Figure 1.3.

As can be seen from Figure 1.3, the difference in access time to each archive level is significant and it is not feasible to use the same value for access to all of them. In here we assume the possibility of two different access times, i.e. two different "read" times. However the analysis (in chapter 5) can be extended to any number of them. For this environment we propose the service mechanism, shown in Figure 2.11. Depending on where the image is located, an exam request forces the archive process to spend a random amount of time (server 1) to retrieve the image, this happens with probability α_i , or spend an additional time (server 2) with probability β_i (where $\alpha_i+\beta_i=1$) to retrieve that image. After the packet departs from the servers (both servers empty) and only then the next packet is allowed in.

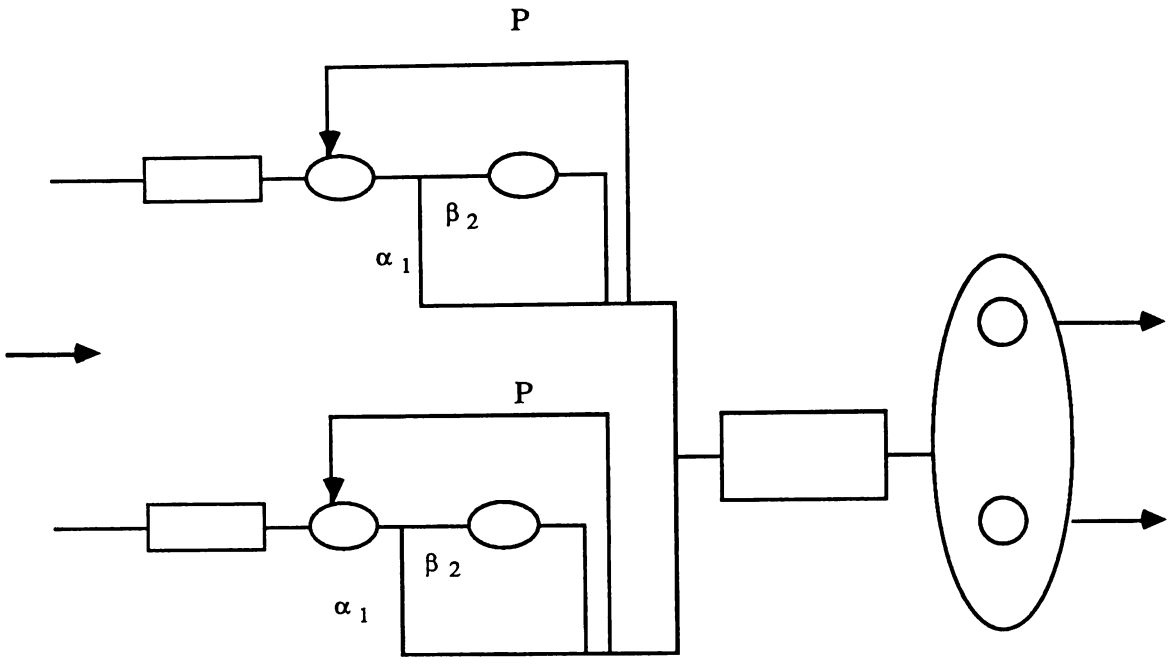

Figure 2.11. $E_2/Cox_2/1$ database queue with spawning and its communication channels.

We assume that the service time of both servers is exponentially distributed. This type of service mechanism is called Coxian-2. We have the same assumption with regard to the size of a "request packet" as in model 2, i.e. the spawning mechanism. This spawning mechanism is as described in section 2.3.

We also assume that request packets from picture viewing stations arrive according to a Poisson process.

With the scheduling of request packets as described in section 2.3, if we have r processes in the database (i.e. r queues), the inter-arrival intervals will have an Erlang-r distribution. Therefore each queue in the database will be an $E_r/Cox_2/1$ queueing system with spawning. We further assume that the two communication servers have exponentially distributed service times, because of that and the size of images the picture viewing stations are modeled as M/G/1 queues with bulk service.

CHAPTER 3

MODEL 1: E_r/M/ 1 DATABASE QUEUES AND M/G/1 IMAGE PROCESSOR QUEUE

3.1 - Model description

This model covers the case in which the medical exam requests are for one image only, and this image consists of a single block of data stored in the database. We assume that there are r database queues and 2 communication channels, see Figure 3.1.

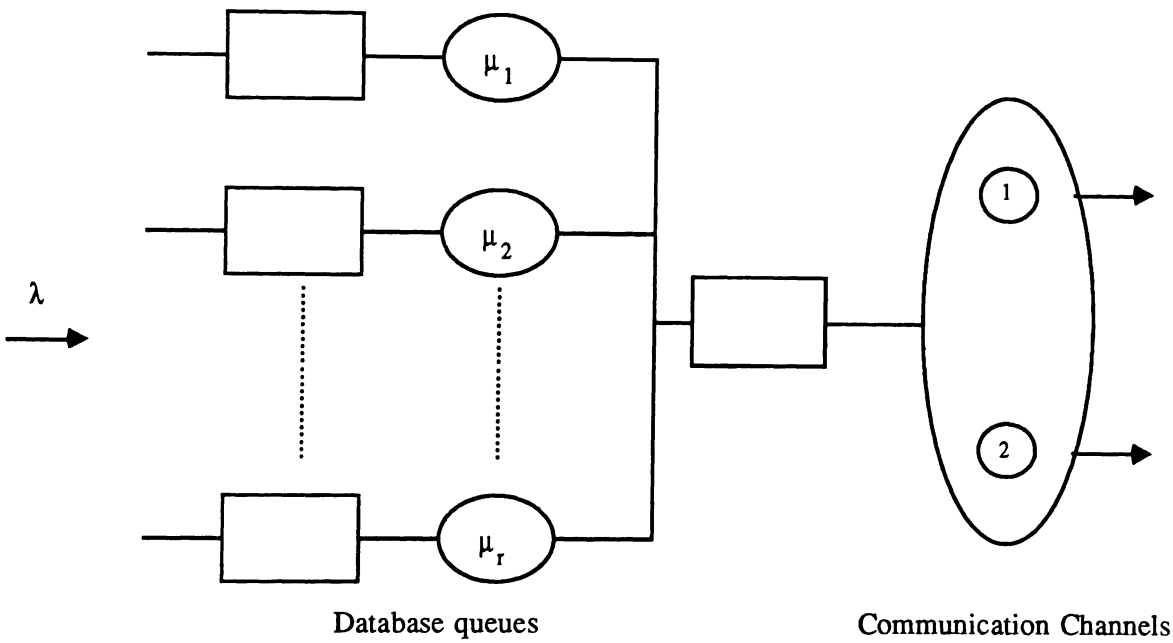

Figure 3.1. Queueing model of the database and the communication channels.

The assumptions for this model are given in section 2.6.1. Here we only add that the Poisson arrival process of the request packets has a rate λ. With the Poisson arrival process and the scheduling mechanism described in section 2.3, the database queues become G/M/1 queueing systems with inter-arrival time which has an Erlang-r distribution.

A number of results are available for G/M/1 queues. In the following section we present results for the distributions of number of packets and

waiting time in the database queues, for the case of an Erlang-r arrival process.

3.2-Analysis of the database queues

In this section the database queues are analyzed. We use the results for G/M/1 queues and apply them for the case of Erlang-r distributed inter-arrival intervals. We also find the distribution of inter-departure intervals for each queue in the database. These departure processes are superimposed (in section 3.4) to find the arrival process of the data packets to the communication channels. Throughout our analysis we use "pdf" for probability density function and "PDF" for probability distribution function.

3.2.1-Distribution of number of packets and average delay in the database queues

Here we concentrate on one of the queues in the database Figure 3.2, the results can be easily applied to the other queues by using the appropriate parameters.

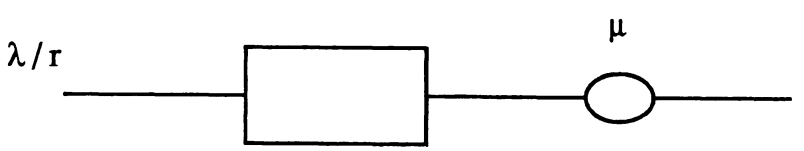

Figure 3.2. A single $E_r/M/1$ database queue.

We have the following parameters for this queue

μ - service rate

$\frac{\lambda}{r}$ - arrival rate

a(t)- probability density function (pdf) of inter_arrival time, is equal to $\frac{\lambda x(\lambda x)^{r-1} e^{-\lambda x}}{(r-1)!}$

$b(x)$ - pdf of service time, is equal to $\mu e^{-\mu x}$

$A^*(s)$ - Laplace transform of the density function of inter_arrival intervals is equal to $\left(\frac{\lambda}{s+\lambda}\right)^r$

$B^*(s)$ - Laplace transform of the density function of service time is equal to $\frac{\mu}{s+\mu}$

For this $E_r/M/1$ queue we can of course use existing results for G/M/1 queues to solve for the equilibrium distribution of number of packets in the system, P_k. From [27] we have

$$P_k = \rho(1-\sigma)\sigma^{k-1} \qquad k \geq 1 \qquad (3.1)$$

Where ρ is the utilization of the server, $\rho = \frac{\lambda}{r\mu}$, and σ should satisfy the following equation $\sigma = A^*(\mu-\mu\sigma)$, and $0 \leq \sigma < 1$. By substituting for σ and ρ , $\bar{N}$ the average number of request packets in a database queue can be evaluated from relation (3.1) as, $\bar{N} = \frac{\rho}{1-\sigma}$. For the distribution of the waiting time we have, from [27]

$$W(y) = 1 - \sigma e^{-\mu(1-\sigma)y} \qquad (3.2)$$

and by straightforward calculation the mean waiting time is $\bar{W} = \frac{\sigma}{\mu(1-\sigma)}$, and the mean delay, T_1, for a request packet in the database is $\bar{W} + \frac{1}{\mu}$.

3.2.2-Distribution of inter_departure intervals from the database queues

The departure process of G/G/1 and G/M/1 queues were extensively analyzed by Daley in [28]. He has shown that for G/M/1 queues the inter_departure intervals are correlated and he also finds the distribution of these intervals. Here we present the distribution of

inter_departure intervals for the case r=2, that is two database queues. Let the random variable D denote the inter_departure interval from the database queue in Figure 3.2. In general we have

$$D = V + B$$

where

V - random variable denoting the idle time of the server
B - random variable denoting the service time of the server

From the properties of convolution of two independent random variables [27], we have

$$D^*_{(s)} = V^*_{(s)} \; B^*_{(s)}$$

where $D^*_{(s)}$, $V^*_{(s)}$, and $B^*_{(s)}$ are the Laplace transforms of the density functions of random variables D, V, and B respectively. Daley in [28] has shown that

$$D^*_{(s)} = \frac{\mu}{s+\mu} \frac{\sigma s - \mu(1-\sigma) A^*_{(s)}}{s - \mu(1-\sigma)} \qquad (3.3)$$

Substituting for $A^*_{(s)}$, for the queue $E_r/M/1$ we have

$$D^*_{(s)} = \frac{\mu}{s+\mu} \frac{\sigma s^2 + [\mu\sigma(1-\sigma) + 2\lambda\sigma] s + \lambda^2}{(s+\lambda)^2}$$

Using partial fraction expansion, we get for $\lambda \neq \mu$

$$D^*_{(s)} = \frac{A_{11}}{s+\mu} + \frac{A_{21}}{(s+\lambda)^2} + \frac{A_{22}}{s+\lambda}$$

Where

$$A_{11} = (s+\mu) \, D^*_{(s)} \Big|_{s=-\mu}$$

$$A_{21} = (s+\lambda)^2 \, D^*_{(s)} \Big|_{s=-\lambda}$$

$$A_{22} = \frac{d(s+\lambda)^2 D^*_{(s)}}{ds}\Big|_{s=-\lambda}$$

From the Laplace transform of the density function of the inter-departure intervals given above, the density function, $d(x)$, can be found using the inverse of the Laplace transforms

$$d(x) = A_{11}e^{-\mu x} + A_{21}x\, e^{-\lambda x} + A_{22}e^{-\lambda x} \qquad (3.4)$$

As described in the queueing model of the image archive in chapter 2, as soon as a block of data is retrieved from the database, it is sent to the input buffer of the communication channels for transmission to the picture viewing station which requested it, see Figure 3.1. Because of that the arrival process to the queue representing the communication channels is created by merging the departure processes of the queues in the database. In our analysis, we assume that these departure processes are independent and we use the results from the superposition of independent processes to find the arrival process to the communication channels. The comparison between the analytical and the simulation results (in chapter 6) of the three queueing models of chapters 3, 4, and 5 indicate that this is a valid assumption and the results are very close.

In the next section we evaluate the distribution of the process formed by superimposing the departure processes, the analyses are due to Cox [29]. In section 3.4 we use this result to find the distribution of the inter-arrival time of the data packets to the communication channels.

3.3-Superposition of k independent processes

Here we present the density function of the process created by superimposing k independent processes [29]. We then apply this result to the parallel queues in the database to find the distribution of inter_arrival time to the queue representing the communication medium.

Suppose that we have k independent processes and a new process is formed by superimposing the k separate processes. Figure 3.3 shows an example with k=2.

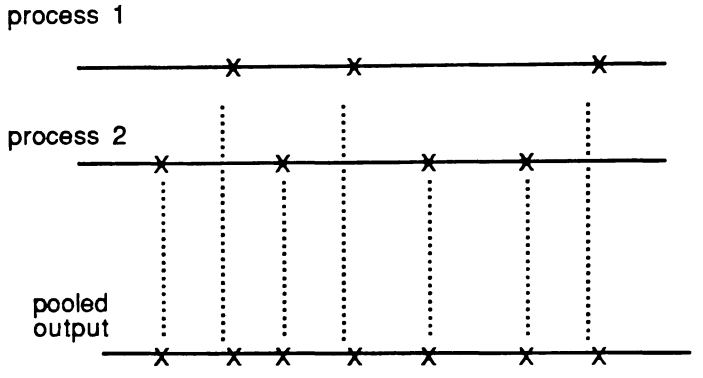

Figure 3.3. Superposition of two processes.

Let $f_i(x)$ denote the pdf of intervals between successive events in process i ($1 \leq i \leq k$) with mean m_i , and $F_i(x)$ the corresponding PDF . Let V_k denote the forward recurrence time of the pooled output as shown below.

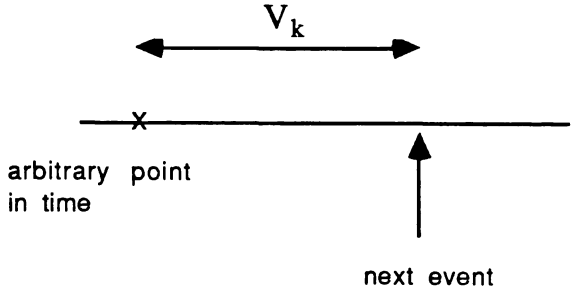

Denoting the forward recurrence time of process i by t_i we have

$$P[V_k \leq x] = P[\min(t_1,t_2,.....,t_k) \leq x] = 1 - P[\min(t_1,t_2,.....,t_k) > x]$$

and because of independence between the processes, we can write

$$P[V_k \leq x] = 1 - P[t_1>x]P[t_2>x].....P[t_k>x]$$

and using the formula for the distribution of the mean residual life [27], we arrive at

$$P[V_k \leq x] = 1 - \prod_{i=1}^{k} \int_{x}^{\infty} \frac{1 - F_{i(u)}}{m_i} du \qquad (3.5)$$

Denoting the pdf of V_k by $f_{v_k}(x)$, and the pdf of intervals in the pooled process by $a_k(x)$, we can write

$$f_{v_k}(x) = \sum_{i=1}^{k} \frac{1 - F_i(x)}{m_i} \prod_{\substack{j=1 \\ j \neq i}}^{k} \left[\int_{x}^{\infty} \frac{1 - F_j(u)}{m_j} du \right] \qquad (3.6)$$

and by using the residual life formula

$$f_{v_k}(x) = \frac{\int_{x}^{\infty} a_k(u)\, du}{n_k} \qquad (3.7)$$

where n_k is the mean of the intervals between successive events in the pooled output, $\frac{1}{n_k} = \sum_{i=1}^{k} \frac{1}{m_i}$.

Therefore from (3.6) and (3.7) we can write the pdf of intervals in the pooled process as

$$a_k(x) = - \frac{d}{dx} \left[n_k f_{v_k}(x) \right]$$

or

$$a_k(x) = \left(\frac{1}{\sum_{i=1}^{k} \frac{1}{m_i}} \right) \qquad (3.8)$$

$$\sum_{i=1}^{k} \left[\frac{f_i(x)}{m_i} \prod_{\substack{j=1 \\ j \neq i}}^{k} \int_x^{\infty} \frac{(1-F_j(u))}{m_j} du + \sum_{\substack{n=1 \\ n \neq i}}^{k} \left[\frac{(1-F_i(x))}{m_i} \frac{(1-F_n(x))}{m_n} \prod_{\substack{m=1 \\ m \neq i \\ m \neq n}}^{k} \int_x^{\infty} \frac{(1-F_m(u))}{m_m} du \right] \right]$$

for k=2 we have

$$a_2(x) = \left(\frac{1}{m_1+m_2} \right) \left(f_1(x) \int_x^{\infty} (1-F_2(u))\, du + \left(1-F_1(x)\right)\left(1-F_2(x)\right) \right.$$

$$\left. + f_2(x) \int_x^{\infty} (1-F_1(u))\, du + \left(1-F_1(x)\right)\left(1-F_2(x)\right) \right) \qquad (3.9)$$

It should be noted that, since the inter_departure intervals from the database queues are correlated (see section 3.2.2), in the pooled process which represents the arrival process to the communication channels the inter_arrival intervals are also correlated. In our analysis of the queueing system representing the communication channels we assume that these intervals are independently distributed. Our results from the simulation of the queueing systems indicate that this is a good assumption and our analytical and simulation results are very close.

3.4-Analysis of the communication channels

In this section, we first use the results of section 3.3 and apply it to the case of having two database queues to find the distribution of the inter-arrival time to the G/M/2 queue which represents the communication medium. We then find the delay in the G/M/2 queue for transmission of medical exams to the picture viewing stations.

3.4.1-Distribution of inter_arrival time to the communication channels

In our model we assume that the blocks retrieved from the database form a single queue, and as soon as a communication channel is available the first packet is taken from the head of the queue for transmission.

The inter_arrival time to the communication channels is a process formed by superimposing the departure processes from the database queues, see Figure 3.1. Here we assume, the database queues have output processes that are independent in order to be able to use the results in section 3.3 . To show the accuracy of this assumption we compare the analytical results with the results that we obtain from a simulation model of the system. From the results in the previous section for r=2, i.e. two database queues, $c_{2(x)}$ the pdf of inter_arrival time to the communication channels is given by

$$c_{2(x)} = \left(\frac{\lambda_1\lambda_2}{\lambda_1+\lambda_2}\right)$$

$$\left(d_{1(x)} \int_x^{\infty}(1-D_{2(u)})du + 2\left[1-D_{1(x)}\right]\left[1-D_{2(x)}\right] + d_{2(x)} \int_x^{\infty}(1-D_{1(u)})du \right) \quad (3.10)$$

Where λ_1 and λ_2 are the arrival rates to queues 1 and 2 respectively, i.e. $\lambda_1=\lambda_2=\lambda/2$. From (3.4), for the queues in the database we have

$$d_{i(x)} = A_{11}^{(i)} e^{-\mu_i x} + A_{21}^{(i)} x e^{-\lambda x} + A_{22}^{(i)} e^{-\lambda x} \quad (3.11)$$

The superscript and subscript 'i' denote the queue number, i.e. 'i' is either 1 or 2 in this case. The corresponding PDF of the inter_departure time is

$$D_{i(x)} = 1 - B_{11}^{(i)} e^{-\mu_i x} - B_{21}^{(i)} x e^{-\lambda x} - B_{22}^{(i)} e^{-\lambda x} \quad (3.12)$$

where $B_{11}^{(i)} = \frac{A_{11}^{(i)}}{\mu_i}$, $B_{21}^{(i)} = \frac{A_{21}^{(i)}}{\lambda}$, $B_{22}^{(i)} = \frac{A_{21}^{(i)}}{\lambda^2} + \frac{A_{22}^{(i)}}{\lambda}$ and

$$\int_{x}^{\infty}(1-D_{i(u)})du = C_{11}^{(i)} e^{-\mu_i x} + C_{21}^{(i)} x\, e^{-\lambda x} + C_{22}^{(i)} e^{-\lambda x} \qquad (3.13)$$

where $C_{11}^{(i)} = \frac{B_{11}^{(i)}}{\mu_i}$, $C_{21}^{(i)} = \frac{B_{21}^{(i)}}{\lambda}$, $C_{22}^{(i)} = \frac{B_{21}^{(i)}}{\lambda^2} + \frac{B_{22}^{(i)}}{\lambda}$. Substituting the values from equations (3.11), (3.12), and (3.13) in (3.10), and taking the Laplace transform of $c_{2(x)}$, we have

$$C_{2(s)}^{*} = \left(\frac{\lambda_1\lambda_2}{\lambda_1+\lambda_2}\right)\Bigg(\Bigg[C_{11}^{(2)} D_{1(s+\mu_2)}^{*} - C_{21}^{(2)}\frac{d\, D_{1(s+\lambda)}^{*}}{d\,s} + C_{22}^{(2)} D_{1(s+\lambda)}^{*} +$$

$$C_{11}^{(1)} D_{2\,(s+\mu_1)}^{*} - C_{21}^{(1)}\frac{d\, D_{2(s+\lambda)}^{*}}{d\,s} + C_{22}^{(1)} D_{2(s+\lambda)}^{*}\Bigg] +$$

$$2\Bigg[\frac{B_{11}^{(1)} B_{21}^{(2)}}{(s+\mu_1+\mu_2)} + \frac{B_{11}^{(1)} B_{21}^{(2)}}{(s+\mu_1+\lambda)^2} + \frac{B_{11}^{(1)} B_{22}^{(2)}}{(s+\mu_1+\lambda)} +$$

$$\frac{B_{11}^{(2)} B_{21}^{(1)}}{(s+\mu_2+\lambda)^2} + \frac{2B_{21}^{(1)} B_{21}^{(2)}}{(s+2\lambda)^3} + \frac{B_{21}^{(1)} B_{22}^{(2)}}{(s+2\lambda)^2} +$$

$$\frac{B_{22}^{(1)} B_{11}^{(2)}}{(s+\mu_2+\lambda)} + \frac{B_{22}^{(1)} B_{21}^{(2)}}{(s+2\lambda)^2} + \frac{B_{22}^{(1)} B_{22}^{(2)}}{(s+2\lambda)}\Bigg]\Bigg) \qquad (3.14)$$

where $D_{i}^{*}(s) = \int_{x=0}^{\infty} e^{-sx}\, d_{i(x)}\, dx$. Substituting the values for $D_{i}^{*}(s)$ and $\frac{d\, D_{i}^{*}(s)}{d\,s}$, and using the inverse of the Laplace transforms the pdf of inter_arrival time to the communication channels can be found.

3.4.2-Average number of packets and delay in the communication channels

In this section we evaluate the delay and the average number of packets in the system for the case where we have 2 communication channels

each with service rate μ , i.e the G/M/2 queue. The distribution of number of packets in the system P_k is given by

$$P_k=\rho r_{k-1} \qquad k=2,3,4,..... \tag{3.15}$$

from [27], and $P_1=\frac{(\lambda_1+\lambda_2)r_0}{\mu}$, where r_k = P[an arrival finds k packets in the system] , $r_k=K\sigma^k$ for $k\geq 1$, $r_0=\frac{K\sigma(1-2A^*_{(\mu)})}{(1-2\sigma)A^*_{(\mu)}}$, and $\rho=(\lambda_1+\lambda_2)/2\mu$. For the G/M/2 queue from [27]

$$K= A^*_{(\mu)}\frac{(1-\sigma)(1-2\sigma)}{\sigma[1-\sigma-A^*_{(\mu)}]} \tag{3.16}$$

Where $A^*_{(s)}$ denotes the Laplace transform of the inter_arrival time. From equation (3.15) the average number of packets in the system, $\bar{N}=\sum_{k=0}^{\infty} kP_k$, is

$$\bar{N} = P_1 + \rho K\sigma \frac{2-\sigma}{(1-\sigma)^2} \tag{3.17}$$

The distribution of waiting time for the G/M/2 queue [27] is given by

$$W_{(y)}= 1 - \frac{\sigma(1-2\sigma)A^*_{(\mu)}}{1-\sigma-A^*_{(\mu)}} e^{-2\mu(1-\sigma)y} \tag{3.18}$$

and the corresponding mean waiting time is

$$\bar{W} = \frac{K\sigma^2}{2\mu(1-\sigma)^2} \tag{3.19}$$

and the average delay in transmitting an exam through the communication channels, T_2 is $\bar{W}+\frac{1}{\mu}$. By using the Laplace transform of

the inter_arrival time from section 3.4.1 the delay in our model (two database queues and two communication channels) can be found.

3.5-Analysis of the picture viewing station

As mentioned in chapter 2, for this model we use an M/G/1 queueing system to represent the image processor in the picture viewing station. A number of results are available for M/G/1 queues, and we use them in the next section to find the average delay in displaying an image in the picture viewing station.

3.5.1-Average number of packets in the picture viewing station

Since the amount of processing required to display an image varies between different type of images, we assume a service mechanism as shown in Figure 3.4. Here we are assuming that the image processor is designed to display two types of image, where each image type requires a different amount of processing.

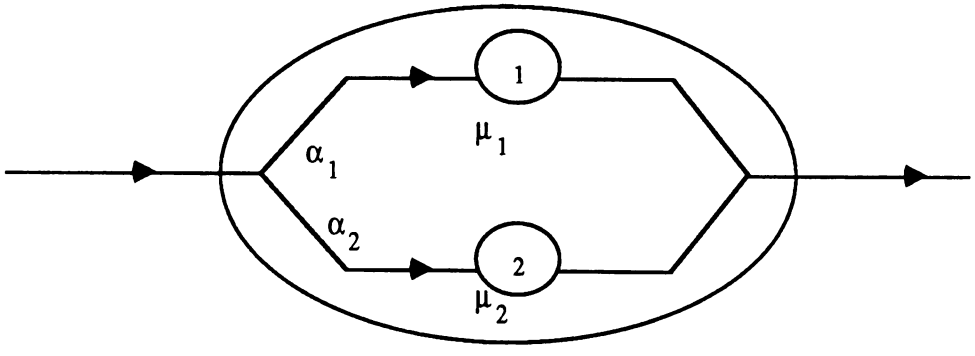

Figure 3.4. Service mechanism of the image processor.
A two-stage parallel server.

Upon entry, a data packet is provided service at a rate of μ_1, with probability α_1, or at the rate of μ_2, with probability α_2 , where $\alpha_1+\alpha_2 = 1$. It should be obvious that this analysis can be extended to any number of image types. It is clear from the above description that the service time pdf will be given by

$$b(x)= \alpha_1\mu_1 e^{-\mu_1 x} + \alpha_2\mu_2 e^{-\mu_2 x}$$

and for the Laplace transform we have

$$B^*(s)= \alpha_1 \frac{\mu_1}{s+\mu_1} + \alpha_2 \frac{\mu_2}{s+\mu_2}$$

The average number of packets in an M/G/1 queueing system is given by the well known Pollaczek-Khinchin (P-K) mean-value formula [27]

$$\bar{q} = \rho + \frac{\rho^2[\,1+C_b^2]}{2(1-\rho)} \qquad (3.20)$$

where $\rho = \lambda \left[\frac{\alpha_1}{\mu_1} + \frac{\alpha_2}{\mu_2} \right]$, λ is the arrival rate, and C_b^2 is the squared coefficient of variation for service time.

3.5.2-Average delay in the picture viewing station

The distribution of waiting time in a M/G/1 queue is given in [27] as

$$W^*(s)= \frac{1-\rho}{1-\rho\left(\frac{1-B^*(s)}{s\bar{x}}\right)} \qquad (3.21)$$

where $\bar{x} = -B^{*(1)}(0)$. The average delay in displaying an image, T_3 is $\bar{W} + \frac{\alpha_1}{\mu_1} + \frac{\alpha_2}{\mu_2}$, where $\bar{W} = -W^{*(1)}(0)$.

The results obtained in this chapter are used in chapter 6 to draw the performance curves for model 1.

CHAPTER 4

MODEL 2: $E_r/M/1$ DATABASE QUEUES WITH SPAWNING AND M/G/1 IMAGE PROCESSOR QUEUE WITH BULK SERVICE

4.1-Model description

This model covers the more general case where exam requests are for a number of images which in turn consists of a number of blocks of data stored in the database. As described in section 2.3, for this case we have a spawning mechanism which generates sibling requests for more data until all blocks of data in a medical exam are removed. We assume that there are r database processes and 2 communication channels in the system. This model is shown in Figure 4.1.

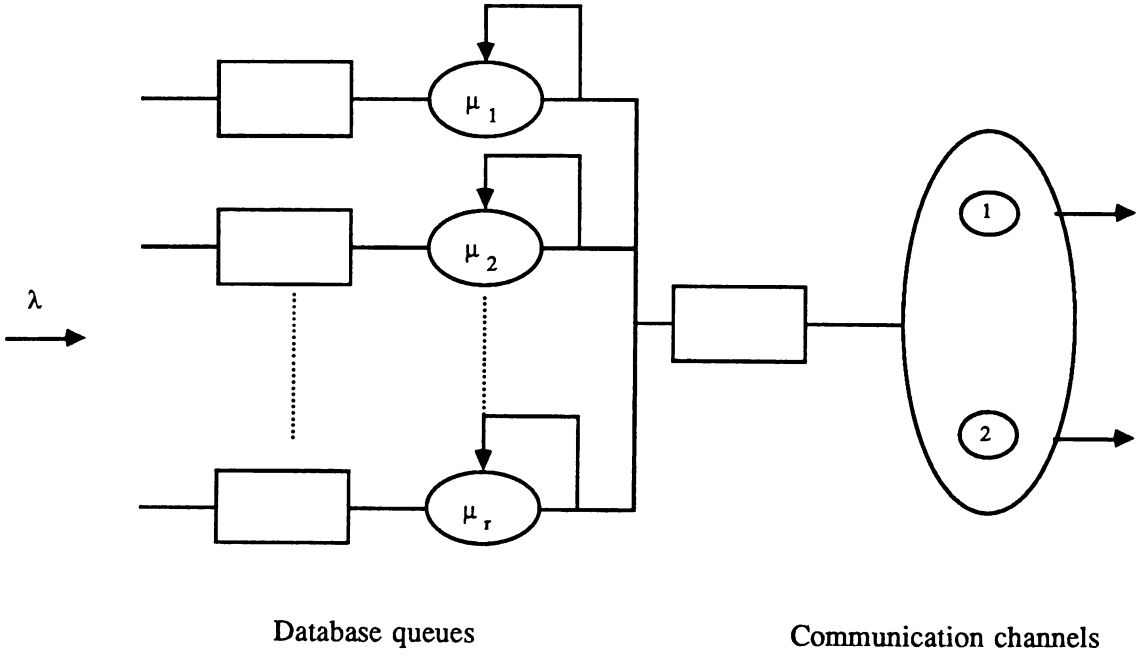

Figure 4.1. Queueing model of the database and the communication channels.

The assumptions for this model are given in section 2.6.2. Here we add that, we assume the request packets from picture viewing stations arrive at a rate of λ.

Queues with feedback have been analyzed for a number of years, Takacs in [30] studied the M/G/1 queue with feedback, Burke [31] has shown that for the M/M/1 queue with feedback as far as the distribution of number of packets in the queue is concerned, the queue behaves as an M/M/1, even though the composite inter_arrival time is not exponentially distributed. Disney et al in [32] studied the processes in the M/G/1 queue with feedback, they studied the arrival, input, output, departure, and feedback processes in excruciating details. They point out that the feedback process is quite difficult to work with and they show that the feedback process is either not independent of the arrival process or not a Poisson process. Melamed in [33] shows that the feedback process is not Poisson except for a very trivial case. Disney et al [32] also show that the departure process from the M/G/1 with feedback is a renewal process if and only if the service time is exponentially distributed, and in that case the departure process is Poisson.

In the following two sections we analyze the database queue $E_r/M/1$ with spawning through the method of stages used by Kleinrock in [27].

In section 4.2.3 we study the departure process of $E_r/M/1$ with spawning using the method of stages. In section 4.2.4 we present numerical results and in section 4.3 we analyze the communication channels. The analysis of the picture viewing station is presented in section 4.4 .

4.2-Analysis of the database queues

In this section, the database queueing system is analyzed in details. We start by finding the distribution of number of packets in the system, we then proceed to find the distribution of the waiting time.

In section 4.2.3 we find the distribution of inter-departure intervals, and present the numerical results in section 4.2.4.

4.2.1-Distribution of number of packets in the database queues

Here we again concentrate on a single queue in the database, see Figure 4.2. However the analysis can be repeated for any other queue by using the appropriate parameters. We still assume that there are r queues in the database and we have 2 communication channels.

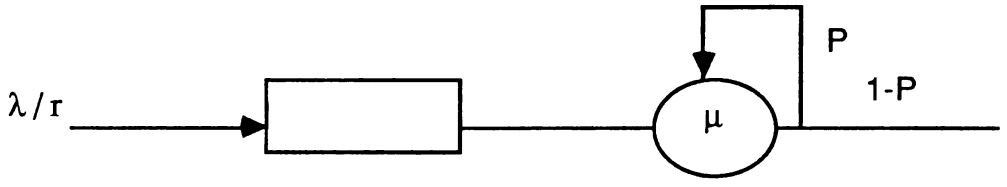

Figure 4.2. A single $E_r/M/1$ database queue with spawning.

For this queue we use the following notations:

μ - Service rate

$\frac{\lambda}{r}$ - Arrival rate

j - The number of arrival stages in the system

k - The number of packets in the system

P_j - P[number of arrival stages is j]

p_k - P[K packets in the system]

To model the routing of request packets in the database we use the arrival facility shown in Figure 4.3.

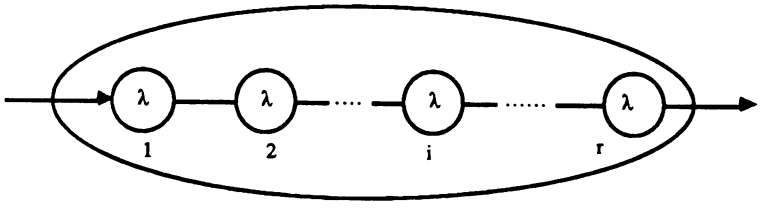

Figure 4.3. Arrival facility.

A request packet enters the arrival facility from left, after going through r exponential servers, it exits from right and enters the queue. After the packet is departed from the facility the next packet is allowed in. The total average time that the packet spends in the arrival facility is r/λ , and the arrival rate to each queue is λ/r . The Laplace transform of the total time spent in the arrival facility is $(\lambda/s+\lambda)^r$, and in the time domain the density function of the total time spent in the service facility is $\lambda x^{r-1} e^{-\lambda x}/(r-1)!$, which is the Erlang-r distribution or gamma distribution. This is exactly what the scheduler does in effect by routing the request packets to the database queues as described in section 2.3. Therefore this arrival facility provides a mechanism for feeding request packets to the archive queues at a rate of λ/r, with the inter-arrival intervals which have an Erlang-r distribution.

With the above model, an appropriate state description for the $E_r/M/1$ with spawning is to specify the number of arrival stages in the system [25]. We consider that a request packet which has arrived (exogenous or feedback) in the system but not yet departed contributes r stages of "arrival" and we also take into account the number of stages that an arriving packet has completed in the "arrival facility". Thus the total number of arrival stages in the system, when we find k request packets in the system and our arriving packet is in the ith stage of arrival is given by

$$j = kr + i - 1 \qquad \text{where } 1 \le i < r$$

Clearly p_k and P_j are related through

$$p_k = \sum_{j=rk}^{r(k+1)-1} P_j \qquad (4.1)$$

The z-transform of P_j is defined as

$$P(z) = \sum_{j=0}^{\infty} P_j \, z^j$$

We may represent the state transition-rate diagram for the arrival stages in the system as shown in Figure 4.4 [27].

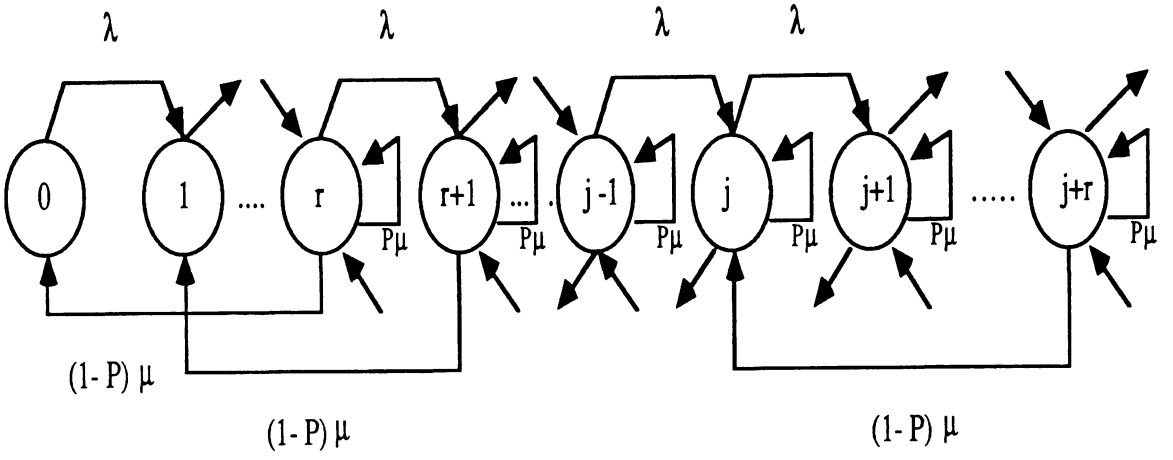

Figure 4.4. State transition diagram for $E_r/M/1$ with spawning.

Writing the equilibrium equations and applying the transform methods it can be shown [27] that the z-transform of P_j is

$$P_{(z)}= \frac{(1-z^r)\sum_{j=0}^{r-1} P_j\, z^j}{r\rho z^{r+1} - (1+r\rho)z^r + 1} \qquad \text{where } \rho = \frac{\lambda}{r\,(1-P)\mu} \qquad (4.2)$$

The denominator has r+1 roots of which z=1 is one, it can be shown that of the remaining r roots, r-1 them lie in the range $|z| < 1$ and the last, which we denote by z_0, is such that $|z_0| > 1$ [27] . Since $P_{(z)}$ is bounded in the range $|z| < 1$, then the numerator must also have the same r-1 roots in the range $|z| < 1$ as the denominator.

The numerator consists of two factors, the first of the form $(1- z^r)$ all of whose roots have absolute value equal to unity, and the second in the form of a summation. Therefore, the "compensating" roots in the numerator must come from the summation (it is a polynomial of degree

r-1 and therefore has exactly r-1 roots). From the above observations we can write

$$\frac{r\rho z^{r+1} - (1+r\rho)z^r + 1}{(1-z)(1- z/z_0)} = K \sum_{j=0}^{r-1} P_j \, z^j \qquad (4.3)$$

Where K is a constant. Since $P_{(1)}=1$ we find that

$$K = \frac{r}{(1- 1/z_0)}$$

and so we have

$$P_{(z)} = \frac{(1- z^r)(1-1/z_0)}{r(1- z)(1- z/z_0)} \qquad (4.4)$$

As shown in [27] we can evaluate P_j from above as

$$P_j = \begin{cases} \frac{1}{r}(1-z_0^{-j-1}) & 0 \le j < r \\ \rho(z_0 - 1)z_0^{r-j-1} & j \ge r \end{cases} \qquad (4.5)$$

and p_k the probability of the number of packets in the system can be evaluated from relation (4.1) as

$$p_k = \begin{cases} 1-\rho & k = 0 \\ \rho(z_0^r - 1)z_0^{-rk} & k > 0 \end{cases} \qquad (4.6)$$

4.2.2-Distribution of waiting time in the database queues

Our model here is as shown in section 4.2.1, see Figure 4.2. Let r_k denote the probability that a request packet finds k packets in the queue upon

arrival, $r_{k-1} = \frac{1}{\rho} P_k$ for $k \geq 1$ [27], and let $W^*(s)$ be the Laplace transform of the waiting time in the database. First we find

$$W^*(s \mid k) = E[e^{-sw} \mid \text{an arrival finds k in the system}]$$

Introducing the conditional transform, we have

$$W^*(s \mid k) = \left(\sum_{i=1}^{\infty} P^{i-1}(1-P) \left(\frac{\mu}{s+\mu} \right)^i \right)^k = \left(\frac{(1-P)\mu}{s+(1-P)\mu} \right)^k \quad (4.7)$$

Note that as mentioned in the description of the queueing model of the image archive (section 2.3), in our model the spawned packet is inserted at the head of the queue since the blocks comprising an image are retrieved consecutively. Now for $W^*(s)$ we have

$$W^*(s) = r_0 E[e^{-s\,0}] + \sum_{k=1}^{\infty} r_k \, W^*(s \mid k)$$

where $r_k = (z_0^r - 1) z_0^{-r(k+1)}$, and we get

$$W^*(s) = \left(1 - \frac{1}{z_0^r}\right) + \left(1 - \frac{1}{z_0^r}\right) \left(\frac{(1-P)\mu}{z_0^r \left(s + \mu(1-P)\left(1 - \frac{1}{z_0^r}\right) \right)} \right) \quad (4.8)$$

Therefore the pdf of waiting time is

$$w(y) = \left(1 - \frac{1}{z_0^r}\right) u_0(y) + \left(1 - \frac{1}{z_0^r}\right) \frac{(1-P)\mu}{z_0^r} \exp\left(-\mu(1-P)\left(1 - \frac{1}{z_0^r}\right) y\right) \quad (4.9)$$

where $u_0(y)$ is the impulse function, using Kleinrock's notation. The corresponding PDF of the waiting time is

$$W(y) = 1 - \frac{1}{z_0^r} \exp(-\mu(1-P)(1 - \frac{1}{z_0^r})y) \qquad (4.10)$$

and the mean waiting time $\bar{W} = \frac{1}{\mu(1-P)(z_0^r-1)}$. The average delay, T_1 is $\bar{W} + \frac{1}{\mu}$.

4.2.3-Distribution of inter_departure intervals from the database queues

Let d_j denote the probability that a departing packet leaves j arrival stages behind in the system, and the random variable 'd' the inter_departure time from the queue in Figure 4.2. The d_j can be found as

$$d_j = \begin{cases} \dfrac{\mu(1-P)P_{j+r} + (\mu P)P_j}{\mu \sum_{k=r}^{\infty} P_k} & j \geq r \\ \dfrac{\mu(1-P)P_{j+r}}{\mu \sum_{k=r}^{\infty} P_k} & 0 \leq j < r \end{cases} \qquad (4.11)$$

The Laplace transform of inter-departure time, $D^*(s)$, can be expressed as

$$D^*(s) = E\left[e^{-sd} \mid j \geq r\right]P[j \geq r] + E\left[e^{-sd} \mid j < r\right]P[0 \leq j < r]$$

Therefore we have

$$D^*(s) = \sum_{j=r}^{\infty} \frac{\mu}{s+\mu} d_j + \sum_{j=0}^{r-1} \frac{\mu}{s+\mu} \left(\frac{\lambda}{s+\lambda}\right)^{r-j} d_j \qquad (4.12)$$

Substituting for P_j in (4.11) we get

$$d_j = \begin{cases} (1-P)(z_0-1)z_0^{-j-1} + P(z_0-1)z_0^{r-j-1} & j \geq r \\ \dfrac{(1-P)(z_0-1)}{z_0^{j+1}} & 0 \leq j < r \end{cases} \qquad (4.13)$$

We also find that $\sum_{j=r}^{\infty} d_j = \dfrac{1-P}{z_0^r} + P$.

The denominator of (4.2) must be zero for $z=z_0$, which gives us $\dfrac{1}{z_0^r} = 1 - r\rho(z_0-1)$.

Substituting the values in (4.12) we can write

$$D^*(s) = \left(\frac{\mu}{s+\mu}\right)\left(1-r\rho(1-P)(z_0-1)\right) + \left(\frac{\mu}{s+\mu}\right)\left(\frac{\lambda}{s+\lambda}\right)^r (1-P)\frac{(z_0-1)}{z_0}\sum_{j=0}^{r-1}\left(\frac{s+\lambda}{\lambda z_0}\right)^j$$

Using the inverse of the Laplace transforms we can evaluate the density function of inter_departure time. In the next section numerical results are given for the case r=2, i.e. two database queues.

4.2.4-Numerical results

For r=2 from (4.2) we have $2\rho z^3 - (1+2\rho)z^2+1=0$ which after factorizing 1-z gives $z_0 = \dfrac{1+\sqrt{1+8\rho}}{4\rho}$ and clearly $|z_0| > 1$. As an example for P=0.5 , $\lambda=1$, $\mu=2$, z_0 is 1.62 . Substituting the above values in (4.13) we get d_0= 0.19 and d_1=0.12. From equation (4.12),

$$D^*(s) = \frac{\mu}{s+\mu}\sum_{j=2}^{\infty} d_j + \left(\frac{\lambda}{s+\lambda}\right)^2\frac{\mu}{s+\mu}d_0 + \left(\frac{\lambda}{s+\lambda}\right)\frac{\mu}{s+\mu}d_1 \qquad (4.14)$$

using partial fraction expansion and inverting the Laplace transform, the density function $d(x)$ of inter-departure interval is given by

$$d(x)= a\, e^{-\mu x}+ b\, x\, e^{-\lambda x} + c\, e^{-\lambda x} \qquad (4.15)$$

Where a=1.53 , b= 0.38 , and c= - 0.15 , for this case.

4.3-Analysis of the communication channels

Our analysis here is for the case of having two database queues. We first use the results in the previous section and the results from section 3.3 to find the inter-arrival time to the communication channels which is represented by a G/M/2 queueing system. We then find the delay in transmitting the medical exams to the picture viewing stations.

4.3.1-Distribution of inter_arrival time to the communication channels

As in model 1, the inter_arrival time to the communication channels is a process formed by superimposing the departure processes from the parallel queues in the database. From the results in section 3.3 and the independence assumption (see section 3.4.1), for r=2 $c_{2(x)}$ the pdf of inter_arrival time to the communication channel is

$$c_{2(x)} = \left(\frac{\lambda_1\lambda_2}{\lambda_1+\lambda_2}\right)\left(d_{1(x)} \int_x^\infty (1 - D_{2(u)})du \; + 2\left[1 - D_{1(x)}\right]\left[1-D_{2(x)}\right] + d_{2(x)} \int_x^\infty (1 - D_{1(u)})du \right) \qquad (4.16)$$

Where λ_1 and λ_2 are the total arrival rates, exogenous and spawned, to queues one and two respectively, $\lambda_1 = \lambda_2 = \lambda/2(1-P)$. From equation (4.12) , the pdf of inter_departure time for queue i is

$$d_{i(x)} = A_{11}^{(i)} e^{-\mu_i x} + A_{21}^{(i)} x\, e^{-\lambda x} + A_{22}^{(i)} e^{-\lambda x} \qquad (4.17)$$

where

$$A_{11}^{(i)} = \frac{\lambda^2 \mu_i d_0^{(i)}}{(-\mu_i+\lambda)^2} + \frac{\lambda \mu_i d_1^{(i)}}{(-\mu_i+\lambda)} + \mu \sum_{j=2}^{\infty} d_j$$

$$A_{21}^{(i)} = \frac{\lambda^2 \mu_i d_0^{(i)}}{(-\lambda+\mu_i)}$$

$$A_{22}^{(i)} = \frac{-\lambda^2 \mu_i d_0^{(i)}}{(-\lambda+\mu_i)^2} + \frac{\lambda \mu_i d_1^{(i)}}{(-\lambda+\mu_i)}$$

and the corresponding PDF is given by

$$D_{i(x)} = 1 - B_{11}^{(i)} e^{-\mu_i x} - B_{21}^{(i)} x e^{-\lambda x} - B_{22}^{(i)} e^{-\lambda x} \qquad (4.18)$$

where

$$B_{11}^{(i)} = \frac{A_{11}^{(i)}}{\mu_i}, \; B_{21}^{(i)} = \frac{A_{21}^{(i)}}{\lambda}, \; B_{22}^{(i)} = \frac{A_{21}^{(i)}}{\lambda^2} + \frac{A_{22}^{(i)}}{\lambda}$$

and

$$\int_x^{\infty} (1-D_{i(u)}) du = C_{11}^{(i)} e^{-\mu_i x} + C_{21}^{(i)} x e^{-\lambda x} + C_{22}^{(i)} e^{-\lambda x} \qquad (4.19)$$

where $C_{11}^{(i)} = \frac{B_{11}^{(i)}}{\mu_i}$, $C_{21}^{(i)} = \frac{B_{21}^{(i)}}{\lambda}$, $C_{22}^{(i)} = \frac{B_{21}^{(i)}}{\lambda^2} + \frac{B_{22}^{(i)}}{\lambda}$. Substituting the values from equations (4.12), (4.13), and (4.14) in (4.11), and taking the Laplace transform of $c_{2(x)}$, we have

$$C_{2(s)}^{*} = \left(\frac{\lambda_1\lambda_2}{\lambda_1+\lambda_2}\right)\Bigg(\Bigg[C_{11}^{(2)} D_{1(s+\mu_2)}^{*} - C_{21}^{(2)} \frac{d\, D_{1(s+\lambda)}^{*}}{d\,s} + C_{22}^{(2)} D_{1(s+\lambda)}^{*} + C_{11}^{(1)} D_{2(s+\mu_1)}^{*} - C_{21}^{(1)} \frac{d\, D_{2(s+\lambda)}^{*}}{d\,s} + C_{22}^{(1)} D_{2(s+\lambda)}^{*} \Bigg] +$$

$$2\Bigg[\frac{B_{11}^{(1)} B_{11}^{(2)}}{(s+\mu_1+\mu_2)} + \frac{B_{11}^{(1)} B_{21}^{(2)}}{(s+\mu_1+\lambda)^2} + \frac{B_{11}^{(1)} B_{22}^{(2)}}{(s+\mu_1+\lambda)} +$$

$$\frac{B_{11}^{(2)} B_{21}^{(1)}}{(s+\mu_2+\lambda)^2} + \frac{2B_{21}^{(1)} B_{21}^{(2)}}{(s+2\lambda)^3} + \frac{B_{21}^{(1)} B_{22}^{(2)}}{(s+2\lambda)^2} +$$

$$\frac{B_{22}^{(1)} B_{11}^{(2)}}{(s+\mu_2+\lambda)} + \frac{B_{22}^{(1)} B_{21}^{(2)}}{(s+2\lambda)^2} + \frac{B_{22}^{(1)} B_{22}^{(2)}}{(s+2\lambda)} \Bigg] \Bigg) \qquad (4.20)$$

where $D_i^{*}(s) = \int_{x=0}^{\infty} e^{-sx}\, d_{i(x)}\, dx$ and i=1 or 2. Substituting the values for $D_i^{*}(s)$ and $\frac{d\, D_i^{*}(s)}{d\,s}$, and using the inverse of the Laplace transforms the pdf of inter_arrival time to the communication channels can be found.

4.3.2-Average number of packets and delay in the communication channels

Using results obtained in section 3.4.2 and the Laplace transform of the inter_arrival time to the communication channels from section 4.3.1 , the average number of packets in the system and the average delay in transmitting an image, T_2, through the communication channels in this model (two database queues and two communication channels) can be found easily. We do not repeat the analysis here, since it is exactly the same as in section 3.4.2 .

4.4-Analysis of the picture viewing station

As mentioned in chapter 2, we model the image processor in the picture viewing station as a M/G/1 queuing system with bulk service. In section 4.4.1 we first find the z-transform of number of packets in the system, then we solve it for the case of a 2-stage parallel server. In section 4.4.2 we find the average delay in the picture viewing station.

4.4.1-Distribution of number of packets in the image processor

In [34] Baily used the imbedded Markov chains generated by the length of queue, q , at the epoches just before service is due to take place, to solve for the z-transform of the probability of number of packets in the system, π_j .

In his analysis, Baily assumes a constant bulk size of m, but as mentioned in chapter 2 our assumption is that an image consists of a random number of SIFs, i.e. a random bulk size. In the analysis here, we assume that m, is the average size of an image ($\bar{n}$ in chapter 2).

Here we first present Bailey's result and then find π_j for a 2-stage parallel server. We assume that when the server becomes free he will accept a "bulk" of exactly m packets (m is the average image size in number of packets) from the queue if they are available, or if not will accept less than m if any are available.

From section 3.5.1, for the density function of a two stage parallel server and its Laplace transform we have

$$b(x)= \alpha_1\mu_1 e^{-\mu_1 x} + \alpha_2\mu_2 e^{-\mu_2 x}$$

$$B^*(s)= \alpha_1 \frac{\mu_1}{s+\mu_1} + \alpha_2 \frac{\mu_2}{s+\mu_2} \qquad (4.21)$$

Let β_k = P[k arrivals during a service interval] and $V(z)=\sum_{k=0}^{\infty} \beta_k z^k$. It is well known that for any interval $V(z)=B^*(\lambda-\lambda z)$ [27], where λ is the arrival rate. Baily has shown that for the z-transform of π_j , $\Pi(z)$, the following relation holds

$$\Pi(z)=\frac{\sum_{j=0}^{m-1} \pi_j (z^m - z^j)}{z^m/V(z) - 1} \qquad (4.22)$$

where the m unknowns π_j's are determined by considering the roots of the numerator and the denominator within the unit circle. We now solve the above equation for the distribution given in 4.21, using the Laplace transform of the service time and we have

$$V(z)=\frac{\lambda(1-z)(\alpha_1\mu_1 + \alpha_2\mu_2) + \mu_1\mu_2}{(\lambda(1-z) + \mu_1)(\lambda(1-z) + \mu_2)}$$

Substituting for $V(z)$ in equation (4.22) we get

$$\Pi(z)=\frac{\left[\lambda(1-z)(\alpha_1\mu_1 + \alpha_2\mu_2) + \mu_1\mu_2\right] \sum_{j=0}^{m-1} \pi_j (z^m - z^j)}{A(z)} \qquad (4.23)$$

where

$$A(z)=\lambda^2 z^{m+2} - (2\lambda+\mu_1+\mu_2)\lambda z^{m+1} + \left[\lambda(\lambda+\mu_1+\mu_2) + \mu_1\mu_2\right]z^m + \lambda(\mu_1\alpha_1+\mu_2\alpha_2)z - \lambda(\mu_1\alpha_1+\mu_2\alpha_2) - \mu_1\mu_2$$

Now $A(z)$ is a polynomial of degree m+2, therefore it has m+2 roots. Using Rouche's theorem (see section 5.2.1), it can easily be shown that of these roots, m of them are within the unit circle (one is such that $|z|=1$), and the other two roots z_0 and z_1 are such that $|z_0| >1$, $|z_1| > 1$. Since $\Pi(z)$ should be

bounded for $|z| \leq 1$, then the summation in the numerator of (4.23) must have the same m roots in $|z| \leq 1$ as the denominator. These observations lead us to write

$$\frac{A(z)}{(z-z_0)(z-z_1)} = K\sum_{j=0}^{m-1} \pi_j \, (z^m - z^j)$$

where K is a constant to be evaluated. Since $\Pi(1)=1$ we can write

$$K = \frac{\mu_1\mu_2}{(1-z_0)(1-z_1)}$$

Substituting for the summation in equation (4.23) we get

$$\Pi(z) = \frac{\left[\lambda(1-z)(\alpha_1\mu_1 + \alpha_2\mu_2) + \mu_1\mu_2\right]}{K(z-z_0)(z-z_1)} \qquad (4.24)$$

using partial fractions expansion we can rewrite equation (4.24) as

$$\Pi(z) = \frac{-1}{K}\left[\frac{A_1/z_0}{1 - z/z_0} + \frac{A_2/z_1}{1 - z/z_1}\right]$$

where

$$A_1 = \frac{\left[\lambda(1-z_0)(\alpha_1\mu_1 + \alpha_2\mu_2) + \mu_1\mu_2\right]}{(z_0-z_1)}$$

$$A2 = \frac{\left[\lambda(1-z_1)(\alpha_1\mu_1 + \alpha_2\mu_2) + \mu_1\mu_2\right]}{(z_1-z_0)}$$

Using the inverse of the Laplace transform we have

$$\pi_i = \frac{-1}{K}\left[\frac{A_1}{z_0}\left(\frac{1}{z_0}\right)^i + \frac{A_2}{z_1}\left(\frac{1}{z_1}\right)^i\right] \qquad (4.25)$$

and the mean number of packets, $\bar{N}$, in the system is

$$\bar{N} = \frac{-1}{K}\left(\frac{A_1}{z_0^2} \frac{1}{\left(1 - \frac{1}{z_0}\right)^2} + \frac{A_2}{z_1^2} \frac{1}{\left(1 - \frac{1}{z_1}\right)^2} \right)$$

4.4.2-Distribution of waiting time in the image processor

In [35] Downton continued Bailey's work and found the Laplace transform of waiting time, $W^*(s)$, in terms of the average service time, E[X], the Laplace transform of service time distribution, $B^*(s)$, and the z-transform of the distribution of number of packets in the system. The derivations here are due to him.

It is intuitively obvious that in equilibrium the average number of packets arriving during a service interval is equal to the average bulk size actually served. Therefore we have

$$\lambda E[X] = \sum_{j=0}^{m} j\pi_j + m \sum_{j=m+1}^{\infty} \pi_j \qquad (4.26)$$

Let the conditional waiting time distribution of packets who are rth in a bulk, that is when their bulk is on the point of being served, they are in fact rth in the queue be $W_r(x)$

$$W_r(x) = P[\text{packet's waiting time} \leq x \mid \text{packet is rth in bulk}]$$

It follows that the distribution of the waiting time, W(x), is given by

$$W(x) = \sum_{r=1}^{m} P_r W_r(x) \qquad (4.27)$$

Where P_r is the probability that a packet, when service starts, finds itself rth in the bulk, where $1 \leq r \leq m$. To determine these probabilities we note that, P[a packet arrives in interval $dt = \lambda\, dt$. Thus the probability of a packet, who is rth in a bulk, arriving in any interval dt is $P_r \lambda dt$. Therefore

λP_r = Expected number of rth packets arriving in unit time,
= Expected number of rth packets being served in unit time,

since the queue is in statistical equilibrium. At every service epoch an rth packet will be served if and only if, the queue length is at least r. Therefore, $\sum_{j=r}^{\infty} \pi_j$ = P[queue is at least of length r]= Expected number of rth packets being served at each service epoch.

Using a theorem from renewal theory [36], the expected number of service epoches in unit time is $\frac{1}{E[X]}$, and therefore the expected number of rth

packets served in unit time is $\frac{\sum_{j=r}^{\infty} \pi_j}{E[X]}$, from which we have

$$P_r = \frac{\sum_{j=r}^{\infty} \pi_j}{\lambda E[X]} \qquad (4.28)$$

From equations (2.26) and (4.28) the necessary condition $\sum_{r=1}^{m} P_r = 1$, is satisfied.

Now consider that the rth packet in a bulk is about to be served, and suppose that it has been waiting for a time x , the probability that there are j+r packets in the queue, given that there are at least r, is

$$\frac{\pi_{j+r}}{\sum_{i=r}^{\infty}\pi_i} = \int_0^{\infty} \frac{(\lambda x)^j}{j!} e^{-\lambda x}\, dW_{r(x)}$$

Now since $\sum_{j=0}^{\infty} \pi_{j+r}\, z^{j+r} = \sum_{j=r}^{\infty} \pi_j\, z^j$, for the z-transform of the number of packets in the system, $\Pi(z)$, from above we have

$$\Pi(z) = \sum_{j=0}^{r-1} \pi_j z^j + \left(\sum_{i=r}^{\infty} \pi_i\right) z^r \int_0^{\infty} \sum_{j=0}^{\infty} \frac{(\lambda z x)^j}{j!} e^{-\lambda x}\, dW_{r(x)}$$

or we can write

$$\Pi(z) = \sum_{j=0}^{r-1} \pi_j z^j + \left(\sum_{i=r}^{\infty} \pi_i\right) z^r M_{r(z)} \qquad (4.29)$$

where $M_{r(z)} = \int_0^{\infty} e^{-\lambda(1-z)x}\, dW_{r(x)}$. Obviously from relation (4.26) we have

$$M(z) = \int_0^{\infty} e^{-\lambda(1-z)x}\, dW(x) = W^*(\lambda - \lambda z) \qquad (4.30)$$

Where $M(z) = \sum_{r=1}^{m} P_r M_{r(z)}$. Multiplying equation (4.29) by z^{s-r}, we can rewrite it as

$$z^s P_r M_{r(z)} = \frac{1}{E[X]} \left[z^{s-r}\, \Pi(z) - z^{s-r} \sum_{j=0}^{r-1} \pi_j z^j \right]$$

Multiplying by 1-z and summing over r gives

$$(1-z)z^s M(z) = \frac{\left((1-z^s)\Pi(z) - \sum_{j=0}^{r-1} \pi_j (z^j - z^s)\right)}{E[X]}$$

Substituting for $\Pi(z)$ from equation (4.22) we get

$$M(z) = \frac{(1-z^s)\sum_{j=0}^{m-1} \pi_j (z^m - z^j) - \left(z^m/V(z) - 1\right)\sum_{j=0}^{m-1} \pi_j (z^j - z^m)}{\left(z^m/V(z) - 1\right)(1-z)z^s E[X]}$$

or

$$M(z) = \frac{1/V(z) - 1}{(1-z)E[X]} \frac{\sum_{j=0}^{m-1} \pi_j (z^m - z^j)}{(z^m/V(z) - 1)} = \frac{1/V(z) - 1}{(1-z)E[X]} \Pi(z)$$

From equation (4.30) and above, we have

$$W^*(s) = \frac{\Pi\left(\frac{\lambda - s}{\lambda}\right)}{\left(1 - \frac{\lambda - s}{\lambda}\right)E[X]} \left[\frac{1}{B^*(s)} - 1\right] \qquad (4.31)$$

Where by substituting for π_j in equation (4.26) we get

$$E[X] = \frac{-1}{K\lambda}\left[\sum_{j=0}^{m} j \left[\frac{A_1}{z_0}\left(\frac{1}{z_0}\right)^j + \frac{A_2}{z_1}\left(\frac{1}{z_1}\right)^j\right] + m\sum_{j=m+1}^{\infty}\left[\frac{A_1}{z_0}\left(\frac{1}{z_0}\right)^j + \frac{A_2}{z_1}\left(\frac{1}{z_1}\right)^j\right]\right]$$

or

$$E[X] = \frac{-1}{K\lambda}\left[\left(\frac{A_1}{z_0}\right)\left(\frac{1}{z_0}\right)\frac{-(m+1)(1/z_0)^m(1-1/z_0) + (1-(1/z_0)^{m+1})}{(1-1/z_0)^2} + \left(\frac{A_2}{z_1}\right)\left(\frac{1}{z_1}\right)\frac{-(m+1)(1/z_1)^m(1-1/z_1) + (1-(1/z_1)^{m+1})}{(1-1/z_1)^2} + m\left(\frac{A_1}{z_0}\frac{(1/z_0)^{m+1}}{(1-1/z_0)} + \frac{A_2}{z_1}\frac{(1/z_1)^{m+1}}{(1-1/z_1)}\right)\right] \quad (4.32)$$

Substituting the values for $\Pi\left(\frac{\lambda-s}{\lambda}\right)$, E[X] , and $B^*(s)$ in equation (4.31) the Laplace transform of the waiting time in the image processor queue can be evaluated. The average waiting time for an image is, $\bar{W} = -W^{*(1)}(0)$, and the average delay, T_3 , is $\bar{W} + \frac{\alpha_1}{\mu_1} + \frac{\alpha_2}{\mu_2}$.

The results obtained in this chapter are used in chapter 6 to sketch the performance curves for this model. These curves are for the delay and occupancy of the queueing systems in the database, the communication channels and the image processor in the picture viewing stations.

CHAPTER 5

MODEL 3: $E_r/Cox_2/1$ DATABASE QUEUES WITH SPAWNING AND M/G/1 IMAGE PROCESSOR QUEUE WITH BULK SERVICE

5.1-Model description

This model covers the case where the large image archive has a hierarchy of storage with different access times. As described in section 2.6.1, this model consists of $E_r/Cox_2/1$ database queues with spawning, a G/M/2 queue representing the communication channels, and a G/M/1 queue with bulk service representing the image processor in the picture viewing station, see Figure 5.1.

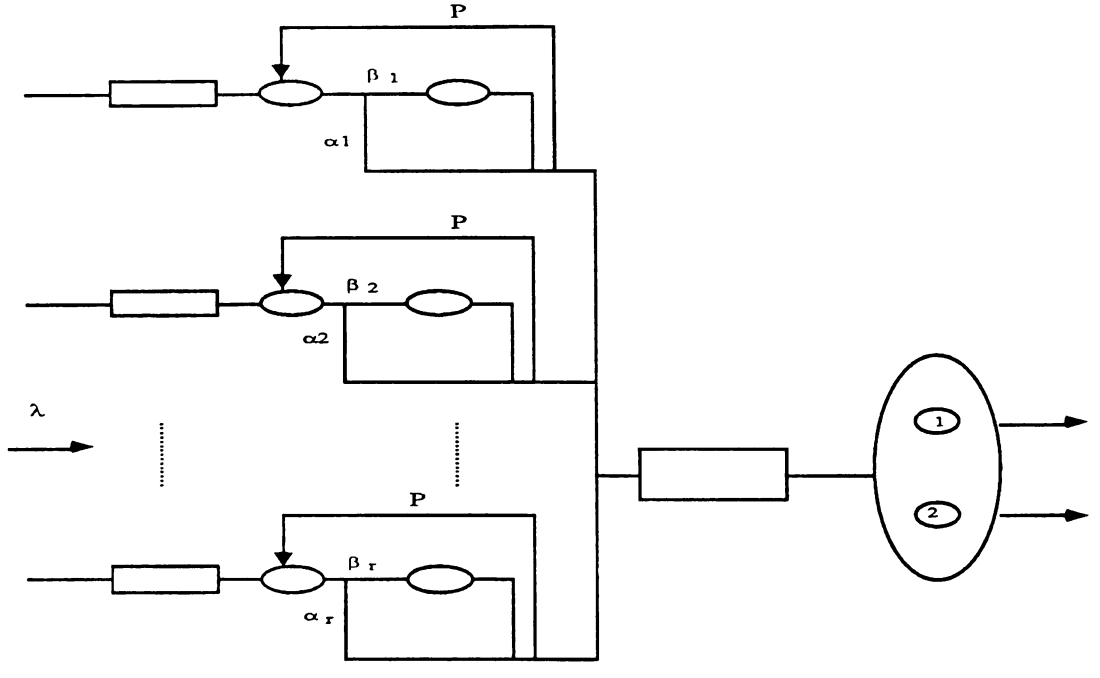

Figure 5.1. Queueing model of the database and the communication channels.

The assumptions for this model are given in section 2.6.1. We only add that the Poisson arrival process of request packets from picture viewing stations has a rate of λ.

5.2-Analysis of the database queues

In this section the database queues are analyzed in details. We first find the distribution of number of request packets in these queues. Then in section 5.2.2 we find the distribution of waiting time and the average delay. Distribution of inter-departure intervals is presented in section 5.2.3.

5.2.1-Distribution of number of packets in the database queues

In the analysis here we concentrate on a single queue in the database, but clearly the analysis can be applied to other queues by using the appropriate parameters, we assume that there are r queues in the database. Our state variable in this model is a pair (j,i), where j is the number of arrival stages in the system (as in model 2) and i is a binary variable indicating the server currently in use (server 1 or 2). For server one we set i to 1 and for server 2 , i is equal to 2. To indicate an empty system we set i to zero. In Figure 5.2 we show an $E_r/Cox_2/1$ with spawning together with the arrival facility for an Erlang-r arrival process. From Figure 5.2, it is clear that the mean inter_arrival time to the queue is $\frac{r}{\lambda}$, and the arrival rate is $\frac{\lambda}{r}$.

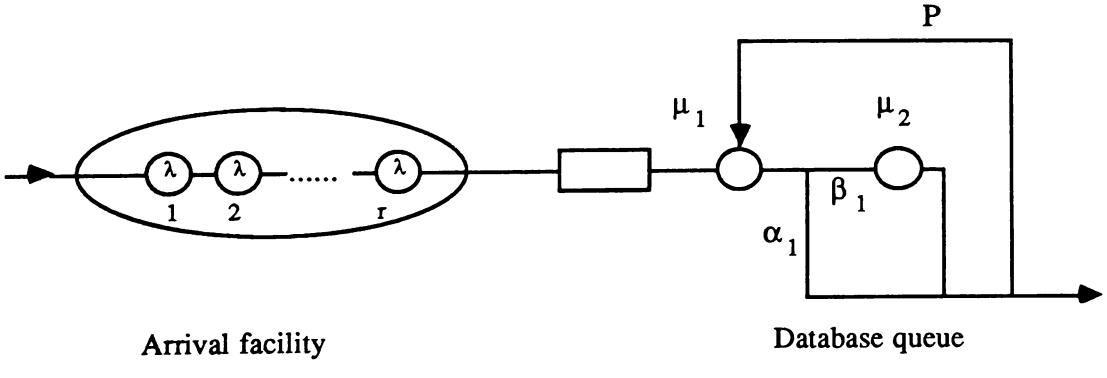

Figure 5.2. A single $E_r/Cox_2/1$ database queue with spawning.

The state transition diagram for an $E_r/Cox_2/1$ with spawning is shown below

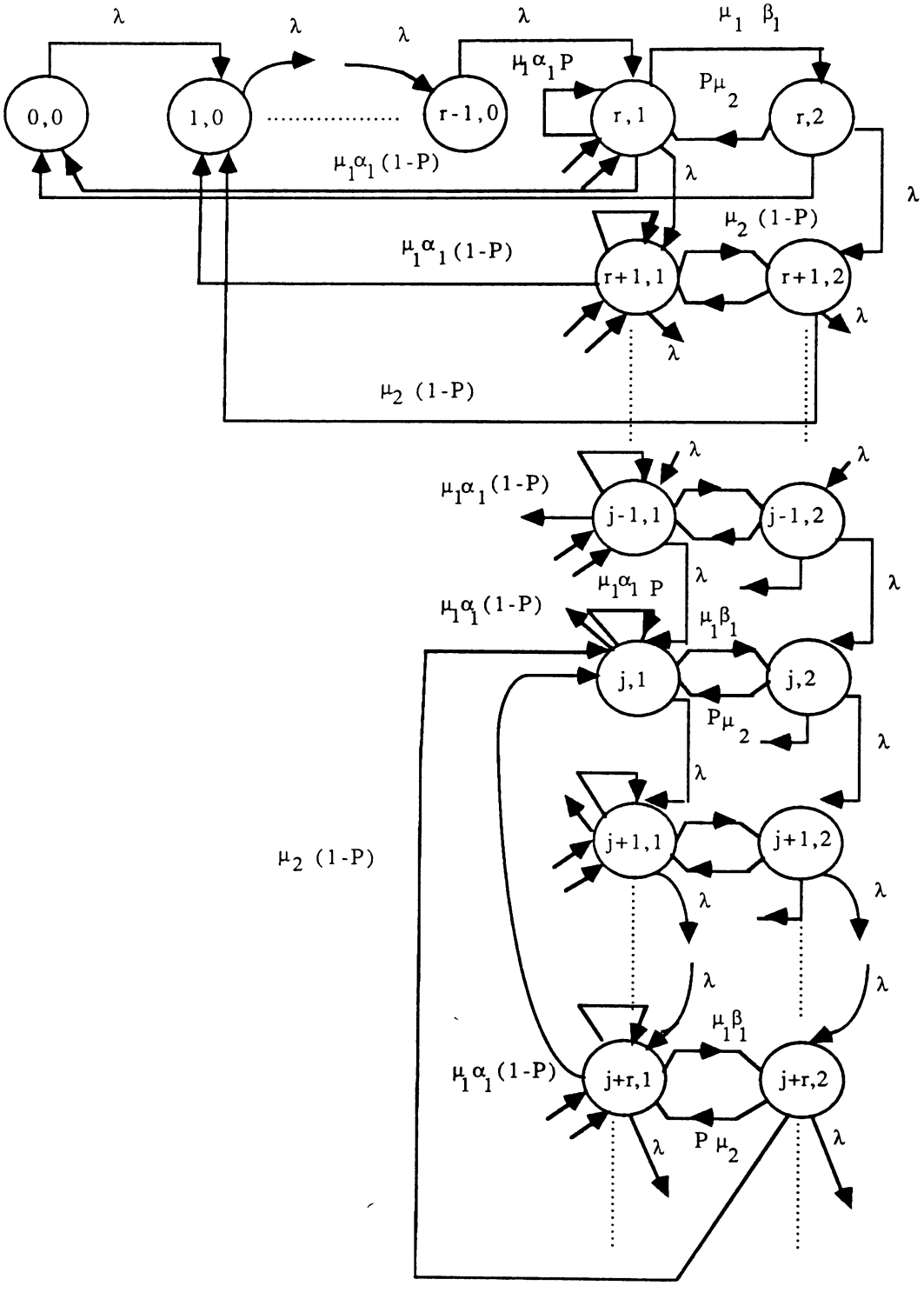

Figure 5.3. State transition diagram for $E_r/Cox_2/1$ with spawning

We define $P_{(j,i)}$ as the probability of having j stages of arrival in the system and server i in use, i.e. $P_{(j,1)} = P_{(j,2)} = 0$ for $j < r$. As in model 2, the total number of stages of arrival in the system when our arriving packet is in the nth stage of arrival ($1 \leq n \leq r$) and the number of request packets in the system is k, is given by

$$j = rk + n - 1$$

Let P_k denote the equilibrium probability of having k packets in the system, then we can write

$$P_k = \sum_{j=rk}^{r(k+1)-1} \left[P_{(j,1)} + P_{(j,2)} \right] \qquad (5.1)$$

We may write down the equilibrium equations for the state transition rate diagram of Figure 5.3 as

$$\lambda P_{(0,0)} = \mu_1\alpha_1(1-P)P_{(r,1)} + \mu_2(1-P)P_{(r,2)} \qquad j = 0 \qquad (5.2)$$

$$\lambda P_{(j,0)} = \lambda P_{(j-1,0)} + \mu_1\alpha_1(1-P)P_{(j+r,1)} + \mu_2(1-P)P_{(j+r,2)} \qquad 1 \leq j < r \qquad (5.3)$$

$$(\lambda+\mu_1\alpha_1(1-P)+\mu_1\beta_1)P_{(r,1)} = \lambda P_{(r-1,1)}+\mu_2 P\, P_{(r,2)}+ \mu_1\alpha_1(1-P)P_{(2r,1)}+\mu_2(1-P)P_{(2r,2)} \qquad j = r \qquad (5.4)$$

$$(\lambda+\mu_1\alpha_1(1-P)+\mu_1\beta_1)P_{(j,1)} = \lambda P_{(j-1,0)}+\mu_2 P\, P_{(j,2)}+ \mu_1\alpha_1(1-P)P_{(j+r,1)}+\mu_2(1-P)P_{(j+r,2)} \qquad j > r \qquad (5.5)$$

$$(\mu_2(1-P)+P\mu_2+\lambda)P_{(r,2)} = \mu_1\beta_1 P_{(r,1)} \qquad j = r \qquad (5.6)$$

$$(\mu_2(1-P)+P\mu_2+\lambda)P_{(j,2)} = \lambda P_{(j-1,2)}+\mu_1\beta_1 P_{(j,1)} \qquad j \geq r \qquad (5.7)$$

We define the z-transform for the probabilities $P_{(j,1)}$ and $P_{(j,2)}$ as

$$G(z,1)= \sum_{j=0}^{\infty} P(j,1)\, z^{j} \qquad \text{for } |z| < 1$$

$$G(z,2)= \sum_{j=0}^{\infty} P(j,2)\, z^{j} \qquad \text{for } |z| < 1$$

Multiplying equations (5.2), (5.3), (5.4), (5.5), (5.6), and (5.7) by z^{j}, summing for all applicable values of j and adding equations (5.2) and (5.3), (5.4) and (5.5), (5.6) and (5.7) we get

$$z^{r}\Big[\lambda P_{(r-1,0)} z^{r-1} - (\lambda z-\lambda) \sum_{j=0}^{r-2} P(j,i)\, z^{j}\Big] = \mu_1\alpha_1(1-P) \sum_{j=r}^{2r-1} P(j,1)\, z^{j} + \mu_2(1-P) \sum_{j=r}^{2r-1} P(j,2)\, z^{j} \qquad (5.8)$$

$$\Big[\big[(\lambda+\mu_1-\mu_1\alpha_1 P)\big]z^{r} - \lambda z^{r+1} - \mu_1\alpha_1(1-P)\Big] G(z,1) = \Big[\mu_2 P z^{r} + \mu_2(1-P)\Big] G(z,2) + z^{r}\lambda P_{(r-1,0)} z^{r} - \mu_1\alpha_1(1-P) \sum_{j=r}^{2r-1} P(j,1)\, z^{j} - \mu_2(1-P) \sum_{j=r}^{2r-1} P(j,2)\, z^{j} \qquad (5.9)$$

$$G(z,2) = \frac{\mu_1\beta_1}{\big[\mu_2+\lambda(1-z)\big]} G(z,1) \qquad (5.10)$$

From equations (5.8), (5.9), and (5.10) solving for $G(z,1)$ we have

$$G(z,1) = \frac{z^{r}\big[\mu_2+\lambda(1-z)\big](\lambda z-\lambda) \sum_{j=0}^{r-1} P(j,0)\, z^{j}}{A(z)} \qquad (5.11)$$

where $A(z)$ is

$$A(z) = \lambda^2 z^{r+2} - \lambda(2\lambda+\mu_1+\mu_2-\mu_1\alpha_1 P)\, z^{r+1} + \left[\lambda(\lambda+\mu_1+\mu_2-\mu_1\alpha_1 P)+\mu_1\mu_2(1-P)\right]z^r + \lambda\mu_1\alpha_1(1-P)z - \lambda\mu_1\alpha_1(1-P)-\mu_1\mu_2(1-P)$$

We must now study the zeros of the denominator for this function. Rouche's theorem [37] states that *"If $f(z)$ and $g(z)$ are analytic functions of z inside and on a closed contour C, and also if $|g(z)| < |f(z)|$ on C, then $f(z)$ and $f(z)+g(z)$ have the same number of zeros inside C."*. Taking $f(z)= \left[\lambda(\lambda+\mu_1+\mu_2-\mu_1\alpha_1 P)+\mu_1\mu_2(1-P)\right]z^r - \lambda\mu_1\alpha_1(1-P)-\mu_1\mu_2(1-P)$ and $g(z)= \lambda^2 z^{r+2} - \lambda(2\lambda+\mu_1+\mu_2-\mu_1\alpha_1 P)z^{r+1} + \lambda\mu_1\alpha_1(1-P)z$, and the contour C as the unit circle around the origin on the complex plane. It can be easily shown that $\min(|f(z)|) > |g(z)|$ for $|z|=1$, and therefore $|f(z)| > |g(z)|$. The denominator polynomial has r+2 zeros of which unity is one. Now by applying Rouche's theorem, of the remaining r+1 roots, r-1 of them lie in the region $|z| < 1$, and two of them (z_0, z_1) are such that $|z_0| > 1$ and $|z_1| > 1$.

Since $G(z,1)$ must be bounded in the range $|z| < 1$, these r-1 roots must be compensated by the roots of the numerator. These observations allow us to equate the summation in the numerator to the denominator, after its three roots at $z=1$, $z=z_0$, and $z=z_1$ are factored out.

$$\frac{A(z)}{(1-\frac{z}{z_0})(1-\frac{z}{z_1})(1-z)} = K\sum_{j=0}^{r-1} P(j,0)\, z^j \qquad (5.12)$$

Where K is a constant to be determined.

From equations (5.11) and (5.12) we have

$$G(z,1) = \frac{z^r\left[\mu_2+\lambda(1-z)\right]\lambda}{K(1-\frac{z}{z_0})(1-\frac{z}{z_1})} \qquad (5.13)$$

From (5.10) and (5.13) we have

$$G_{(z,2)} = \frac{\lambda\mu_1\beta_1 z^r}{K(1 - \frac{z}{z_0})(1 - \frac{z}{z_1})} \tag{5.14}$$

For z=1 we get

$$G_{(1,1)} = \frac{\lambda\mu_2}{K(1 - \frac{1}{z_0})(1 - \frac{1}{z_1})} \tag{5.15}$$

and

$$G_{(1,2)} = \frac{\lambda\mu_1\beta_1}{K(1 - \frac{1}{z_0})(1 - \frac{1}{z_1})} \tag{5.16}$$

Now from the definitions of z-transforms, $G_{(z,1)}$ and $G_{(z,2)}$, we have

$$G_{(1,1)} + G_{(1,2)} = \rho \tag{5.17}$$

Where ρ is the utilization of the system, $\rho = \left(\frac{\lambda}{2(1-P)}\right)\left(\frac{\mu_2+\mu_1\beta_1}{\mu_1\mu_2}\right)$.

From equations (5.15), (5.16), and (5.17), we can now evaluate the constant K as

$$K = \frac{\lambda(\mu_2 + \mu_1\beta_1)}{\rho(1 - \frac{1}{z_0})(1 - \frac{1}{z_1})} \tag{5.18}$$

We can rewrite equation (5.13) as

$$G_{(z,1)} = \frac{\lambda z^r}{K}\left[\frac{A_1}{1 - \frac{z}{z_0}} + \frac{A_2}{1 - \frac{z}{z_1}}\right] \tag{5.19}$$

Where A_1 and A_2 are

$$A_1 = \frac{\mu_2+\lambda(1-z_0)}{1-\frac{z_0}{z_1}} \qquad A_2 = \frac{\mu_2+\lambda(1-z_1)}{1-\frac{z_1}{z_0}} \tag{5.20}$$

If we denote the inverse of the Laplace transform in the brackets (eq. (5.19)) as f_j, from the properties of Laplace transforms [27] we must have

$$P_{(j,1)}= \frac{\lambda}{K} f_{j-r} \tag{5.21}$$

Where f_j is given by

$$f_j = \begin{cases} A_1\left(\frac{1}{z_0}\right)^j + A_2\left(\frac{1}{z_1}\right)^j & j \geq 0 \\ 0 & j < 0 \end{cases} \tag{5.22}$$

therefore

$$P_{(j,1)}= \frac{\lambda}{K}\left[A_1\left(\frac{1}{z_0}\right)^{j-r} + A_2\left(\frac{1}{z_1}\right)^{j-r}\right] \qquad j \geq r \tag{5.23}$$

Repeating the same for $P_{(j,2)}$ we get

$$P_{(j,2)}= \frac{\lambda\mu_1\beta_1}{K} f'_{j-r}$$

where

$$f'_j = \begin{cases} A'_1\left(\frac{1}{z_0}\right)^j + A'_2\left(\frac{1}{z_1}\right)^j & j \geq 0 \\ 0 & j < 0 \end{cases} \tag{5.24}$$

and

$$A'_1 = \frac{1}{1 - \frac{z_0}{z_1}} \qquad A'_2 = \frac{1}{1 - \frac{z_1}{z_0}}$$

therefore

$$P_{(j,2)} = \frac{\lambda\mu_1\beta_1}{K}\left[A'_1\left(\frac{1}{z_0}\right)^{j-r} + A'_2\left(\frac{1}{z_1}\right)^{j-r}\right] \tag{5.25}$$

From equations (5.1), (5.23), and (5.25) the steady state distribution of number of packets in the system can be found as

$$P_k = \frac{\lambda}{K}\left(A_1 + A'_1\mu_1\beta_1\right)\frac{\left(\frac{1}{z_0}\right)^{r(k-1)} - \left(\frac{1}{z_0}\right)^{rk}}{\left(1 - \frac{1}{z_0}\right)} + \frac{\lambda}{K}\left(A_2 + A'_2\mu_1\beta_1\right)\frac{\left(\frac{1}{z_1}\right)^{r(k-1)} - \left(\frac{1}{z_1}\right)^{rk}}{\left(1 - \frac{1}{z_1}\right)} \tag{5.26}$$

5.2.2-Distribution of waiting time in the database queues

Our analysis here is similar to the one in section 4.2.2 for model 2. Referring to Figure 5.2, let r_k denote the probability that a request packet finds k packets in the queue upon arrival, $r_{k-1} = \frac{1}{\rho}P_k$ for $k \geq 1$, where $\rho = \frac{\lambda}{r(1-P)}\frac{\mu_2+\beta_1\mu_1}{\mu_1\mu_2}$.

Let $W^*(s)$ the Laplace transform of the waiting time in the database and $W^*(s \mid k) = E[e^{-sw} \mid$ an arrival finds k packets in the system] , therefore

$$W^*_{(s \mid k)} = \left(\sum_{i=1}^{\infty} P^{i-1}(1-P) \left(\frac{\mu_1}{s+\mu_1} + \beta_1 \frac{\mu_1}{s+\mu_1} \frac{\mu_2}{s+\mu_2} \right)^i \right)^k$$

or

$$W^*_{(s \mid k)} = \left(\frac{(1-P) \left(\frac{\mu_1}{s+\mu_1} + \beta_1 \frac{\mu_1}{s+\mu_1} \frac{\mu_2}{s+\mu_2} \right)}{1 - P \left(\frac{\mu_1}{s+\mu_1} + \beta_1 \frac{\mu_1}{s+\mu_1} \frac{\mu_2}{s+\mu_2} \right)} \right)^k$$

Again here we assume that the spawned packet is inserted at the head of the queue. Let S denote the term inside the brackets. Now for $W^*_{(s)}$ we have

$$W^*_{(s)} = r_0 E[e^{-s0}] + \sum_{k=1}^{\infty} r_k S^k \qquad (5.27)$$

where $r_k = \frac{\lambda}{\rho K} \Bigg((A_1 + A'_1 \mu_1 \beta_1) \frac{\left(\frac{1}{z_0}\right)^{rk} - \left(\frac{1}{z_0}\right)^{r(k+1)}}{\left(1 - \frac{1}{z_0}\right)} + (A_2 + A'_2 \mu_1 \beta_1) \frac{\left(\frac{1}{z_1}\right)^{rk} - \left(\frac{1}{z_1}\right)^{r(k+1)}}{\left(1 - \frac{1}{z_1}\right)} \Bigg)$

Let $B = \frac{(A_1 + A'_1 \mu_1 \beta_1)}{1 - \frac{1}{z_0}}$ and $C = \frac{(A_2 + A'_2 \mu_1 \beta_1)}{1 - \frac{1}{z_1}}$. Substituting the values in equation (5.27) we have

$$W^*_{(s)} = r_0 + \frac{1}{\rho K}\left[B\sum_{k=1}^{\infty} S^k\left[\left(\frac{1}{z_0}\right)^{rk} - \left(\frac{1}{z_0}\right)^{r(k+1)}\right] + C\sum_{k=1}^{\infty} S^k\left[\left(\frac{1}{z_1}\right)^{rk} - \left(\frac{1}{z_1}\right)^{r(k+1)}\right]\right]$$

or

$$W^*_{(s)} = r_0 + \frac{1}{\rho K}\left[B\left(1 - \frac{1}{z_0}\right)\frac{S\left(\frac{1}{z_0}\right)^r}{1 - S\left(\frac{1}{z_0}\right)^r} + C\left(1 - \frac{1}{z_1}\right)\frac{S\left(\frac{1}{z_1}\right)^r}{1 - S\left(\frac{1}{z_1}\right)^r}\right]$$

Using the inverse of Laplace transform the distribution of waiting time can be found. The mean waiting time $\bar{W} = - W^{*(1)}(0)$, and the average delay in the database to retrieve an exam, T_1 is $\bar{W} + \frac{\mu_2 + \beta_1\mu_1}{\mu_1\mu_2}$.

5.2.3- Distribution of inter_departure intervals from the database queues

Let d_j denote the probability of a departing packet from the database queue in Figure 5.2 leaving j stages of arrival behind. d_j can be found as

$$d_j = \begin{cases} \dfrac{\mu_1\alpha_1(1-P)P_{(j+r,1)} + \mu_2(1-P)P_{(j+r,2)}}{\sum_{k=r}^{\infty}\mu_1 P_{(k,1)} + \mu_2 P_{(k,2)}} & j < r \qquad (5.28) \\ \dfrac{\mu_1\alpha_1(1-P)P_{(j+r,1)} + \mu_1\alpha_1 P\ P_{(j,1)} + \mu_2(1-P)P_{(j+r,2)} + \mu_2 P\ P_{(j,2)}}{\sum_{k=r}^{\infty}\mu_1 P_{(k,1)} + \mu_2 P_{(k,2)}} & j \geq r \end{cases}$$

Let the random variable 'd' denote the inter_departure intervals from the queue . The Laplace transform of the inter_departure time, $D^*(s)$, can be expressed as

$$D^*(s) = E[e^{-sd} \mid j \geq r]\, P[j \geq r] + E[e^{-sd} \mid j < r]\, P[j < r] \qquad (5.29)$$

Therefore for r=2 we have

$$D^*(s) = \sum_{j=2}^{\infty} \left[\alpha_1 \frac{\mu_1}{s+\mu_1} + \beta_1 \left(\frac{\mu_1}{s+\mu_1}\right)\left(\frac{\mu_2}{s+\mu_2}\right) \right] d_j \qquad (5.30)$$

$$+ \sum_{j=0}^{1} d_j \left(\frac{\lambda}{s+\lambda}\right)^{2-j} \left[\alpha_1 \frac{\mu_1}{s+\mu_1} + \beta_1 \left(\frac{\mu_1}{s+\mu_1}\right)\left(\frac{\mu_2}{s+\mu_2}\right) \right]$$

using partial fraction expansion, we have

$$D^*(s) = \frac{\alpha_1\mu_1 \sum_{j=2}^{\infty} d_j}{s+\mu_1} + \frac{A11}{s+\mu_1} + \frac{A21}{s+\mu_2} + \frac{B11}{(s+\lambda)^2} + \frac{B12}{s+\lambda} + \frac{B21}{s+\mu_1} \qquad (5.31)$$

$$+ \frac{C11}{(s+\lambda)^2} + \frac{C12}{s+\lambda} + \frac{C21}{s+\mu_1} + \frac{C31}{s+\mu_2}$$

$$+ \frac{D11}{s+\lambda} + \frac{D21}{s+\mu_1} + \frac{E11}{s+\lambda} + \frac{E21}{s+\mu_1} + \frac{E31}{s+\mu_2}$$

where

$$A11 = \frac{\beta_1\mu_1\mu_2 \sum_{j=2}^{\infty} d_j}{-\mu_1 + \mu_2} \qquad A21 = \frac{\beta_1\mu_1\mu_2 \sum_{j=2}^{\infty} d_j}{-\mu_2 + \mu_1}$$

$$B11 = \frac{d_0\lambda^2\alpha_1\mu_1}{-\lambda+\mu_1} \qquad B12 = \frac{-d_0\lambda^2\alpha_1\mu_1}{(-\lambda+\mu_1)^2} \qquad B21 = \frac{d_0\lambda^2\alpha_1\mu_1}{(\lambda-\mu_1)^2}$$

$$C_{11} = \frac{d_0\lambda^2\beta_1\mu_1\mu_2}{(-\lambda+\mu_1)(-\lambda+\mu_2)} \quad C_{12} = \frac{-d_0\lambda^2\beta_1\mu_1\mu_2[(-\lambda+\mu_1) + (-\lambda+\mu_2)]}{(-\lambda+\mu_1)^2(-\lambda+\mu_2)^2}$$

$$C_{21} = \frac{d_0\lambda^2\beta_1\mu_1\mu_2}{(-\mu_1+\lambda)^2(-\mu_1+\mu_2)} \quad C_{31} = \frac{d_0\lambda^2\beta_1\mu_1\mu_2}{(-\mu_2+\lambda)^2(-\mu_2+\mu_1)}$$

$$D_{11} = \frac{d_1\lambda\alpha_1\mu_1}{-\lambda+\mu_1} \quad D_{21} = \frac{d_1\lambda\alpha_1\mu_1}{-\mu_1+\lambda}$$

$$E_{11} = \frac{d_1\lambda\beta_1\mu_1\mu_2}{(-\lambda+\mu_1)(-\lambda+\mu_2)} \quad E_{21} = \frac{d_1\lambda\beta_1\mu_1\mu_2}{(-\mu_1+\lambda)(-\mu_1+\mu_2)} \quad E_{31} = \frac{d_1\lambda\beta_1\mu_1\mu_2}{(-\mu_2+\lambda)(-\mu_2+\mu_1)}$$

The pdf of the inter_departure time, $d(x)$, can be found from (5.31) as

$$d(x) = A_1 e^{-\mu_1 x} + A_2 e^{-\mu_2 x} + A_3 x e^{-\lambda x} + A_4 e^{-\lambda x} \qquad (5.32)$$

where $A_1 = \mu_1\alpha_1 \sum_{j=2}^{\infty} d_j + A_{11} + B_{21} + C_{21} + D_{21} + E_{21}$, $A_2 = A_{21} + C_{31} + E_{31}$, $A_3 = B_{11} + C_{11}$, $A_4 = B_{12} + C_{12} + D_{11} + E_{11}$.

The corresponding PDF, $D(x)$, is

$$D(x) = 1 - B_1 e^{-\mu_1 x} - B_2 e^{-\mu_2 x} - B_3 x e^{-\lambda x} - B_4 e^{-\lambda x} \qquad (5.33)$$

where $B_1 = \frac{A_1}{\mu_1}$, $B_2 = \frac{A_2}{\mu_2}$, $B_3 = \frac{A_3}{\lambda}$, $B_4 = \frac{A_3}{\lambda^2} + \frac{A_4}{\lambda}$. We also have

$$\int_x^{\infty} (1 - D(u))\, du = C_1 e^{-\mu_1 x} + C_2 e^{-\mu_2 x} + C_3 x e^{-\lambda x} + C_4 e^{-\lambda x} \qquad (5.34)$$

where $C_1 = \frac{B_1}{\mu_1}$, $C_2 = \frac{B_2}{\mu_2}$, $C_3 = \frac{B_3}{\lambda}$, $C_4 = \frac{B_3}{\lambda^2} + \frac{B_4}{\lambda}$.

5.3-Analysis of the communication channels

The analysis here are for the case of having 2 queues in the database. In section 5.3.1 we find the Laplace transform of the arrival process to the queueing system representing the communication channels, this is done by superimposing the two departure processes of the database queues. In section 5.3.2, we use this Laplace transform to solve for the distribution of number of packets and the average delay in the communication channels.

Since the analysis are similar to the one carried out for model 1, we will not repeat it here.

5.3.1-Distribution of inter_arrival time to the communication channels

Here we apply equation 3.9 from section 3.3 to our model. We add a subscript/superscript to the parameters to indicate to which parallel queue in the database they belong, refer to Figure 5.4. As in the previous models, we find the distribution of inter_arrival time to the communication channels for the case r=2 , i.e. two database queues, however these analysis can be generalized to any number of queues. As in Figure 5.2, we have a Poisson arrival process with rate λ.

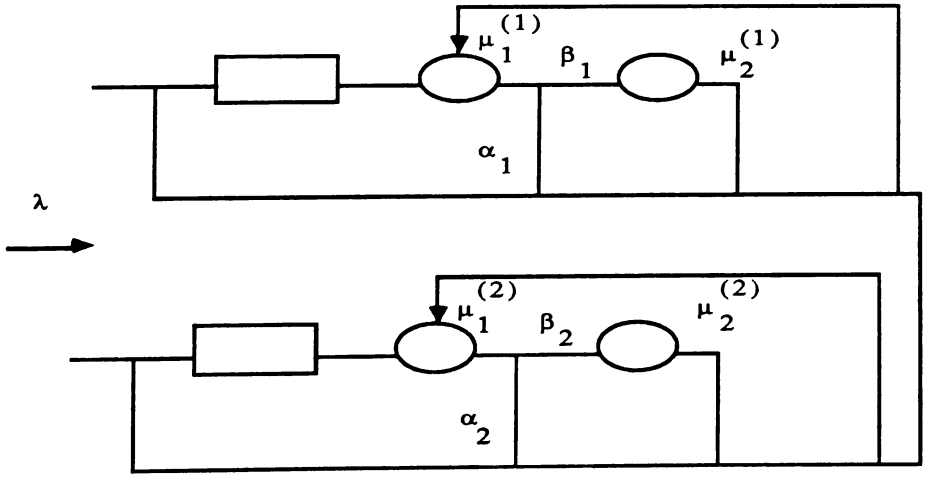

Figure 5.4. Two database queues with Coxian-2 service times.

Using equation 3.9 and substituting the values from previous section, for the pdf of the inter_arrival time $c_{2(x)}$, we have

$$c_{2(x)} = \frac{\lambda_1\lambda_2}{\lambda_1+\lambda_2}\ \Big[d_{1(x)}\ \big(C_1^{(2)} e^{-\mu_1^{(2)}x} + C_2^{(2)} e^{-\mu_2^{(2)}x} + C_3^{(2)}\, x\, e^{-\lambda x} + C_4^{(2)} e^{-\lambda x}\big) + d_{2(x)}\ \big(C_1^{(1)} e^{-\mu_1^{(1)}x} + C_2^{(1)} e^{-\mu_2^{(1)}x} + C_3^{(1)}\, x\, e^{-\lambda x} + C_4^{(1)} e^{-\lambda x}\big) + 2\ \big(B_1^{(1)} e^{-\mu_1^{(1)}x} + B_2^{(1)} e^{-\mu_2^{(1)}x} + B_3^{(1)}\, x\, e^{-\lambda x} + B_4^{(1)} e^{-\lambda x}\big)\ \big(B_1^{(2)} e^{-\mu_1^{(2)}x} + B_2^{(2)} e^{-\mu_2^{(2)}x} + B_3^{(2)}\, x\, e^{-\lambda x} + B_4^{(2)} e^{-\lambda x}\big)\Big] \quad (5.35)$$

where λ_1 and λ_2 are the departure rates from queues one and two respectively, i.e. $\lambda_1 = \lambda_2 = \frac{\lambda}{2(1-P)}$. Taking the Laplace transform we get

$$C^*_{2(s)} = \left(\frac{\lambda_1\lambda_2}{\lambda_1+\lambda_2}\right)\Big[\ C_1^{(2)} D^*_{1(s+\mu_1^{(2)})} + C_2^{(2)} D^*_{1(s+\mu_2^{(2)})} + - C_3^{(2)} \frac{d\ D^*_{1(s+\lambda)}}{ds} + C_4^{(2)} D^*_{1(s+\lambda)} + C_1^{(1)} D^*_{2(s+\mu_1^{(1)})} + C_2^{(1)} D^*_{2(s+\mu_2^{(1)})} + - C_3^{(1)} \frac{d\ D^*_{2(s+\lambda)}}{ds} + C_4^{(1)} D^*_{2(s+\lambda)}$$

$$2\ \Big(\frac{B_1^{(1)}\ B_1^{(2)}}{s+\mu_1^{(1)}+\mu_1^{(2)}} + \frac{B_1^{(1)}\ B_2^{(2)}}{s+\mu_1^{(1)}+\mu_2^{(2)}} + \frac{B_1^{(2)}\ B_3^{(2)}}{(s+\mu_1^{(1)}+\lambda)^2} + \frac{B_1^{(1)}\ B_4^{(2)}}{s+\mu_1^{(1)}+\lambda} + \frac{B_2^{(1)}\ B_1^{(2)}}{s+\mu_2^{(1)}+\mu_1^{(2)}} + \frac{B_2^{(1)}\ B_2^{(2)}}{s+\mu_2^{(1)}+\mu_2^{(2)}} + \frac{B_2^{(1)}\ B_3^{(2)}}{(s+\mu_2^{(1)}+\lambda)^2} + \frac{B_2^{(1)}\ B_4^{(2)}}{s+\mu_2^{(1)}+\lambda} + \frac{B_3^{(1)}\ B_1^{(2)}}{(s+\mu_1^{(2)}+\lambda)^2} + \frac{B_3^{(1)}\ B_2^{(2)}}{(s+\mu_2^{(2)}+\lambda)^2} + \frac{2\ B_3^{(1)}\ B_3^{(2)}}{(s+2\lambda)^3} +$$

$$\frac{B_3^{(1)} B_4^{(2)}}{(s+2\lambda)^2} + \frac{B_4^{(1)} B_1^{(2)}}{s+\mu_1^{(2)}+\lambda} + \frac{B_4^{(1)} B_2^{(2)}}{s+\mu_2^{(2)}+\lambda} + \frac{B_4^{(1)} B_3^{(2)}}{(s+2\lambda)^2} + \frac{B_4^{(1)} B_4^{(2)}}{s+2\lambda}\Big)\Big] \qquad (5.36)$$

where $D_i^*(s) = \int_{x=0}^{\infty} e^{-sx}\, d_i(x)\, dx$, i=1 or 2. Substituting the values for $D_i^*(s)$ and $\frac{d\, D_i^*(s)}{d\, s}$, and using the inverse of the Laplace transforms the pdf of inter_arrival time to the communication channels can be found.

5.3.2-Distribution of number of packets and delay in the communication channels

Using results obtained in section 3.4.2 and the Laplace transform of the inter_arrival time to the communication channels from section 5.3.1 , the average number of packets in the queueing system G/M/2 representing the communication channels and the average delay, T_2, in the communication channels for this model (two database queues and two communication channels) can be found easily. We do not repeat the analyses here, since they are exactly the same as in section 3.4.2 .

5.4-Analysis of the picture viewing station

The image processor in the picture viewing station is modeled as a M/G/1 with bulk service. The analysis is as presented in section 4.4 and is not repeated here.

The results obtained in this chapter are used in chapter 6 to present the performance curves for this model. These curves are for the delay and occupancy of the queueing systems in the database, the communication channels and the image processor in the picture viewing stations.

CHAPTER 6

RESULTS AND DISCUSSIONS

6.1-Introduction

In this chapter we use the analytical results of chapters 3, 4, and 5 together with the results of our simulation of models 1, 2, and 3 to draw the performance curves for the three queueing models of PACS presented in chapter 2. We use performance parameters of PACS such as the access time to the optical disks in a jukebox or the size of digital images from the data provided in chapter 1.

Our performance curves are not for a specific commercial or research PACS since these systems are still being engineered and their performance parameters are constantly changed. However we have chosen realistic parameters based on the information available in the literature. We present the performance curves for the delay in retrieving images from the database, in the transmission of images, and in processing them in the image processor.

The end to end delay, that is the time it takes for a radiologist to view a medical exam from the moment that his request packet is sent to the image database till the time he has the images on his console is the sum of all the delays mentioned above. From the curves provided in this chapter the end to end delay for various amount of load in the system can be accurately estimated.

We present curves for the buffer occupancy in the input buffers of the communication channels and the buffers in the picture viewing stations. For models 2 and 3 we also present the average number of exam requests in the database. These curves can be used in the design phase of a product to estimate the buffer requirements and also to allow for the future expansion of these buffers as the traffic increases in the system. Due to the huge amount of data involved, it is paramount that enough memory space be available for the smooth running of the system.

Otherwise unnecessary delays will be introduced because of buffer shortages.

6.2-Performance curves for model 1

Here we present the performance curves for model 1. We have used the following parameters:

1) Each SIF consists of 512^2x16 bits.
2) Average number of SIFs in an image is 0.9.
3) Average number of images in an exam is 5.
4) Average number of exam requests in a request packet is 1.
5) Average "read" time from the database is 6 secs.
6) Two communication channels of 1 Mbps.

In Figures 6.1 and 6.2, we show the average delay in the communication channels plus the database and the average delay in the communication channels, respectively. On each curve we have the delays from our analytical and the simulation models. In Figure 6.2 we also have the delay from an M/M/2 queueing model of the communication channels. As can be seen from Figure 6.2, the M/M/2 queueing system represents a very good approximation of our G/M/2 model and a practitioner can use this queueing system for performance evaluation of the communication channels. In appendix 1, the pdf of the arrival process to the communication channels for the G/M/2 queueing system and the pdf of an exponentially distributed arrival process are plotted. From the Figure 1 in appendix 1, it is obvious that these two distributions are almost the same for all practical purposes.

The proximity of the simulation and analytical curves in Figures 6.1 and 6.2 indicate that the independence assumption between the departure processes of the queues in the database is valid and our analytical results based on this assumption are quite valid.

In Figures 6.3 and 6.4, we show the average buffer occupancy in the communication channels versus the arrival rate, and the utilization of the

communication channels for the analytical and simulation models, respectively. These curves can be used by a designer to estimate the buffer requirements at the interface between the database and the communication channels. Again our simulation results indicate that the independence assumption in the analytical model is quite good and the two results are very close. Figure 6.5 shows the average delay in the database. In Figure 6.6 we show the utilization of the database and the communication channels, this type of curve is useful to a designer of PACS as an indicator of how much of the capacity of each component can be utilized under certain conditions. For example, with our performance parameters of the database and the communication channels we can see that the capacity of the communication channels is somewhat underutilized at half the utilization rate of the database.

Comparing figure 6.5, 6.2 and figure 6.6 indicates that the delay in the database is almost twice as large as the delay in the communication channels until the utilization of the database reaches 60%, after this point the database queues start to overload and the delay increases at a very high rate.

For the image processor we assume that half of the images require an average service time of 25 seconds and the other half an average service time of 12.5 seconds. In Figures 6.7 and 6.8 we present the delay and the average buffer occupancy in the picture viewing stations.

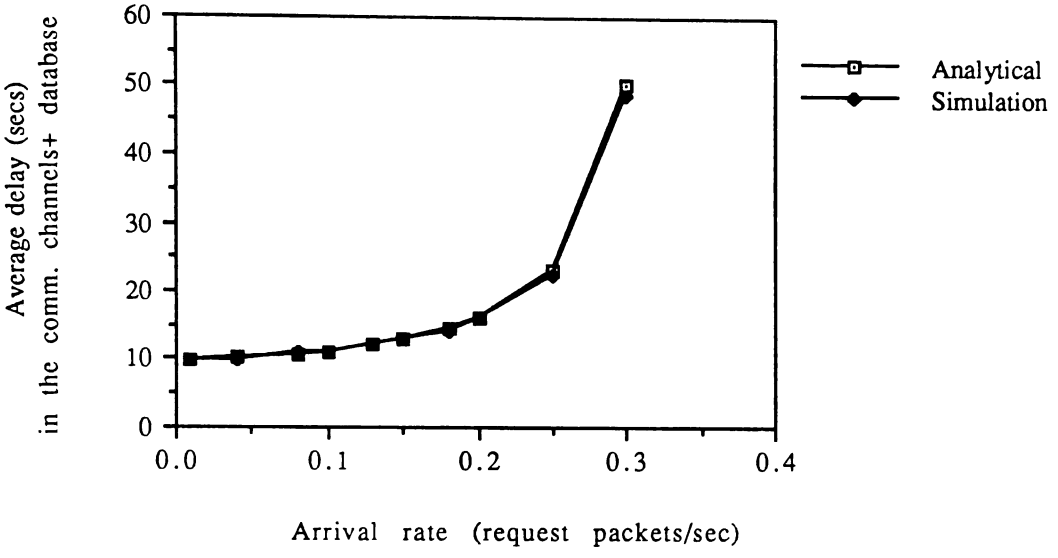

Figure 6.1. Average delay in the comm. channels and the database.

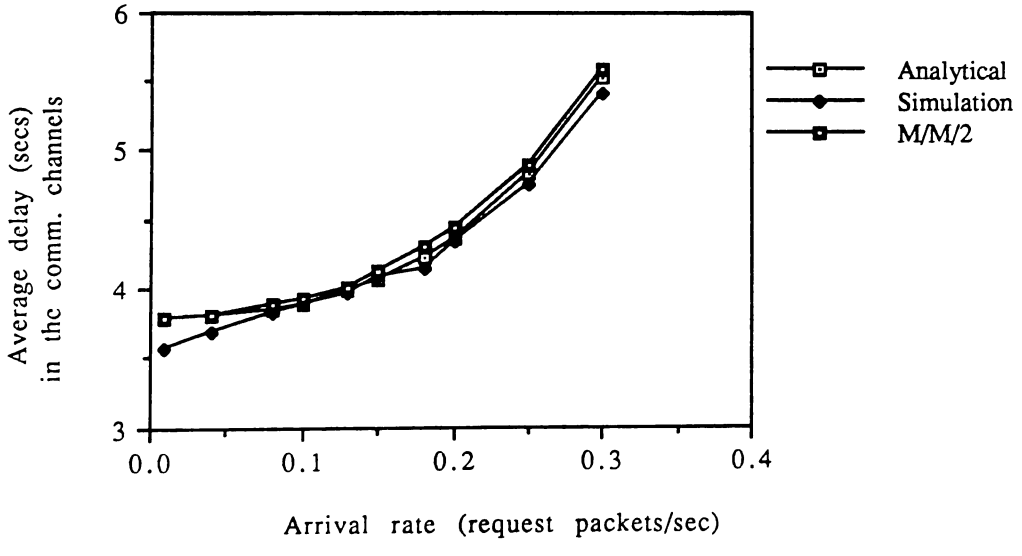

Figure 6.2. Average delay in the communication channels.

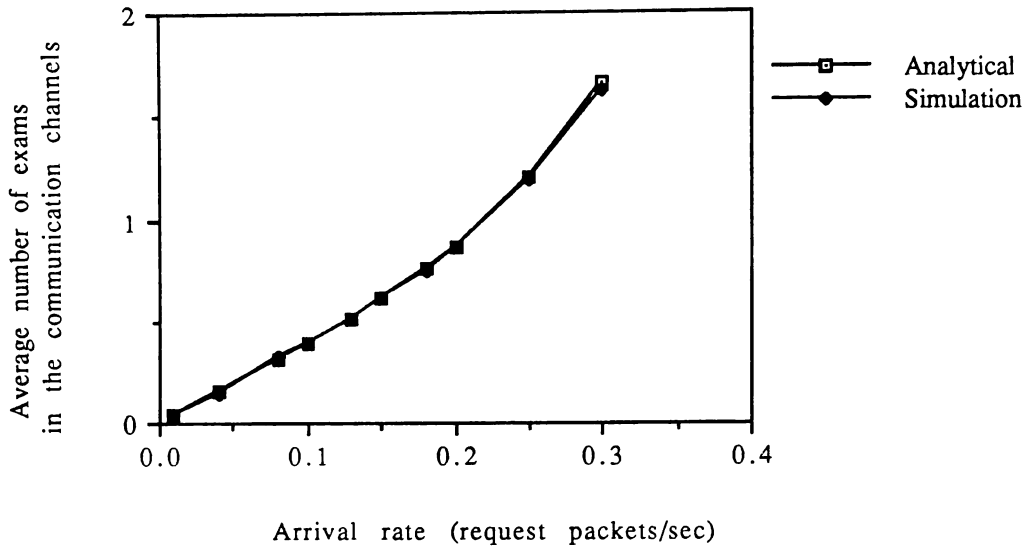

Figure 6.3. Average buffer occupancy in the communication channels versus the arrival rate.

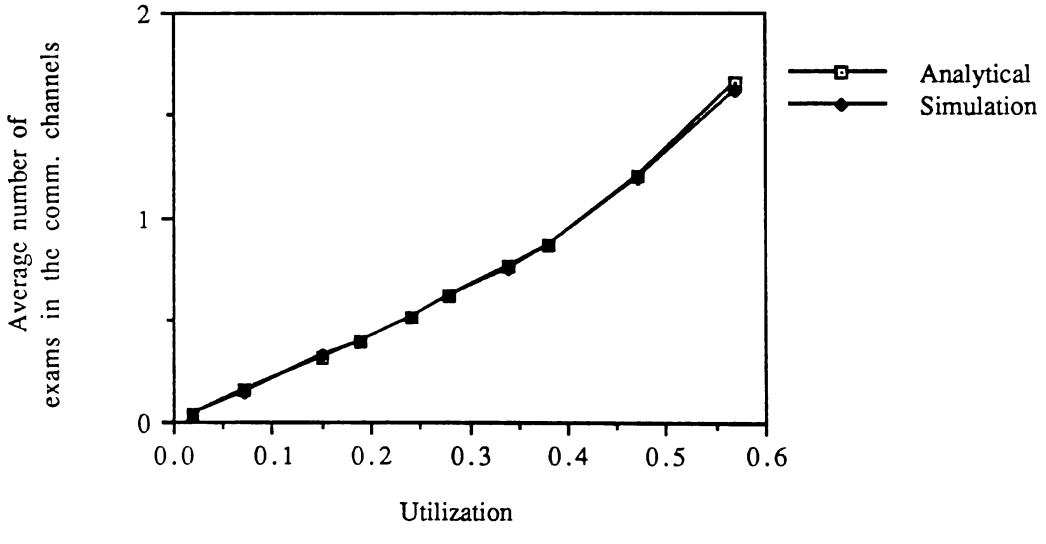

Figure 6.4. Average buffer occupancy in the communication channels versus the utilization.

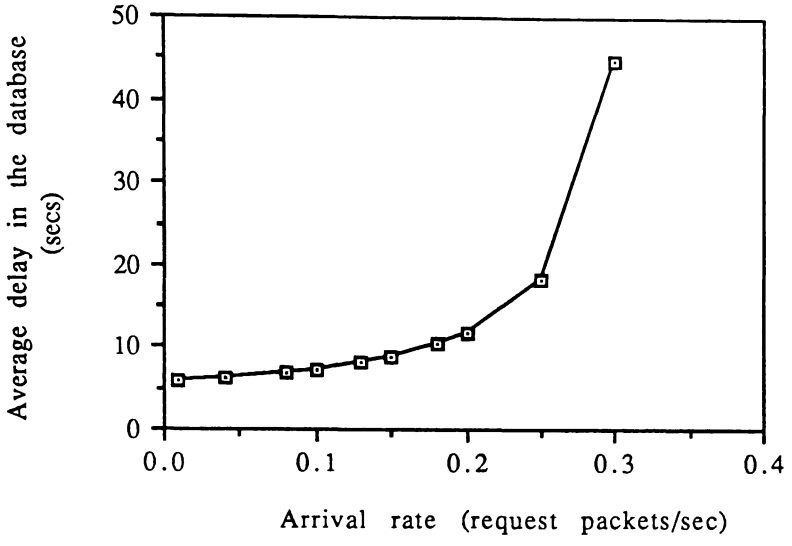

Figure 6.5. Average delay in the database.

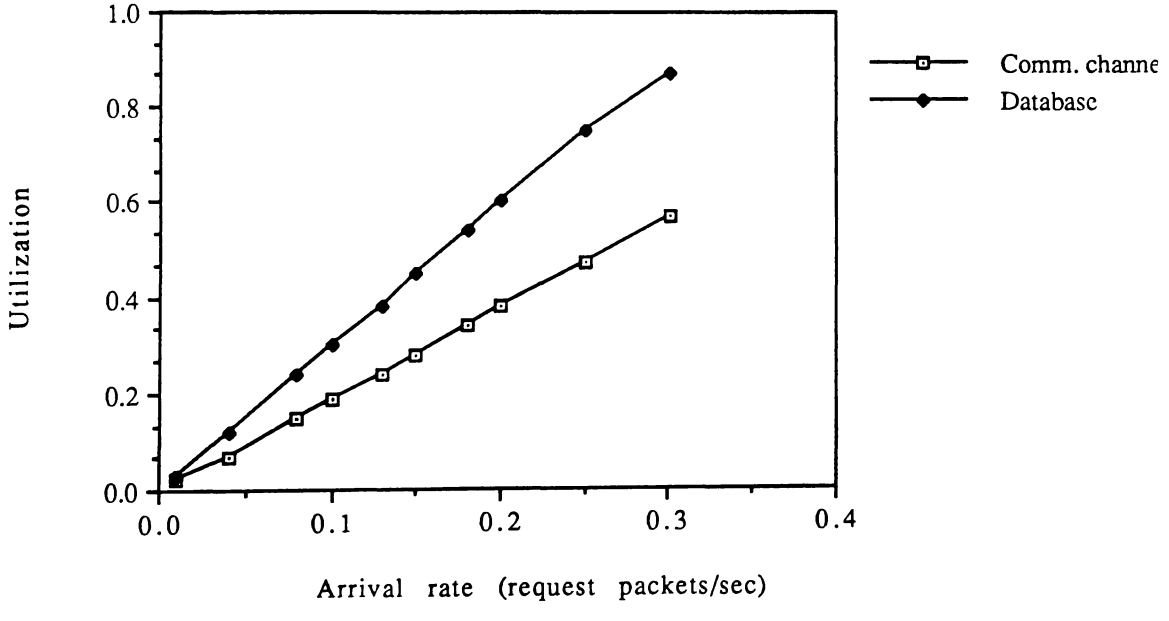

Figure 6.6. Utilization of the database and the comm. channels.

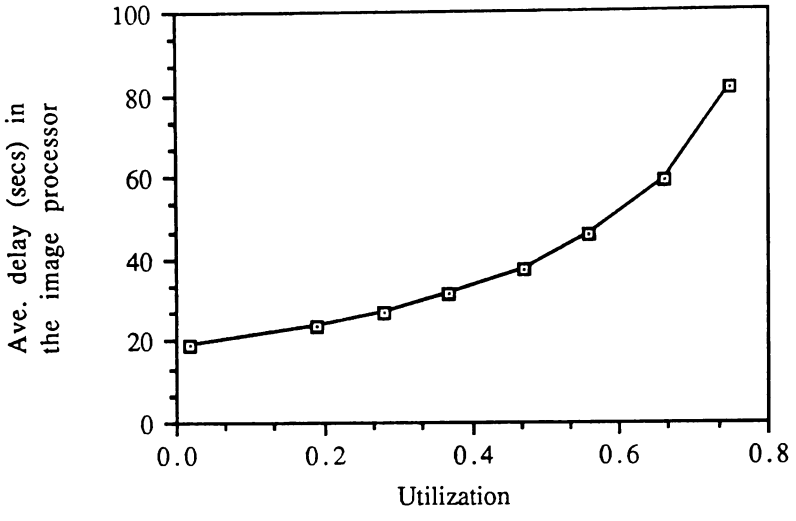

Figure 6.7. Average delay in processing images.

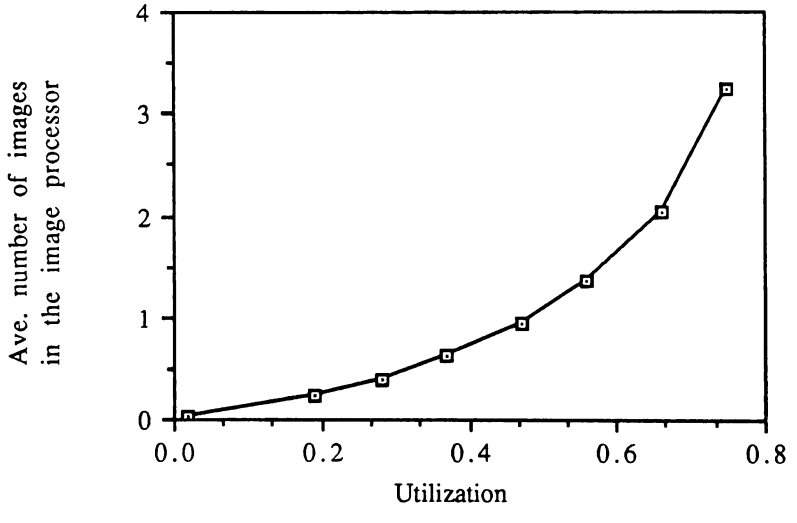

Figure 6.8. Average buffer occupancy in the picture viewing stations.

6.3-Performance curves for model 2

Here we present the performance curves for model 2. We have used the following parameters:

1) Each SIF consists of 512^2x8 bits.
2) Average number of SIFs in an image is 2.
3) Average number of images in an exam is 5.
4) Average number of exam requests in a request packet is 4.
5) Average "read" time from the database is 6 secs.
7) Two communication channels of 4 Mbps.

In Figure 6.9 and 6.10, we show the average delay in the communication channels plus the database and the delay in the communication channels, respectively. As can be seen from the analytical and the simulation curves the independence assumption between the departure processes in the database queues in the analytical model is valid in this case too, and this assumption produces results which are very close to the simulation results. The results of M/M/2 queueing system is also shown in Figure 6.10. The approximation of the queueing model of the communication channels by an M/M/2 queueing system, generates results that are on the average 9% lower that the results from the G/M/2 system.

In Figure 6.11, we show the average buffer occupancy in the communication channels. This curve can be used to estimate the buffer requirements at the interface between the database and the communication channels. Figures 6.12 and 6.13 show the delay and the average number of exam requests in the database, respectively. In Figure 6.14, we present the utilization of the database and the communication channels. Comparing this figure with figure 6.6 indicates a better utilization of the communication channels capacity in this model. These types of curves are useful in fine tuning a PACS, so that the resources are used in an optimal way and the capacity is not wasted.

In Figures 6.15 and 6.16 we show the average number of images and the average delay in the image processor. We assume that half the images

that arrive at the picture viewing station require an average processing time of 11.11 seconds and the other half require 16.67 seconds.

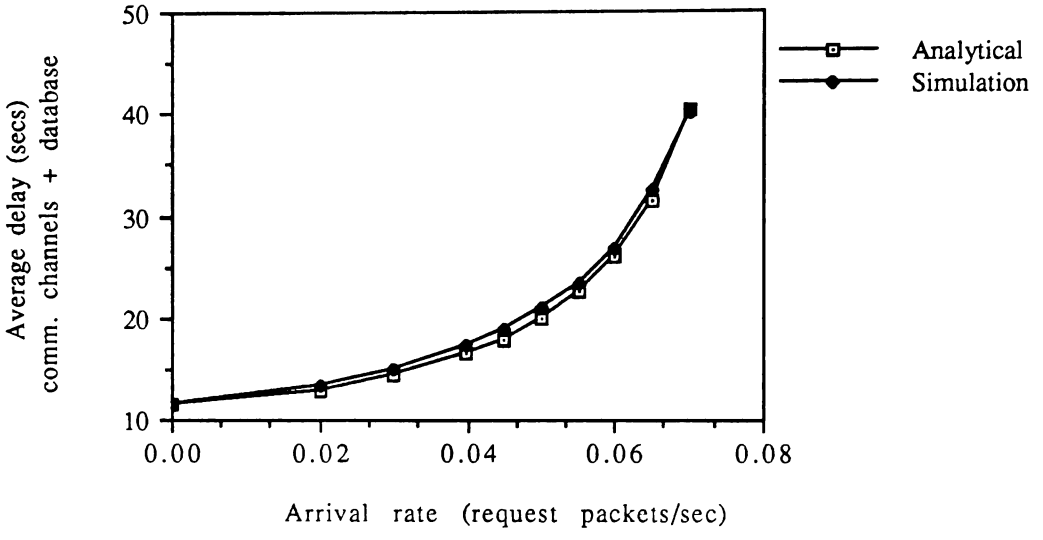

Figure 6.9. Average delay in the comm. channels and the database.

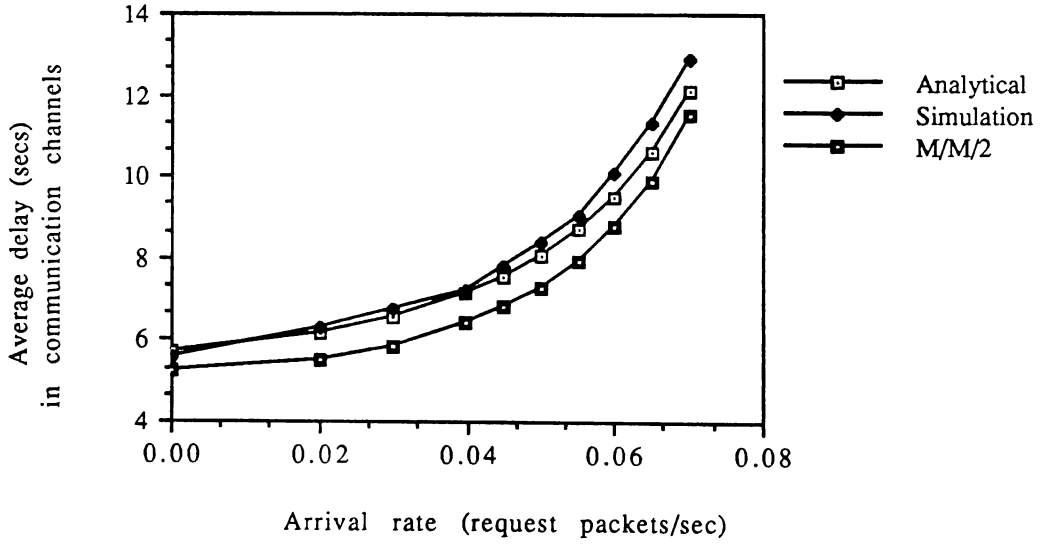

Figure 6.10. Average delay in the comm. channels.

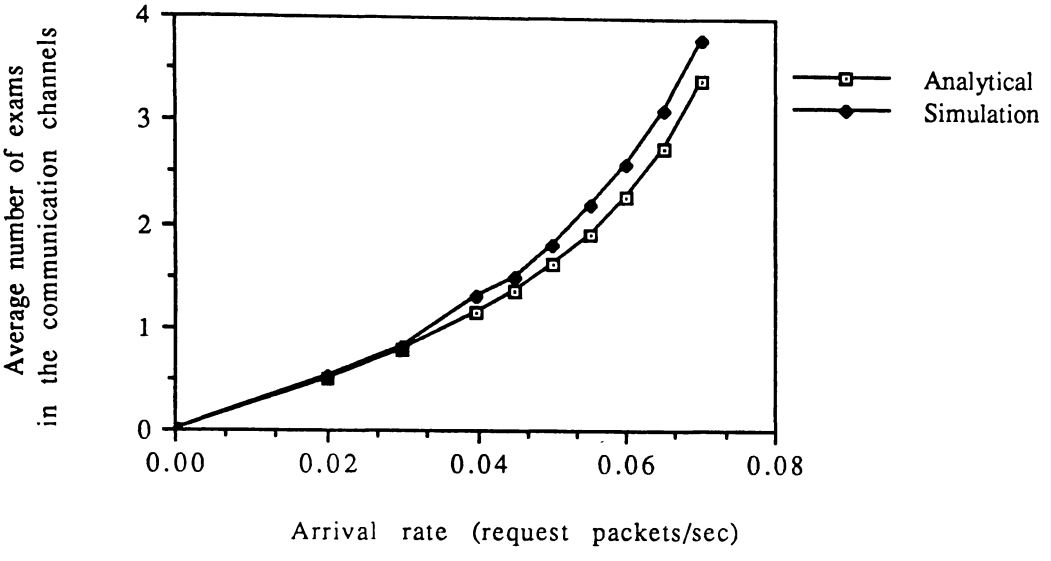

Figure 6.11. Average buffer occupancy in the comm. channels.

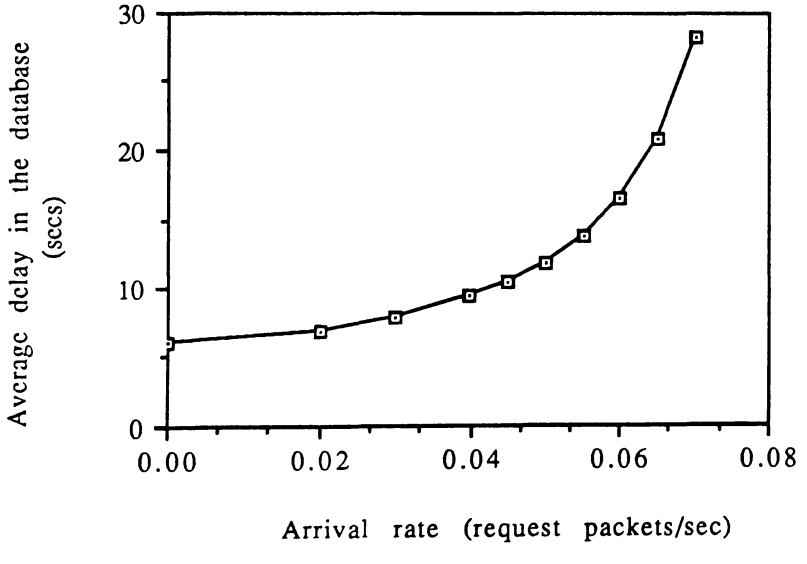

Figure 6.12. Average delay in the database.

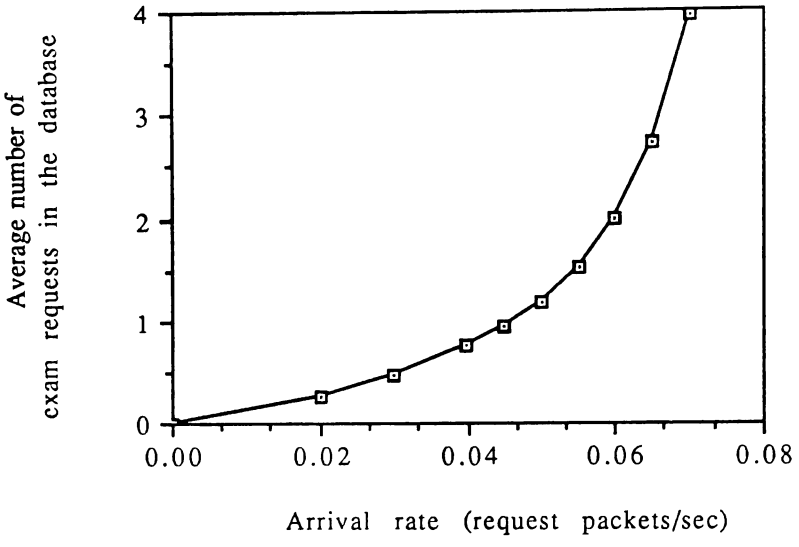

Figure 6.13. Average number of exams in the database.

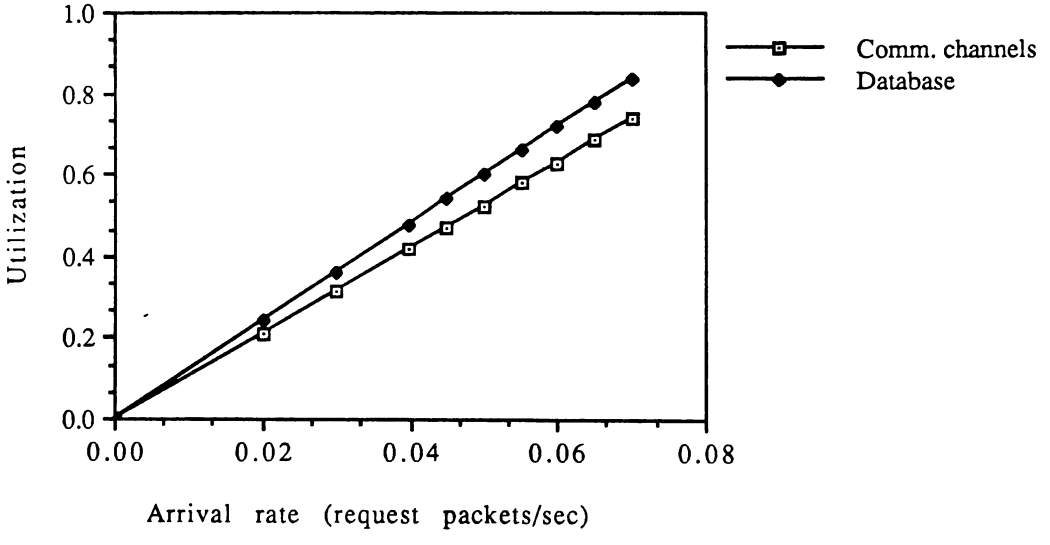

Figure 6.14. Utilization of the communication channels and the database.

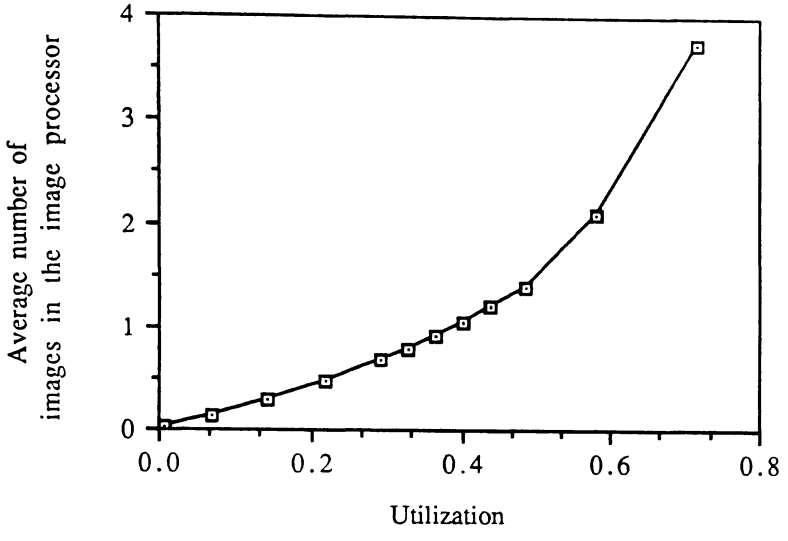

Figure 6.15. Average buffer occupancy in the picture viewing stations.

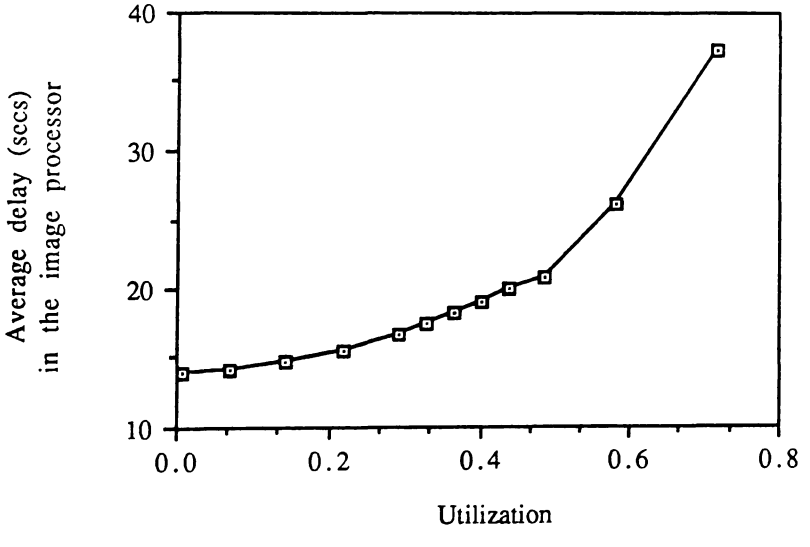

Figure 6.16. Average delay in processing images.

6.4-Performance curves for model 3

Here we present the performance curves for model 3. We have used the following parameters:

1) Each SIF consists of 512^2x8 bits.
2) Average number of SIFs in an image is 2.
3) Average number of images in an exam is 5.
4) Average number of exam requests in a request packet is 4.
5) Two "read" times of 6 and 12 seconds.
6) Two communication channels of 4 Mbps.

In Figure 6.17 we present the delay in the communication channels and the database for the analytical and the simulation models. These curves indicate that as in the previous two models, the independence assumption in the database queues is valid and based on this assumption we obtain analytical results which are very close to the results from simulation of this model. In Figure 6.18 we present the analytical, the simulation and the M/M/2 results for the communication channels. The results from the M/M/2 queueing system model of the communication channels are almost the same as the analytical model for the utilizations of less than 30%, and for higher utilizations the results are in average 6% higher than the analytical results. In Figures 6.19 and 6.20 we present the average buffer occupancy in the input buffers of the communication channels and the buffers of the database queues, respectively. These curves can be used in estimating the buffer requirements in the database and the interface between the database and the communication channels. In Figure 6.21 we show the average delay in th database.

Figure 6.22, shows the utilization of the database and the communication channels. As can be seen the utilization of the communication channels is in average 40% below that of the database queues and at most 53% of the capacity of the channels can be used before the database becomes a bottleneck and gets saturated. As indicated before, these type of curves can be used in fine tuning of the system so that excess capacity is not allocated and the resources are used in an optimal way.

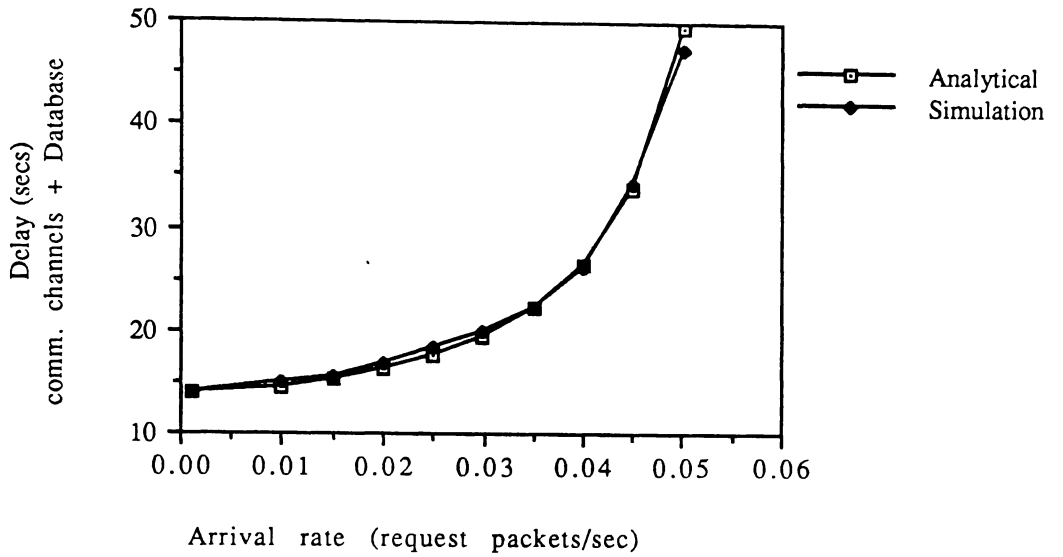

Figure 6.17. Average delay in the comm. channels and the database.

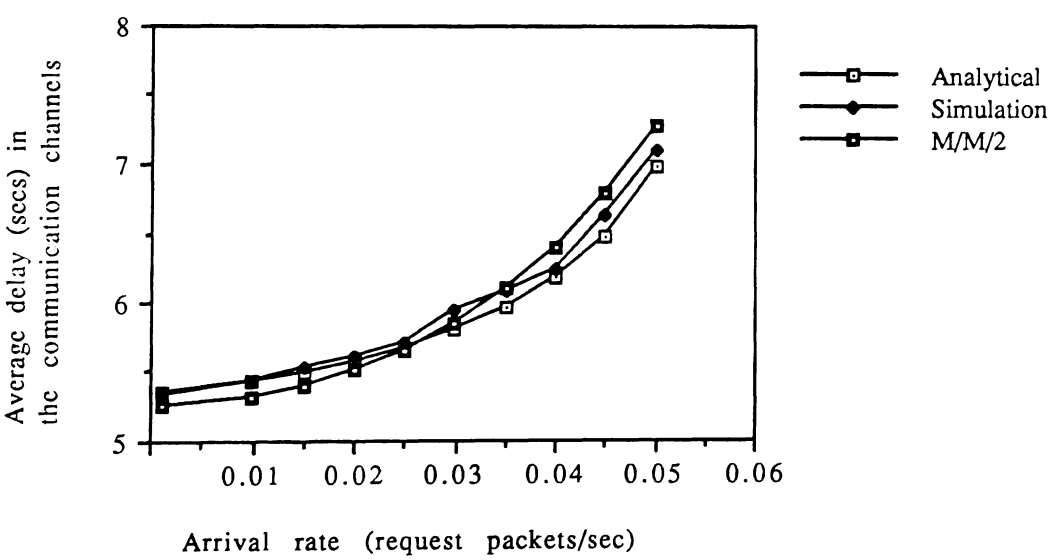

Figure 6.18. Average delay in the communication channels.

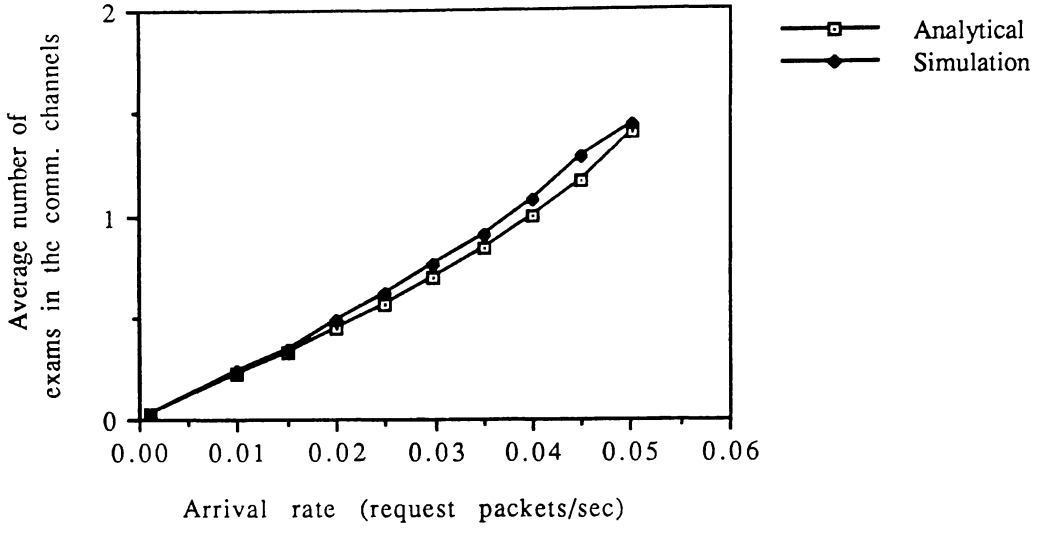

Figure 6.19. Average buffer occupancy in the comm. chznnels.

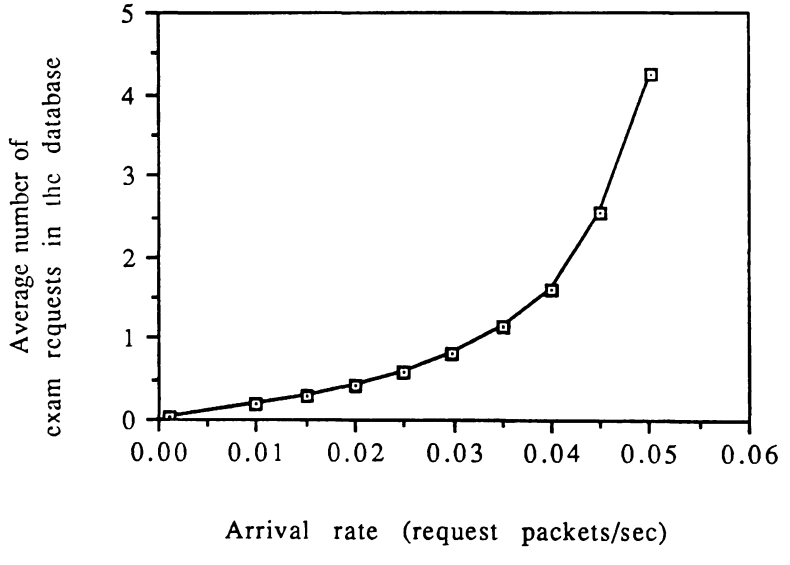

Figure 6.20. Average number of exam requests in the database.

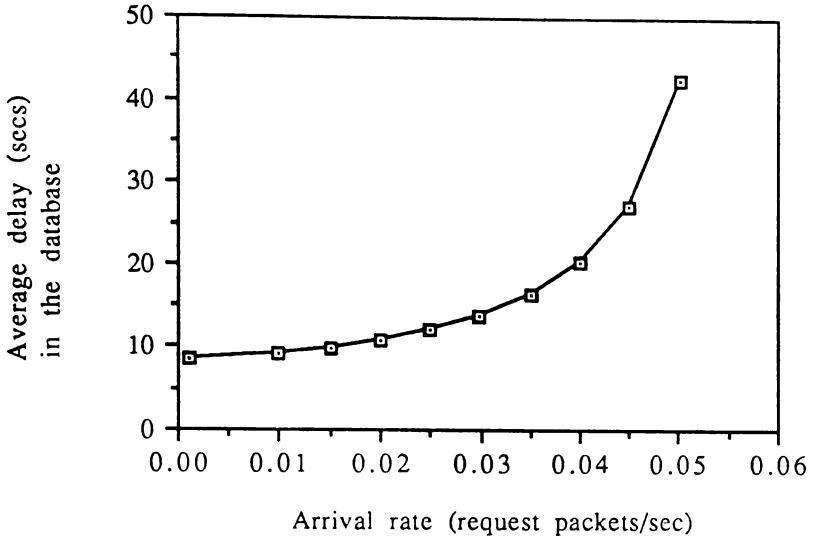

Figure 6.21. Average delay in the database.

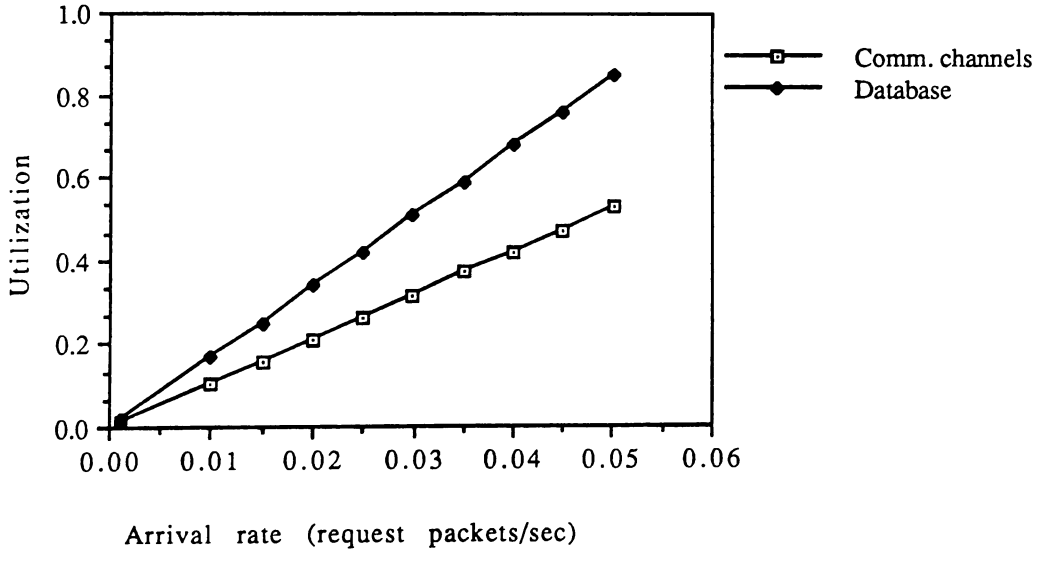

Figure 6.22. Utilization of the database and the comm. channels.

6.5-Conclusions

In this thesis we have presented three generic queueing models of picture archiving and communication systems. These models were for analyzing the performance of the image database, the communication channels and the picture viewing stations.

Our analysis of the queueing model of the communication channels was based on the assumption that the departure processes from the queueing systems in the database were independent and based on that the arrival process to the communication channels was evaluated by superimposing these departure processes.

The simulation results of each model indicated that this assumption is valid and the analytical results that we obtained were very close to the results from the simulation.

Our analytical results in chapters 3, 4, and 5 can be used by a system designer, using the appropriate parameters, to accurately estimate the time it takes to retrieve and display medical images, and also the buffer requirements in a picture archiving and communication system. These type of analysis are essential prior to building a PACS to ensure that the final product is usable and its response time is reasonable. The analysis can also be used to predict the performance of PACS as the system grows and more traffic is generated.

6.6-Future work

In the models that we have studied, we have assumed that request packets for retrieving images from the image database were of the same priority. This assumption could be relaxed in future modeling efforts to incorporate various priority schemes to get the performance measures of the system based on these scheduling mechanisms [38].

In our work, the queueing models of the image database have instantaneous mechanisms for creating siblings of request packet for retrieving more medical exams, which are spawned and put at the head of the queue to generate more requests for retrieving the remaining medical exams that were requested by a "request packet". It could be the case that this spawning mechanism can not be done instantaneously and some delay occurs in creating these siblings. A further study of the performance of the image database can develop models with delayed feedback, to evaluate the response time of the system.

One further work in this area, is to study the communications subnet of PACS in more details. If the delay in passing the data frames through various communication protocols is significant for a specific system, the performance of these protocols have to be analyzed in details to reduce the delay as much as possible.

If the hardware architecture of the image processor in a picture viewing station is such that representing it as a single server queue is not realistic, such as multiprocessor systems with a large amount of parallelism in them, then one can get a more accurate insight into their response time by modeling them as multi-server queues.

REFERENCES

[1] C. Marceau, "What is picture archiving and communication system?," Proc. SPIE, vol. 318 (part 1),1982, pp. 24-29.

[2] S. S. Hedge et al, "AT&T PACS architecture," Proc. SPIE (PACS IV), vol. 626, 1986, pp. 618-625.

[3] R. Arenson, et al, "Fiber optic communication system for medical images," Proc. SPIE, vol. 318 (part 1), 1982, pp.74-79.

[4] R. Vercillo, et al, "Digital image review console," Proc. SPIE, vol. 767, 1987, pp. 708-712.

[5] J. R. Perry, et al, "Performance features for a PACS display console," IEEE computer, August 1983, pp. 51-56.

[6] T. Wendler, et al, "Modular multiprocessor picture computer architecture for distributed picture information systems," Proc. SPIE, vol. 318 (part 1), 1982, pp. 125-132.

[7] K. Tsui, D. Rosenfeld, " A PC-based imaging workstation," Proc. SPIE, vol. 767, 1987, pp. 654-658.

[8] G. Y. Tang, B. Lien, "IBM PC-based multimedium workstation for joint medical diagnosis," Proc. SPIE, vol. 767,1987, pp. 659-662.

[9] H. Lemke, et al, "3-D computer workstation for biomedical information modelling and display," Proc. SPIE, vol. 767,1987, pp. 586-592.

[10] S. Suthasinekul, "Recent development in optical data storage," Proc. SPIE, vol 318 (part 1),1982, pp. 65-71.

[11] J. D. Kuehler, H.R. Kerby, " A photodigital mass storage system," Proc. of the Fall joint computer conference,1966, pp. 735-742.

[12] T. H. Otten, R. H. Nelson, " Human read-machine read microfilm mass storage system," RADC-TR-79-30, Final Technical Report, Rome Air development center, March 1979.

[13] R. A. Bartolini, et al, "Optical disk systems emerge," IEEE Spectrum, August 1978, pp. 20-28.

[14] G. C. Kenney, et al, "An optical disk replaces 25 Mag-tapes," IEEE Spectrum, February 1979, pp. 33-38.

[15] L. L. Burns, "System design of the slidestore," Digest of papers,IEEE symposium on Mass Storage Systems, April 1980, pp. 26-29.

[16] Technical Support Package, "Optical memory stores 10^{12} bits," NASA Tech. briefs, spring 1981, vol. 6, number 1, MFS-25456, Marshal Space Flight Center, Alabama.

[17] G. M. Blom, " Optical disk data storage," Proc. SPIE, vol. 318 (part 1), 1982, pp. 43-46.

[18] D. Meyer-Ebrecht, T. Wendker, "An architecture route through PACS," IEEE Computer, August 1983, pp. 19-28.

[19] R. L. Colby, "Promising rapid access high-capacity mass storage technique for diagnostic information utilizing optical disk," Proc. SPIE, vol. 318 (part 1),1982, pp. 36-42.

[20] N. J. Mankovich, "An image database structure for pediatric radiology," Proc. SPIE, vol. 767 pp. 564-570, 1987.

[21] J. L. Creasy, et al, "Overview of University of North Carolina at Chapel Hill PACS program," Proc. SPIE , vol. 914, 1988, pp. 1349-1355.

[22] J. R. Cox, et al, "Study of a distributed picture archiving and communication system for radiology," Proc. SPIE, vol. 318, 1982, pp. 133-142.

[23] J. Cox, et al, "Some design considerations for picture archiving and communication systems," IEEE Computer, August 1983, pp. 39-49.

[24] J. G. Hoffman, "Reliability requirements in a digital imaging environment," Proc. SPIE, vol. 767, 1987, pp. 834-838.

[25] E. G. Rawson, R. M. Metcalfe, "Fibernet: Multimode optical fibers for local computer networks," IEEE Trans. Communications, Vol. COM-26, No. 7, 1978, pp. 983-990.

[26] N. J. Mankovich, et al, "The software architecture of an integrated optical disk archive for digital radiographic images," Proc. SPIE 695, 1986, pp. .

[27] L. Kleinrock, "Queueing systems vol 1: Theory," Wiley-Interscience (New York) 1975.

[28] D. J. Daley, "The correlation structure of the output process of some single server queueing systems," The Annals of Mathematical Statistics, vol. 39 No. 3, 1968, pp. 1007-1019.

[29] D. R. Cox, H. D. Miller, "The theory of stochastic processes," Chapman and Hall (London) 1965.

[30] L. Takacs, "A single server queue with feedback," Bell System Technical Journal 42, 1963, pp. 509-519.

[31] P. J. Burke, "Proof of a conjecture on the inter_arrival time distribution in M/M/1 queues with feedback," IEEE Trans. on Communications, vol. COM-24, 1976, pp. 575-578.

[32] R. L. Disney, "The M/G/1 queue with instantaneous bernoulli feedback," Naval Res. Logist. Quart. 27, 1980, pp. 635-644.

[33] B. Melamed, "Characterization of Poisson traffic streams in Jackson queueing networks," Advances in Applied probability, 11, 1979, pp. 422-438.

[34] N. T. J. Bailey, "On queueing process with bulk service," J. R. Statist. Soc. (B)16, 1954a, pp. 80-87.

[35] F. Downton, "Waiting time in bulk service queues," J. R. Statis. Soc. B 17, 1955, No. 2 256-261.

[36] S. M. Ross, "Applied probability models with optimization applications," Holden-Day (San Francisco) 1970.

[37] E. A. Guillemin, "The mathematics of circuit analysis," Wiley (New York), 1949.

[38] D. D'Lima, "Performance models of a network interface unit in PACS," CCSP-TR-89/3, Center for Communications and Signal Processing, N. C. State University, Raleigh, North Carolina,1989.

APPENDIX 1

Our point of departure is equation (3.14) of section 3.4.1. After simplifying this equation and using the inverse of the Laplace transforms, we obtain the pdf of the inter_arrival time to the communication channels, $a(x)$, as

$$a(x) = \frac{\lambda_1\lambda_2}{\lambda_1+\lambda_2}\left[D_1e^{-(\mu_1+\mu_2)x} + D_2xe^{-(\mu_2+\lambda)x} + D_3e^{-(\mu_2+\lambda)x} + D_4xe^{-(\mu_2+\lambda)x} + D_5e^{-(\mu_1+\lambda)x} + D_6x^2e^{-2\lambda x} + D_7xe^{-2\lambda x} + D_8e^{-2\lambda x}\right]$$

where

$$D_1=\frac{A_{11}^{(1)}C_{11}^{(2)} + A_{11}^{(2)}C_{11}^{(1)} + 2B_{11}^{(1)}B_{11}^{(2)} +}{(s+\mu_1+\mu_2)}$$

$$D_2=\frac{A_{21}^{(1)}C_{11}^{(2)} + A_{11}^{(2)}C_{21}^{(1)} + 2B_{11}^{(1)}B_{11}^{(2)}}{(s+\lambda+\mu_2)^2}$$

$$D_3=\frac{A_{22}^{(1)}C_{11}^{(2)} + A_{11}^{(2)}C_{22}^{(1)} + 2B_{22}^{(1)}B_{11}^{(2)}}{(s+\lambda+\mu_2)}$$

$$D_4=\frac{A_{21}^{(2)}C_{11}^{(1)} + A_{11}^{(1)}C_{21}^{(2)} + 2B_{11}^{(1)}B_{21}^{(2)}}{(s+\lambda+\mu_1)^2}$$

$$D_5=\frac{A_{22}^{(2)}C_{11}^{(1)} + A_{11}^{(1)}C_{22}^{(2)} + 2B_{11}^{(1)}B_{22}^{(2)}}{(s+\lambda+\mu_1)}$$

$$D_6=\frac{2A_{21}^{(1)}C_{21}^{(2)} + 2A_{21}^{(2)}C_{21}^{(1)} + 4B_{21}^{(1)}B_{21}^{(2)}}{(s+2\lambda)^3}$$

$$D_7=\frac{A_{22}^{(1)}C_{21}^{(2)} + A_{22}^{(2)}C_{21}^{(1)} + C_{22}^{(2)}A_{21}^{(1)} + C_{22}^{(1)}A_{21}^{(2)} + 2B_{21}^{(1)}B_{22}^{(2)} + 2B_{22}^{(1)}B_{21}^{(2)}}{(s+2\lambda)^2}$$

$$D_8=\frac{A_{22}^{(1)}C_{22}^{(2)} + A_{22}^{(2)}C_{22}^{(1)} + 2B_{22}^{(1)}B_{22}^{(2)}}{(s+2\lambda)}$$

Clearly this density function is not exponential, however for all practical purposes it behaves as an exponential distribution. We plot this probability density function of the inter_arrival time and the pdf of an exponentially distributed inter_arrival time in Figure 1 to show how close these two distributions are

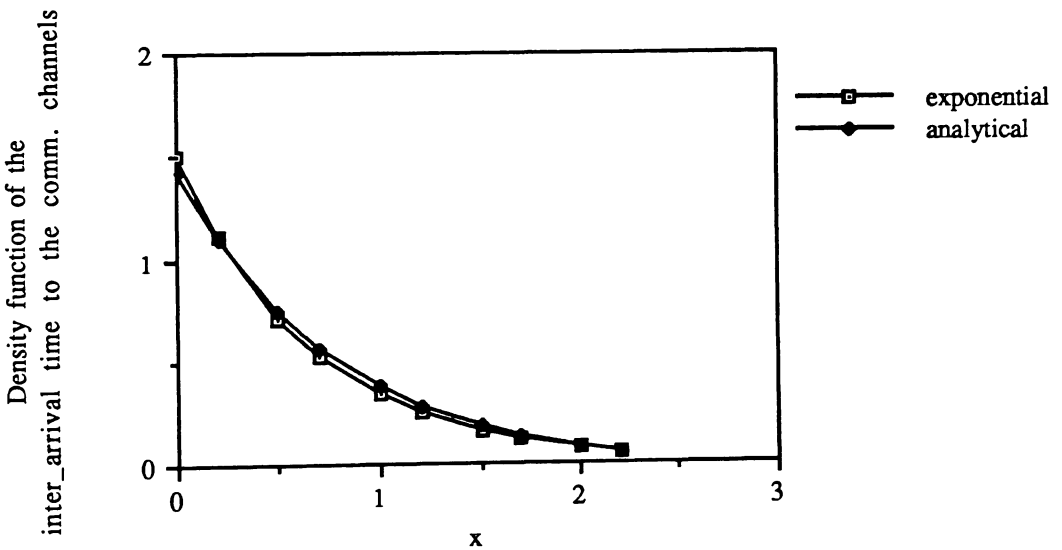

Figure 1. Density function of the inter-arrival time to the comm. channels. λ=0.75, $\mu_1=\mu_2$=1.

ISSN 0894-7066

April, May, June 1989

Spending cuts kill newsletter early; new publication begins in August — page 2. Conservation tips — page 3.

NCSU Computing Center Newsletter
North Carolina State University

Computing facility in 118 Daniels to be reduced 10 May

The 118 Daniels computing facility will close 8-9 May and reopen on 10 May in approximately half its previous space. This change is due to critical need for that space by the College of Engineering.

Beginning 10 May, the smaller Daniels facility will have the present Macintosh cluster, approximately ten Ampex terminals, and a Printronix printer. The RJE equipment will be retired, eliminating the campus' last card-reading capability.

When a replacement facility in Burlington Labs is completed some time in the next fiscal year, the Computing Center will completely vacate 118 Daniels. Because of the student needs which have been expressed, it appears that we will be able to continue Macintosh services in the Burlington facility.

These changes are caused by the priorities and needs of Engineering. We appreciate their willingness to provide the new space in Burlington.

The 118 Daniels facility has been our flagship remote facility since 1980 and provided much-needed services. However, use of the terminals and RJE equipment decreased considerably in the past three years. A severe lack of space in Engineering requires its reduction and eventual closing.

We regret and apologize for any inconvenience caused by these changes.

—Carl Allred
Assistant Director
ALLRED@NCSUVM.BITNET

Spending cuts kill newsletter early; Computing Center to launch successor in August

Because of budget cuts imposed for the remainder of this fiscal year by Governor Martin, this is the last issue of the *NCSU Computing Center Newsletter*. We will replace it with a new publication beginning in August.

The Computing Center had planned to cease publishing the newsletter this summer and replace it with the newly designed publication that we hope will serve our readers better. As part of our adjustment to the spending cuts, however, we will end it a few months early.

The new publication, *Connect*, will appear monthly except in July. It will feature a mix of articles and announcements of interest to faculty, staff, and students who use computers or are interested in their role in society. Each issue should offer key information to both users of mainframes and users of microcomputers.

Connect will continue the technical series of articles on SAS by Susan West, on the Macintosh by Daniel Carr, and on Unix by Sam Moore. It will also contain Mary Edeburn's highly popular profiles of Computing Center staff members and Rhonda Hunter's column on BIS, the online catalog system of the Triangle Research Libraries Network. We also plan several new features in *Connect* which we are not yet ready to announce.

While *Connect* will build upon the solid content the newsletter offered, its most noticeable improvement will be visual. This spring, a team of ten designers led by Bill Deere in the Department of Visual and Product Design developed new and much more readable formats for the Computing Center's publications. Though the necessity of printing our publications on a photocopier limits their visual quality, we look forward to offering much more accessible publications this fall, beginning with the first issue of *Connect*.

We will offer subscriptions to *Connect* to current subscribers to the *NCSU Computing Center Newsletter* and to faculty and staff on campus. Students are welcome to subscribe but will not receive individual invitations. Subscriptions are free to those who receive *Connect* at a NCSU campus mail address and to other computing centers with whom we exchange newsletters.

Computing can be a cost-effective (and often essential) tool of academic life. *Connect* will help our campus wield that tool wisely.

—L. Russell Herman, Jr.
RUSSELL@NCSUVM.BITNET

Keep informed via ENEWS

To keep up during the suspension of printing, you can subscribe to ENEWS, our new electronic mail news service. Subscribers will receive short announcements and schedules of coming events.

To subscribe, send "SUB ENEWS your full name" ("your full name" is replaced by your name) to LISTSERV@NCSUVM.BITNET.

From CMS on NCSUVM, the command is "TELL LISTSERV SUB ENEWS your full name".

From a TSO account at TUCC, type the following commands with a return after each line:

VMSG
NCSUVM LISTSERV
SUB ENEWS your full name
END

From VMS on a VAX, type the single command "SEND LISTSERV@NCSUVM SUB ENEWS your full name".

From Unix, send mail to LISTSERV@NCSUVM.BITNET containing the single line "SUB ENEWS your full name".

If you have any questions, contact a Computing Center consultant by sending e-mail to CONSULT@NCSUVM.BITNET, phoning 737-3035, or visiting the Information Center in Room 106 of the Hillsborough Building. ■

How to compute in a fiscal crisis: conservation tips

The Computing Center's services can often help you conserve university funds. Here are suggestions for reducing your computing expenditures and for using computing to reduce other expenses.

Use electronic mail

Do you collaborate or correspond with colleagues around the world by telephone or mail? If you do and are not currently using electronic mail you should consider e-mail as a cost-saving alternative. You will also find e-mail a convenient method of avoiding telephone tag and time zone irritations.

Contact your computing coordinator and request an allocation to use e-mail. If you do not know who your computing coordinator is, refer to User Memo UM-054, *Departmental Computing Coordinators*, or contact Angie Taylor at the Computing Center (737-2517 or ANGIE@NCSUVM.BITNET).

These tips come from Carl Allred (Assistant Director), Larry Roberson (Manager of Systems), Larry Robinson (head, Information Center), Daniel Carr (technical writer and microcomputing consultant), Ken Aldridge (Manager of Hardware Services), and Dennis Elledge (Manager of Microcomputing and Education).

Check output before printing

Because of the state's budget constraints, we must sharply cut our use of supplies. Please do not print anything that is not essential. Review drafts on your screen and get them correct before committing them to paper. For assistance in reviewing on the screen, contact a consultant by sending e-mail to CONSULT@NCSUVM.BITNET, by phoning 737-3035, or by visiting the Information Center in Room 106 Hillsborough Building.

Compress TUCC printing

TUCC batch users may save paper when printing by requesting vertical output compression. This causes the skipping of blank lines to be suppressed and can result in significant paper savings for some jobs. Compression is specified by the use of "FORMS=COMP" on the JOBPARM statement. See TUCC document GI-081, *Job Control Language (JCL) and Other Job Management Information for TUCC's Batch (Remote Job Entry) System*, for more information.

Happenings! available for newsletters

Happenings!, the campus online videotex system administered by the Computing Center, is available for electronic distribution of campus newsletters and other information. Currently, the *Official Bulletin* and Purchasing newsletters are placed into *Happenings!* on a regular basis. Others include *Omnibus* from Transportation and *NCSU Computing Center Newsletter* articles. *Happenings!* is accessible from terminals or microcomputers with VT100 capability. Call Larry Roberson at 737-2517 for more information or send email to NLCR@NCSUVM.BITNET.

Recycle paper

It's easy to put used paper in a recycling bin instead of the trash. It also saves the University money.

If you are using a laser printer, do not try to "recycle" paper by printing on paper already used. It can damage the laser printer.

If you do not have access to recycling bins, or you would like to learn more about recycling, contact Randy Bowen of Automotive Services (737-2181). He is in charge of NCSU's recycling.

(Continued on next page.)

(Continued from previous page.)

Documentation available online

Many of the publications that the Computing Center produces on paper are also available online on our mainframe computers. The GETDOC command on TUCC TSO, Wylbur, and NCSU VM/CMS provides on-screen versions of most current User Memos, and other useful information. Type "GETDOC" on TSO, Wylbur, or CMS for more information.

Most of the TUCC GI and LS series documents are also available online for TUCC TSO and Wylbur users. The dataset TUCDOC.LIST contains a list of the names and instructions for printing these files. To save money, you can display the file on your screen by editing the corresponding file using either QED or ISPF under TSO. Use the "USE" command in Wylbur. Type "TUCDOC" to see the list of file names.

The "ABSTRACT" command on the TUCC TSO system will display an abstract of any of the items referenced in TUCC document GIR-000, *Index of Computer Programs and Facilities Documented at TUCC.* Type "HELP ABSTRACT" for more information about using the ABSTRACT command.

If you can not afford the manuals that are sometimes needed when using the TUCC TSO or NCSU VM/CMS systems, try out the "HELP" command. Simply type "HELP" on either of these systems for more information.

Information Center may reduce hours

Due to possible cutbacks in our part-time budget, it may be necessary to curtail or eliminate some of the evening and weekend hours that the Computing Center's Information Center is operational. We will endeavor to limit the closings to times of low use. We regret any inconvenience that this schedule change may cause.

Save electricity

Turn off lights, printers, and computers if they're not going to be used for over an hour.

Hardware Services

The Computing Center's Hardware Services (737-2016) is less expensive than commercial services for maintenance and repairs of campus computing equipment. See User Memos UM-060, *Hardware Maintenance Policies*; UM-061, *Maintenance Contract Rates for University-owned Equipment*; and UM-062, *Maintenance Contract Rates for Individually-owned Equipment*, for details.

Site licenses and "Public" save on software

The Computing Center purchased a campus-wide site license for WordPerfect early in 1988. This allows departmental purchases at a large discount off the single-copy price. The suggested retail price of WordPerfect 5.0 is $495 (with an educational discount price of $135 from certain vendors). Under our site license, a new WordPerfect license, with template, may be purchased for $35 and an upgrade to WordPerfect 5.0 from an earlier version is only $5. Manuals are optional at $35 per set.

The Public Software Access Facility (called "Public"), a bulletin board of microcomputer software operated by the Computing Center, contains many utilities and application packages available for little or no cost. Access is available through the campus dataswitch, which can be reached via hardwired terminal or via telephone with a modem.

Kermit is the asynchronous communications package we recommend for accessing many of the Computing Center's services (such as Public). We distribute free copies of Kermit for Macintosh and MS-DOS computers. Kermit allows access to mainframe computers and the uploading and downloading of files. ■

Big changes coming at TUCC; here's the current schedule

Carl Malstrom, director of the Center, has announced that the Computing Center will continue to provide MVS services to the campus even after TUCC closes. Making MVS service available to campus users is not in question. The question is how to provide those services. The Computing Center and the TUCC staff are working on plans for the transition from TUCC.

The following schedule lists events planned so far. We will publish revised schedules in future newsletter issues as plans develop.

14 December 1988

- WYLBUR was "frozen" (i.e., no more updates).

22 December 1988

- TUCCVM frozen. If VM fails and cannot be restarted quickly, MVS will be brought up alone while VM is being worked on.

February 1989

- No major changes are planned to TUCC after February to allow time to make sure the system is stable by May.

1 May 1989

- MVS system (including TSO and WYLBUR) is frozen (except HSM).
- First TUCC staff reductions (includes four of six systems positions, the documentation specialist, and some administrative staff).
- Any datasets remaining under the old TUCC naming convention will be scratched and all backup tapes of them will be recycled.

30 June 1990

- TUCC ceases operation. ■

Some computing schedules change during session break

Some computing facilities will have reduced schedules between spring and summer sessions. Unless otherwise indicated, schedules are normal. For instance, TUCC and Computing Center facilities in Hillsborough, 120 Dabney, and 1139 Burlington will operate normally. ■

	118 Daniels	222 Mann	1404 Broughton	118 Winston
29-30 April	spring	spring	closed	closed
1-2 May	0800-1800	0800-1700	0900-1600	closed
3-5 May	0800-1800	0800-1700	0900-1600	closed
6-7 May	closed	closed	closed	closed
8-12 May	0800-1800	0800-1700	0900-1600	closed
13-14 May	closed	closed	closed	closed
15-19 May	0800-1800	0800-1700	0900-1600	closed
20-21 May	closed	closed	closed	closed
22 May	0800-1800	0800-1700	0900-1600	closed
23 May	0800-1800	0800-1700	1200 summer	summer
24 May	0800 summer	0800 summer	summer	summer

Computing Center directory

Computers and operating systems
NCSU users have access to an IBM 3081K48-PIF running under MVS/XA and VM/SP CMS at the Triangle Universities Computation Center (TUCC) and to an IBM 4381M12 running under VM/SP CMS at the NCSU Computing Center. An IBM 3083 in the Computing Center runs under MVS/XA for administrative computing. In addition, many departments and research projects have their own machines.

General services
The Computing Center is in the Hillsborough Building at the corner of Hillsborough and Gardner Streets. Microcomputing, Education, and Publications are in the Hillsborough Building Annex on the east side of the Hillsborough Building. Hardware Services is at 20 Enterprise Street. Business Services and Data Entry are in the D. H. Hill Library (DHHL). Except where otherwise indicated, the voice telephone number is (919) 737-2517. The fax number is (919) 737-3787.

Service	Contact person	Location	BITNET address
account applications/maintenance	Angie Taylor	1307 DHHL	NANGIE@NCSUVM
consulting	consultant on duty	106 (737-3035)	CONSULT@NCSUVM
courier service	Tommy Whitley	124	VWIT@NCSUVM
education coordinator	Bill Padgett	7 Annex	BILL@NCSUVM
hardware repair	Mary Serianni	Enterprise (737-2016)	MARY@NCSUVM
job submittal and retrieval	operator on duty	dispatcher's window (737-2523)	
keypunch service (data entry)	Shirley Massey	1303A DHHL	QUIZ@NCSUVM
mainframe graphics	Jack Fulton	109A	NJHF@TUCC
microcomputing	Dennis Elledge	2 Annex	DWE@NCSUVM
network communications	Sam Averitt	B16	SFA@NCSUVX
optical mark reading	Shirley Massey	1303A DHHL	QUIZ@NCSUVM
publications	Russell Herman	5 Annex	RUSSELL@NCSUVM
SAS and PC SAS consulting	Susan West	3 Annex	SUSAN@NCSUVM
special forms, special operations	George Stancil	124	NGRSTW@NCSUVM
supercomputing	Jeff Alexander	106 (737-3035)	JEFF@NCSUVM
tape disk registration	Tommy Whitley	124	VWIT@NCSUVM
Computing Center management			
Director	Carl Malstrom	M2	CWM@NCSUVAX
Asst. Dir., Support & Business Planning	Carl Allred	110	ALLRED@NCSUVM
Manager, Business Services	Regina Ekong	1304 DHHL	GINA@NCSUVM
Manager, Mainframe Support Services	Ellen Berry	107	NELLEN@TUCC
Manager, Research & Communications	Sam Averitt	B16B	SFA@NCSUVX
Manager, Operations	George Stancil	124	NGRSTW@NCSUVM
Manager, Systems Support	Larry Roberson	B17G	NLCR@NCSUVM
Manager, User Services	Bill Padgett	7 Annex	BILL@NCSUVM
Manager, Administrative Services	Betty Strickland	M2	NBETTY@NCSUVM
Related computing activities			
Assoc. Provost, Academic Computing	Henry Schaffer	M2	TSCHES@TUCC
Administrative Computing Services	Leo Buckmaster	B21 (737-2794)	NACSHLB@NCSUADM
Management Information Resource Center	Jeff Hunter	18 Leazar Hall	N988483@NCSUADM

The *NCSU Computing Center Newsletter* (ISSN 0894-7066) is published monthly except July by the Computing Center of North Carolina State University.
One thousand seven hundred copies of this public document were printed at a cost of $312, or $.18 per copy.

Computing Center, Campus Box 7109, North Carolina State University, Raleigh, North Carolina 27695-7109 USA

Computing Center facilities

(Please see inter-session schedule on page 5.)

LOCATION	SUMMER HOURS OF OPERATION	TYPE OF AVAILABILITY	CRT	APL	PRINTER	MICROS	CONSULTING	PHONE 737-
Hillsborough[1]	0700 Mon - 2400 Sat 1300-2400 Sun	Network	9	0	4	MTEC[1]	0800-1800 Mon-Fri 1300-1700 Sat-Sun	2517 Operator 2523 Dispatcher 3035 Consultant
1139 Burlington[2]	key access only	Network, RJE	5	0	1	0	none	3165
118 Daniels	0800-2400 Mon-Sat 1300-2400 Sun	Network	12	0	2	Macs[3]	none	3631
Bragaw	closed	Network	10	0	0	0	none	2517
1404 Broughton	1200-2100 Mon-Thu 1200-1800 Fri 1400-2100 Sun	Network	3[4]	0	1[4]	IBM PCs[4]	see note 4	2517
120 Dabney	0600-2200 Mon-Thu 0600-1700 Fri	Network	17	4[5]	1	0	none	2517
222 Mann[6]	0800-1700 Mon-Fri	Network	22	0	1	0	none	2517
Tucker	closed	Network	11	0	0	0	none	2517
118 Winston	1200-1900 Mon-Fri		0	0	1	Macs[7]		

1 The Microcomputer Testing and Evaluation Center (MTEC) is also located in Hillsborough. Software and manuals may be checked out at the dispatcher's window. Various graphics devices are also available.

2 For graduate and faculty users engaged in research. Key access only.

3 Nine Macintosh Plus and three Macintosh SE microcomputers, one ImageWriter II, one LaserWriter Plus, and minimal software.

4 Fifteen IBM PCs, eight IBM graphics printers, a Hewlett-Packard Laserjet printer, and various software packages available. Staff is on duty during operating hours to check out software and manuals to users.

5 One Decwriter and three APL CRTs.

6 The operator in 118 Daniels may keep 222 Mann open if Daniels has an overflow crowd. When it is kept open beyond normal hours, the last person leaving 222 Mann must notify the operator in 118 Daniels.

7 Twelve Macintosh SEs, two Macintosh II computers, and one ImageWriter II.

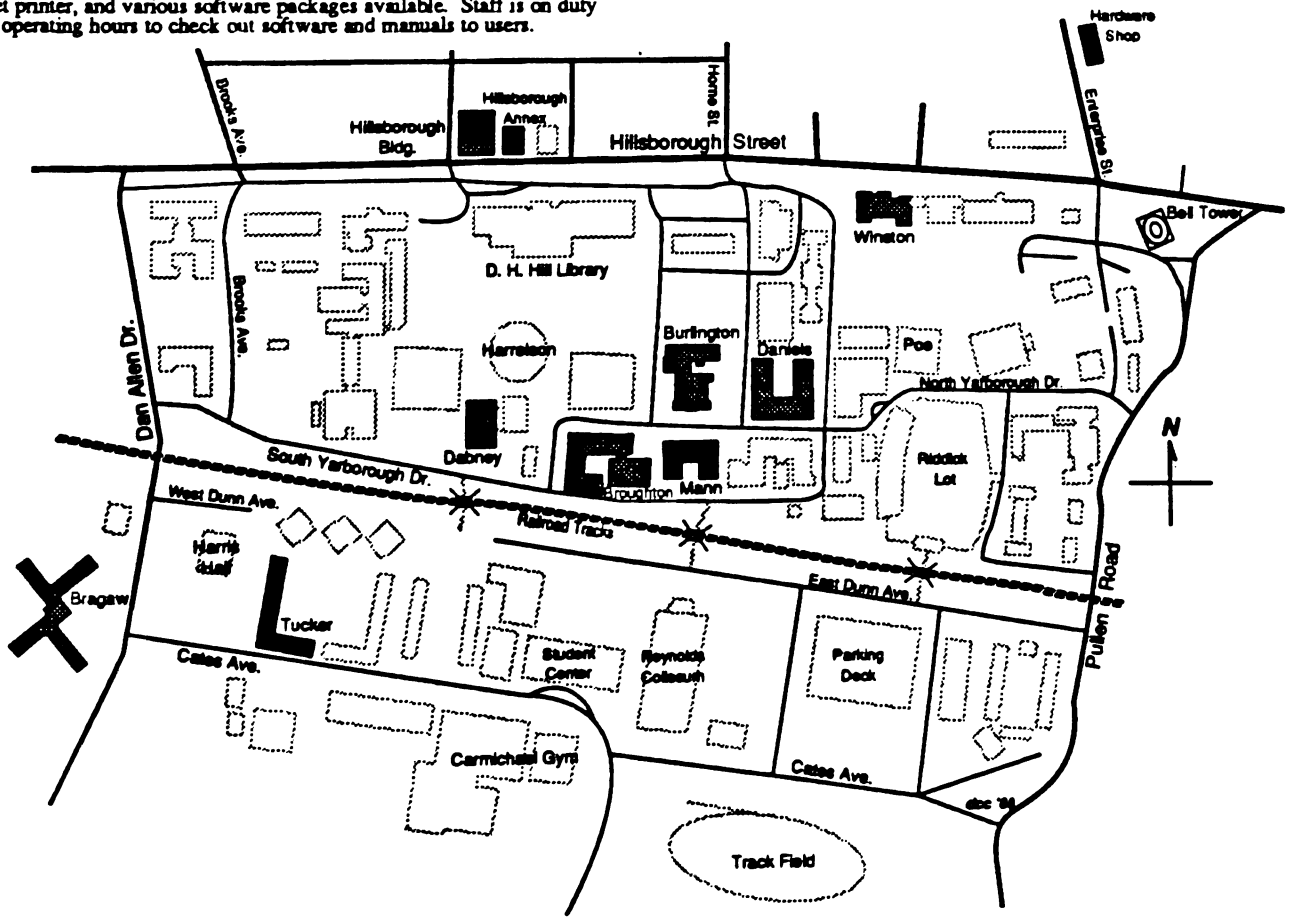

FROM:
Publications Office
Computing Center
Campus Box 7109
North Carolina State University
Raleigh, North Carolina 27695-7109
USA

Betsy Jobe
320 Daniels
Campus Box 7914
Campus mail